

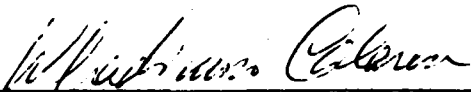
MICROCOPY RESOLUTION TEST CHART
NATIONAL BUREAU OF STANDARDS-1963-A

NOTICE

When Government drawings, specifications, or other data are used for any purpose other than in connection with a definitely related Government procurement operation, the United States Government thereby incurs no responsibility nor any obligation whatsoever; and the fact that the government may have formulated, furnished, or in any way supplied the said drawings, specifications, or other data, is not to be regarded by implication or otherwise as in any manner licensing the holder or any other person or corporation, or conveying any rights or permission to manufacture use, or sell any patented invention that may in any way be related thereto.

This report has been reviewed by the Office of Public Affairs (ASD/PA) and is releasable to the National Technical Information Service (NTIS). At NTIS, it will be available to the general public, including foreign nations.

This technical report has been reviewed and is approved for publication.



Wladimiro Calarese
Aerospace Engineer
High Speed Aero Performance Branch
Aeromechanics Division



Valentine Dahlem
Chief
High Speed Aero Performance Branch
Aeromechanics Division

FOR THE COMMANDER



Donald A. Dreesbach
Colonel, USAF
Chief
Aeromechanics Division

If your address has changed, if you wish to be removed from our mailing list, or if the addressee is no longer employed by your organization please notify AFWAL/FIMG, W-PAFB, OH 45433 to help us maintain a current mailing list.

Copies of this report should not be returned unless return is required by security considerations, contractual obligations, or notice on a specific document.

Unclassified

SECURITY CLASSIFICATION OF THIS PAGE

AD-H174806

REPORT DOCUMENTATION PAGE

1a. REPORT SECURITY CLASSIFICATION Unclassified		1b. RESTRICTIVE MARKINGS	
2a. SECURITY CLASSIFICATION AUTHORITY		3. DISTRIBUTION/AVAILABILITY OF REPORT Approved for Public Release; Distribution Unlimited	
2b. DECLASSIFICATION/DOWNGRADING SCHEDULE			
4. PERFORMING ORGANIZATION REPORT NUMBER(S)		5. MONITORING ORGANIZATION REPORT NUMBER(S) AFWAL-TR-86-3031	
6a. NAME OF PERFORMING ORGANIZATION Complere Inc.	6b. OFFICE SYMBOL (If applicable)	7a. NAME OF MONITORING ORGANIZATION Air Force Wright Aeronautical Laboratories Flight Dynamics Laboratory (AFWAL/FIMG)	
6c. ADDRESS (City, State and ZIP Code) P.O. Box 1697 Palo Alto CA 94302		7b. ADDRESS (City, State and ZIP Code) Wright-Patterson Air Force Base, Ohio 45433	
8a. NAME OF FUNDING/SPONSORING ORGANIZATION	8b. OFFICE SYMBOL (If applicable)	9. PROCUREMENT INSTRUMENT IDENTIFICATION NUMBER F33615-82-C-3022	
8c. ADDRESS (City, State and ZIP Code)		10. SOURCE OF FUNDING NOS.	
		PROGRAM ELEMENT NO. 61102F	PROJECT NO. 2307
		TASK NO. N4	WORK UNIT NO. 51
11. TITLE (Include Security Classification) Turbulent Boundary Layer Measurements (U)			
12. PERSONAL AUTHOR(S) F.K. Owen and A.W. Fiore			
13a. TYPE OF REPORT Final Report	13b. TIME COVERED FROM 10/1/82 TO 3/31/85	14. DATE OF REPORT (Yr., Mo., Day) August 1986	15. PAGE COUNT 134
16. SUPPLEMENTARY NOTATION			
17. COSATI CODES		18. SUBJECT TERMS (Continue on reverse if necessary and identify by block number)	
FIELD 0102	GROUP 2004	SUB. GR. 0101	Supersonic Boundary Layers, Turbulent Flow, Hot Wire Anemometer and Laser Velocimeter Measurements.
19. ABSTRACT (Continue on reverse if necessary and identify by block number)			
<p>This reports reviews the principles and practice of hot wire anemometry for the measurement of turbulent flows. The requirements and pitfalls involved in the use of hot wire anemometers in supersonic flows are addressed and the methods used for data acquisition and reduction are detailed. Examples of measurements obtained in AFWAL facilities are presented. Unfortunately in most flows of practical interest, local fluctuation levels exceed those for which reliable hot wire turbulence measurements can be expected. However, our recent developments in laser velocimetry facilitate the non-intrusive, linear measurement of high speed turbulent flows. Measurements of zero pressure gradient and ramp induced, adverse pressure gradient flows are presented. The results emphasize the need for combined hot wire and laser velocimeter studies to determine the reliable and useful ranges of both instruments.</p>			
20. DISTRIBUTION/AVAILABILITY OF ABSTRACT UNCLASSIFIED/UNLIMITED <input type="checkbox"/> SAME AS RPT. <input checked="" type="checkbox"/> DTIC USERS <input type="checkbox"/>		21. ABSTRACT SECURITY CLASSIFICATION Unclassified	
22a. NAME OF RESPONSIBLE INDIVIDUAL Wladimiro Calarese		22b. TELEPHONE NUMBER (Include Area Code) 513 255-2052	22c. OFFICE SYMBOL AFWAL/FIMG

Table of Contents

Section	Title	Page
1	Introduction	1
2	Definitions and Descriptive Properties of Turbulence	5
3	Turbulence Measurement Requirements	14
4	The Measurement of Turbulent Fluctuations	26
5	The Hot Wire in Compressible Flow	60
6	Practical Procedures for Turbulence Measurement	83
7	Hot Wire and Laser Velocimeter Measurements	118
	References	133

Section 1 Introduction

The word anemometer stems from the Greek "anemos" meaning "wind" and "metron" meaning "measure". A hot-wire anemometer senses any changes in the variables which affect the rate of heat-transfer between the wire and the fluid. Variations in heat transfer coefficient can change both wire temperature and resistance. If the wire is made part of a suitable electrical circuit, these changes can be used to generate a signal which is related to the instantaneous heat transfer. Thus, as Morkovin (ref. 1) points out, for correct interpretation of the electrical signal we need to know: 1) the identity of possible fluid flow variations (eg. turbulence or sound), 2) the laws of heat transfer between the wire and fluid, 3) the variation of wire resistance with temperature and the effects of conduction to the supports, and 4) the response of the associated electrical system which produces the measured current or voltage variations.

Unfortunately, our knowledge in each of these categories is far from complete and could well be responsible for the current lack of reliable data. A review of hot-wire data taken in zero pressure gradient, adiabatic or isothermal wall boundary layers illustrates the problem. Figure 1.1 shows data from several sources for the fluctuating axial velocity component. The scatter is so large that it is impossible to construe that any form of similarity with Reynolds or Mach number exists. The picture is even more confusing when the distributions of the other two normal stresses are plotted. Fig. 1.2 shows the measured shear

stress distributions and again no pattern of similarity can be observed. Indeed, only Klebanoff's incompressible measurements (shown for comparison) approach the anticipated limiting value of unity in the wall region. These results give some indication of the deficiencies in the measurement and data reduction assumptions. Unfortunately, many measurements have been with film gages which have doubtful validity for quantitative turbulence measurements, since substrate thermal feedback causes probe sensitivities to be functions of frequency. It is particularly serious and complex for multiple films mounted on the same substrate - the type of probes used for shear stress and normal stress measurement. Even with crossed-wire probes, data interpretation is involved and can be unreliable. For instance, the time-averaged expression for one component of the compressible turbulent shear stress is $-\overline{(\rho v)'u'}$ whereas the hot-wire, after assumption, measures $\overline{(\rho u)'v'}$ which differs by a first-order term. Thus it is clear that systematic investigations of fluctuating velocities are still needed even in zero-pressure gradient, compressible boundary layers to establish a reliable data base for turbulence modeling.

The effects of wind tunnel freestream turbulent flow quality are known to determine model performance in many test cases. But, for decades, wind tunnel testing has mainly been conducted in test section environments which have not been adequately or consistently documented. In general, the effects of dynamic-flow properties on time-averaged model parameters have been largely ignored. Perhaps the major and most widely recognized question is the influence of freestream

disturbances on model boundary-layer transition. Recent developments in boundary-layer transition research, particularly those of the NASA Transition Study Group, have stressed the dominant role that freestream fluctuations have on model boundary-layer stability at transonic and supersonic speeds. Not only do the external fluctuation amplitudes influence transition, but their energy spectra are also particularly significant. Streamwise turbulence also produces fluctuations in dynamic pressure and local Mach number which lead to time-dependent inviscid forces on the model. The normal turbulence components produce fluctuations in the angles of incidence and side slip. It is important, therefore, that we document the dynamic flow quality of the tunnels which are used for advanced aerodynamic testing. In this way, the list of tunnels can be ranked and judgments made as to the meaningful operating ranges of adequate flow quality in each facility relative to each proposed test program. Problems of wind tunnel flow quality have been addressed recently in ref. 3.

The purpose of this report is to address the requirements and pitfalls involved in the use of hot-wire anemometers in high-speed flows and to detail the measurement techniques required in the study of freestream and shear-layer turbulence.

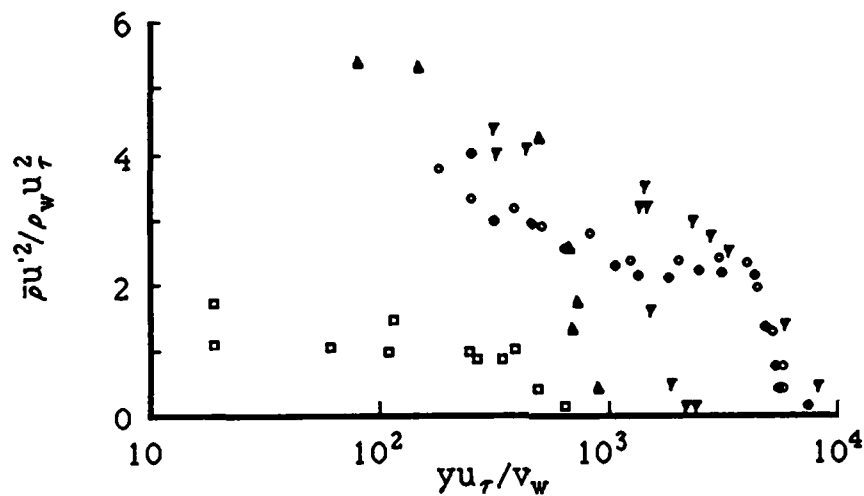


Fig. 1.1 Reynolds normal stress distribution in compressible turbulent boundary layers (ref. 2).

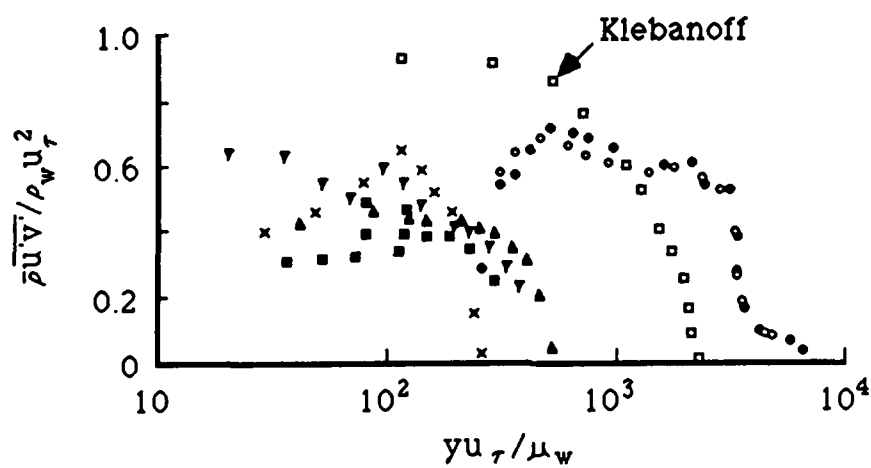


Fig. 1.2 Reynolds shear stress distribution in compressible turbulent boundary layers (ref. 2).

Section 2 Definitions and Descriptive Properties of Turbulence

Turbulence is the usual state of fluid motion except at low Reynolds numbers. It is a three-dimensional irregular flow condition in which the various properties of the fluid show random variations in space and time and in which vortex stretching causes the fluctuations to spread to all wavelengths between a minimum determined by viscosity and a maximum determined by the boundary conditions.

Homogeneous turbulence is statistically independent of position in space but is not necessarily isotropic. Isotropic turbulence is statistically independent of direction, ie., $\overline{u'^2} = \overline{v'^2} = \overline{w'^2}$ and in practice is also homogeneous with $\overline{u'v'} = \overline{v'w'} = \overline{u'w'} = 0$. Scales of turbulence are generally referred to in terms of the dissipating length scale (micro scale) and the energy containing (macro) scales. Wave number is the inverse of wavelength and is defined as the frequency divided by a turbulence velocity, normally the turbulence convection velocity.

Mean square values of fluctuating parameters define their intensity. Probability densities provide information in the amplitude domain. Information on turbulence structure in the space, time and frequency domains can be obtained from auto- and cross-correlation and power spectral density measurements.

The mean square value of a random property is defined as

$$\psi_x^2 = \lim_{T \rightarrow \infty} \frac{1}{T} \int_0^T u^2(t) dt \quad 2.1$$

where ψ_x^2 is the mean square value and the square root ψ is referred to as the root mean square (RMS) value. If we think of the instantaneous value of a fluctuating quantity as a time mean (steady) and a fluctuating (dynamic) component, then $u = \bar{u} + u'$ where the mean value is defined as

$$\mu_x = \lim_{T \rightarrow \infty} \frac{1}{T} \int_0^T u(t) dt \quad 2.2$$

and the variance which is the mean square value about the mean is expressed as

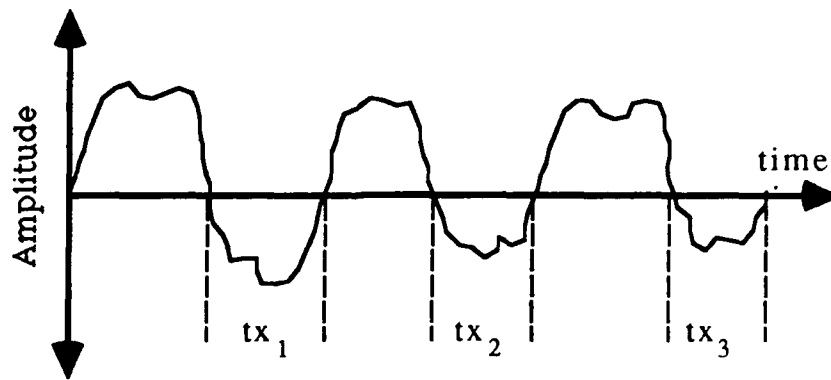
$$\sigma_x^2 = \lim_{T \rightarrow \infty} \frac{1}{T} \int_0^T [u(t) - \mu_x]^2 dt \quad 2.3$$

so that we have

$$\sigma_x^2 = \psi_x^2 - \mu_x^2 \quad 2.4$$

where the positive square root of σ^2 is called standard deviation.

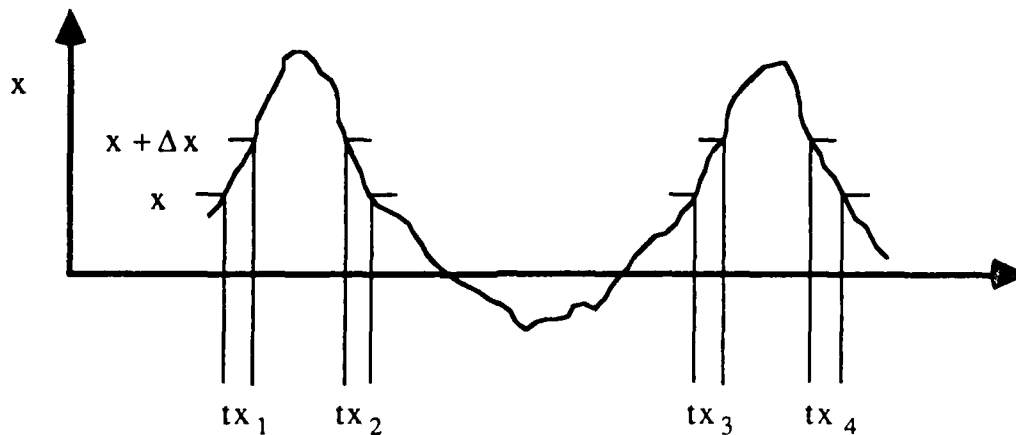
If the variable of interest is random, it can only be defined in terms of its total time history and it must be defined in probabilistic terms. There are two types of probability density function. The amplitude probability function, $[P(x)]$, defines the percentage of the time a property is less than a given threshold level, as shown on the next page.



It is given by

$$\text{Prob} [x(t) \leq x] = P(x) = \lim_{T \rightarrow \infty} \frac{T_x}{T}$$

The complementary distribution function is defined as $1 - P(x)$. The amplitude probability density function $[p(x)]$ defines the percentage of the time a property has a value within a given window width as shown below.



We define the probability that the signal will be in a given window as $p(x)\Delta x$ so that

$$p(x) = \lim_{\Delta x \rightarrow 0} \frac{\text{Prob} [x < x(t) < x + \Delta x]}{\Delta x} = \lim_{\Delta x \rightarrow 0} \lim_{T \rightarrow \infty} \frac{1}{T} \frac{T_x}{\Delta x} \quad 2.5$$

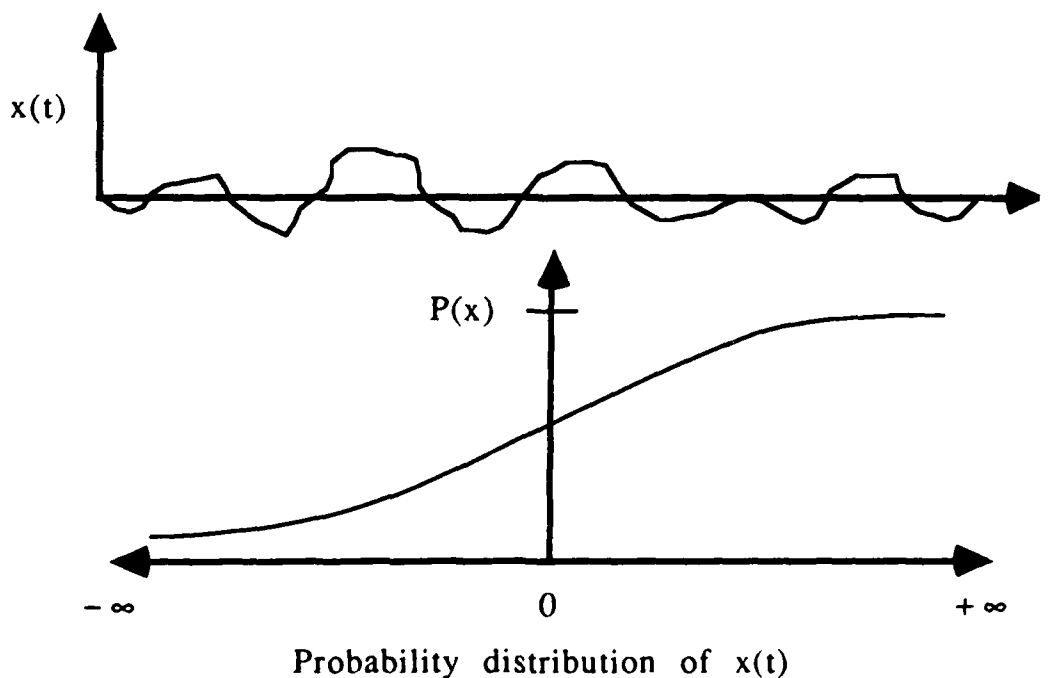
ie. $p(x) = dP(x)/dx$

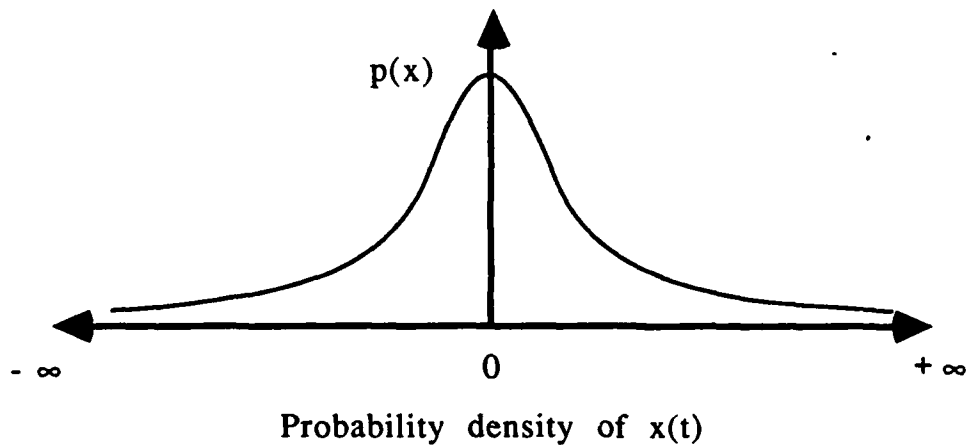
The probability density distribution of a continuous variable, which is the sum of a large number of independent variables, is approximately normal or Gaussian.

$$\text{ie } p(x) = \frac{1}{\sigma\sqrt{2\pi}} e^{-\frac{1}{2\sigma^2}(x-\mu)^2} \quad 2.6$$

Most random processes in nature are Gaussian or have related Maxwell distributions. Unfortunately turbulence is not, since skewness values are not necessarily zero, ie., $u'^2v' \neq 0$ for instance. Turbulence then is the sum of a large number of processes, but they are not quite independent.

Probability densities are used to establish a probabilistic description for the instantaneous values of the data. They are shown below for a signal $x(t)$.





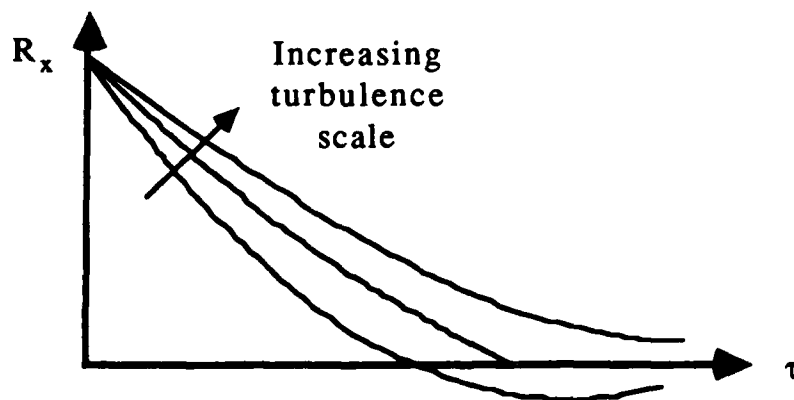
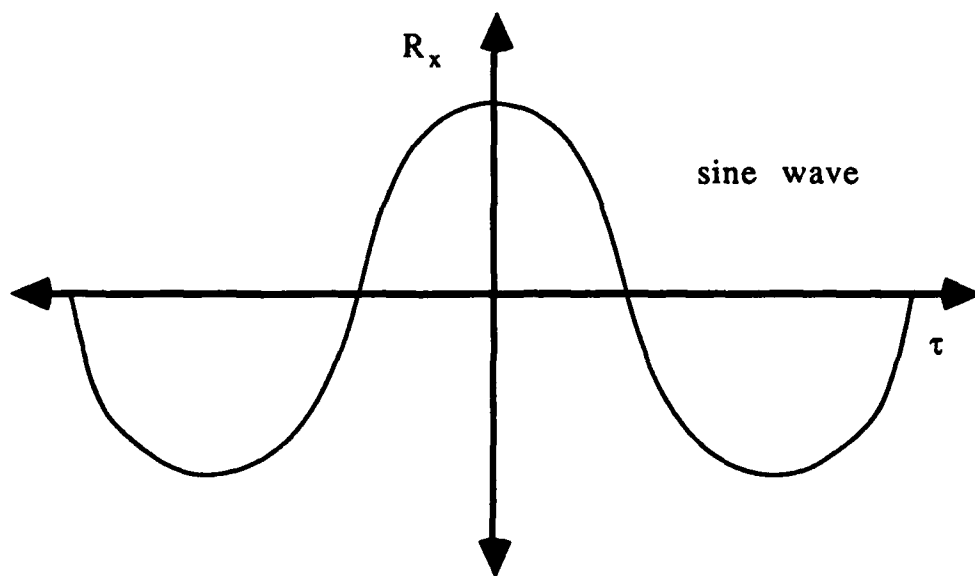
The auto-correlation, or co-variance, describes the general dependence of values of a property between one time and another and is defined as

$$R_x(\tau) = \lim_{T \rightarrow \infty} \frac{1}{T} \int_0^{\infty} x(t) x(t+\tau) dt \quad 2.7$$

The auto-correlation is always a real-valued, even function with a maximum at $\tau = 0$ and may have both positive and negative values so that

$$R_x(-\tau) = R_x(\tau) \text{ and } R_x(0) \geq |R_x(\tau)| \text{ for all } \tau$$

Following are two examples, one for a pure sine wave, the other for turbulence of variable frequency content.



Thus, we can use the auto-correlation to separate coherent from random data and get an idea of the energy-frequency content. The power spectral density function $G_x(f)$ is the Fourier transform of the auto-correlation function. It can also be determined by band-pass filtering and RMS measurement since

$$\psi_x^2 = \int_0^\infty G_x(f) df \quad 2.8$$

The joint probability density may be defined as before, ie.

$$p(x,y) = \lim_{\substack{\Delta x \rightarrow 0 \\ \Delta y \rightarrow 0}} \frac{1}{\Delta x \Delta y} \left[\lim_{T \rightarrow \infty} \frac{T_{xy}}{T} \right] \quad 2.9$$

when x and y are statistically independent.

$$p(x,y) = p(x) p(y) \quad 2.10$$

Cross-correlation measurements can be made with or without time delay

$$R_{xy}(\tau) = \lim_{T \rightarrow \infty} \frac{1}{T} \int_0^T x(t) y(t+\tau) dt \quad 2.11$$

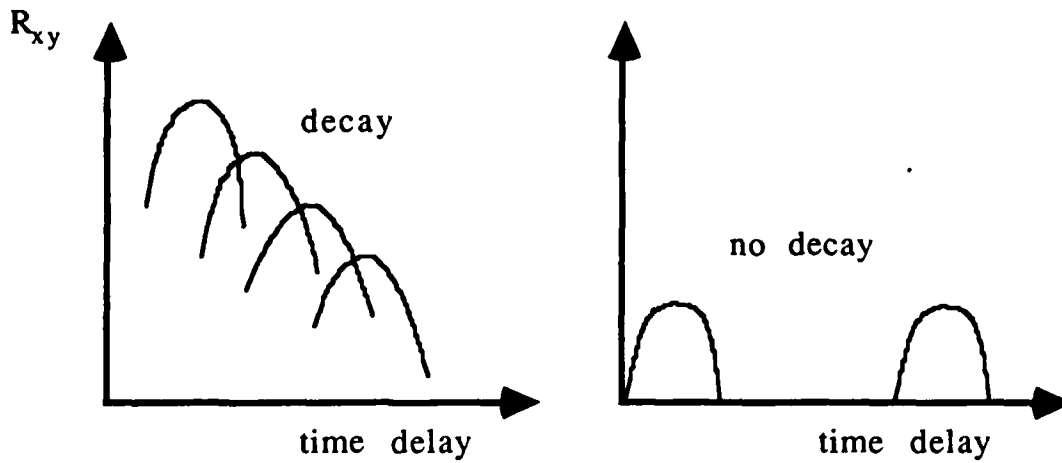
It is not necessarily an even function and $R_{xy}(\tau)$ max is not necessarily at $\tau = 0$. But we can say $R_{xy}(-\tau) = R_{yx}(\tau)$ Also

$$R_x(0)R_y(0) \geq |R_{xy}(\tau)|^2$$

$$1/2[R_x(0) + R_y(0)] \geq |R_{xy}(\tau)|$$

If $R_{xy} = 0$, then $x(t)$ and $y(t)$ are uncorrelated. If $R_{xy} = 0$ for all times, $x(t)$ and $y(t)$ are statistically independent or, if the time average $\neq 0$ then $R_{xy} = \mu_x \mu_y$.

Examples are shown on the next page for frozen and decaying turbulence convection.



As we will see later, the cross-correlation is useful for the determination of convection velocities and determining signal-to-noise ratios.

The cross-spectral density [$G_{xy}(f)$] is the Fourier transformation of cross-correlation. But since R_{xy} is not an even function, $G_{xy}(f)$ is complex and may be written as

$$G_{xy}(f) = C_{xy}(f) - j Q_{xy}(f) \quad 2.12$$

ie.

$$G_{xy}(f) = |G_{xy}(f)| e^{-j \theta_{xy}(f)} \quad 2.13$$

where

$$|G_{xy}| = \sqrt{C_{xy}^2 + Q_{xy}^2} \quad 2.14$$

$$\theta_{xy} = \tan^{-1} \frac{Q_{xy}}{C_{xy}} \quad 2.15$$

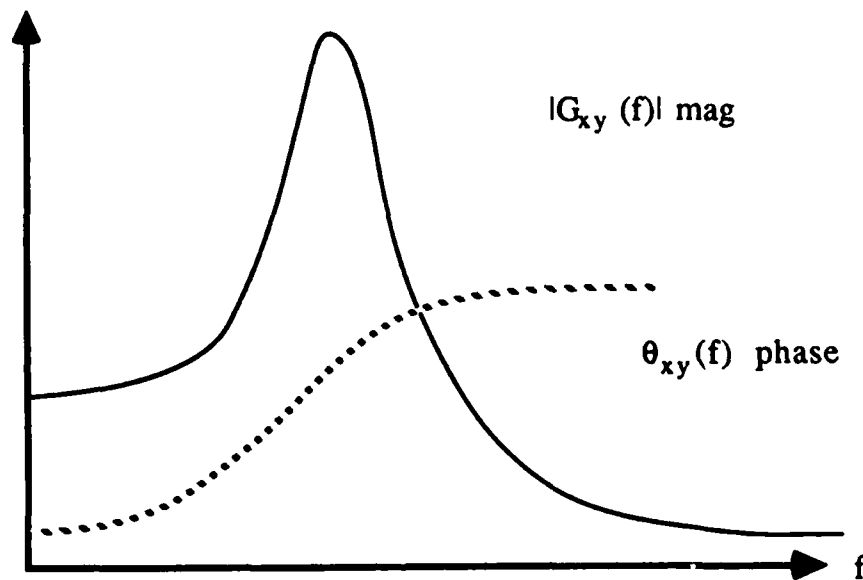
Typical variations of these parameters with frequency are shown in the next figure. A useful relationship is

$$G_x G_y \geq |G_{xy}|^2$$

We generally define the coherence function as

$$\gamma_{xy}^2(f) = \frac{|G_{xy}(f)|^2}{G_x(f) G_y(f)} \leq 1$$

When $\gamma_{xy}^2(f) = 0$ at a given frequency, $x(t)$ and $y(t)$ are incoherent, ie. uncorrelated. Both $x(t)$ and $y(t)$ are statistically independent if $\gamma_{xy}^2(f) = 0$ for all frequencies.



Note also that the time delay $\tau = \theta_{xy}(f)/2\pi f$, so we can determine the time delay as a function of frequency. This provides the relationship between convection velocity and the turbulent scale.

Section 3 Turbulence Measurement Requirements

Most of the measurements required for the definition of turbulent flow fields can be derived by considering the influence of turbulent fluctuations on the overall momentum and energy balances. Consider first the incompressible form of the streamwise momentum equation which may be written as

$$\frac{\partial u}{\partial t} + \frac{\partial u^2}{\partial x} + \frac{\partial uv}{\partial y} + \frac{\partial uw}{\partial z} = -\frac{1}{\rho} \frac{\partial p}{\partial x} + \nu \left(\frac{\partial^2 u}{\partial x^2} + \frac{\partial^2 u}{\partial y^2} + \frac{\partial^2 u}{\partial z^2} \right) \quad 3.1$$

Now if we write $u = \bar{u} + u'$ and noting that $\bar{u} = \overline{u u'} = 0$

$$\text{and that } \frac{\partial(\bar{u} + u')}{\partial x} = \frac{\partial}{\partial x} (\bar{u}^2 + \overline{u'^2} + 2\bar{u}u') = 2\bar{u} \frac{\partial \bar{u}}{\partial x} + \frac{\partial \overline{u'^2}}{\partial x}$$

we obtain

$$\begin{aligned} \frac{\partial \bar{u}}{\partial t} + \bar{u} \frac{\partial \bar{u}}{\partial x} + \bar{v} \frac{\partial \bar{u}}{\partial y} + \bar{w} \frac{\partial \bar{u}}{\partial z} = & -\frac{1}{\rho} \frac{\partial \bar{p}}{\partial x} + \nu \left(\frac{\partial^2 \bar{u}}{\partial x^2} + \frac{\partial^2 \bar{u}}{\partial y^2} + \frac{\partial^2 \bar{u}}{\partial z^2} \right) \\ & - \left(\frac{\partial \overline{u'^2}}{\partial x} + \frac{\partial \overline{u'v'}}{\partial y} + \frac{\partial \overline{u'w'}}{\partial z} \right) \end{aligned} \quad 3.2$$

The last three additional terms have the units of stress and are commonly known as the turbulent or Reynolds shear stresses. These additional stresses are extremely important. If, for example, we have a pipe flow where the velocity fluctuations are $\pm 10\%$ of the mean flow, then the Reynolds stresses are of order $.001\rho u^2$. Since the mean velocity gradient in the pipe is of order u/d then the viscous stress is $\mu(u/d)$. The ratio of turbulent to viscous stress is therefore $.001ud/\mu$. So that, for a pipe flow with a Reynolds number of 100,000, the turbulent stress exceeds the viscous stress by two orders of magnitude.

Thus, it can be seen that turbulent shear stresses are extremely important. The mathematical difficulty in solving the equations of motion for turbulent flow is that they are non-linear; ie., the turbulent fluctuations cannot be superimposed on the mean flow without affecting it. Equations for first order terms involve double correlations and so each equation involves higher order terms. The problem is further complicated by the fact that turbulent cross-correlations (stresses) depend on the phase as well as the magnitude of the two fluctuations.

To determine the turbulent energy balance in a flow we need a relationship for the time rate of change of the individual normal stresses ie.

$$\frac{D \frac{1}{2} \overline{q^2}}{Dt} = \frac{D \frac{1}{2} \overline{u^2}}{Dt} + \frac{D \frac{1}{2} \overline{v^2}}{Dt} + \frac{D \frac{1}{2} \overline{w^2}}{Dt} \quad 3.3$$

where

$$\frac{D}{Dt} = \frac{\partial}{\partial t} + \bar{u} \frac{\partial}{\partial x} + \bar{v} \frac{\partial}{\partial y} + \bar{w} \frac{\partial}{\partial z}$$

To determine this relationship we substitute $u = \bar{u} + u'$ in the equation of motion and multiply each term by u' .

$$\text{Thus } \frac{\partial u}{\partial t} = u' \frac{\partial \bar{u}}{\partial t} + u' \frac{\partial u'}{\partial t} = \frac{\partial \frac{1}{2} \overline{u'^2}}{\partial t}$$

and

$$\begin{aligned} u' \frac{\partial u}{\partial x} &= u' \bar{u} \frac{\partial u'}{\partial x} + u'^2 \frac{\partial \bar{u}}{\partial x} + u'^2 \frac{\partial u'}{\partial x} + u' \bar{u} \frac{\partial \bar{u}}{\partial x} \\ &= \bar{u} \frac{\partial \frac{1}{2} \overline{u'^2}}{\partial x} + \overline{u'^2} \frac{\partial \bar{u}}{\partial x} + \overline{u'^2 \frac{\partial u'}{\partial x}} \end{aligned} \quad 3.4$$

Continuing in this manner and collecting terms we obtain

$$\begin{aligned} \frac{D \frac{1}{2} \overline{u'^2}}{Dt} = & -\frac{1}{\rho} \overline{u' \frac{\partial p'}{\partial x}} + \nu \overline{u' \nabla^2 u'} - \left(\overline{u'^2 \frac{\partial \bar{u}}{\partial x}} + \overline{u' v'} \frac{\partial \bar{u}}{\partial y} + \overline{u' w'} \frac{\partial \bar{u}}{\partial z} \right) \\ & - \left(\overline{u'^2 \frac{\partial u'}{\partial x}} + \overline{u' v' \frac{\partial u'}{\partial y}} + \overline{u' w' \frac{\partial u'}{\partial z}} \right) \end{aligned} \quad 3.5$$

where the first three groups on the RHS represent the spatial transport of turbulent energy by local pressure gradient fluctuations, the viscous dissipation of turbulent kinetic energy and production terms ie. rate of mean work against turbulence. The last group may be rewritten using continuity as

$$-\frac{1}{2} \left(\frac{\partial \overline{u'^3}}{\partial x} + \frac{\partial \overline{u'^2 v'}}{\partial y} + \frac{\partial \overline{u'^2 w'}}{\partial z} \right)$$

and so represents the spatial transport of $\overline{u'^2}/2$ by turbulence. Thus, we have a balance for the turbulence energy in a flow which involves production, dissipation, and convection, where the production term represents an extraction of energy from the mean flow.

In boundary layer flows we can make the approximations

$$\frac{\partial}{\partial z} = 0, \quad \frac{\partial \bar{u}}{\partial x} \ll \frac{\partial \bar{u}}{\partial y}, \quad \text{and } \bar{u} \gg \bar{v}$$

so that the continuity and Navier Stokes equations reduce to the following forms:

$$\frac{\partial \bar{u}}{\partial x} + \frac{\partial \bar{v}}{\partial y} = 0 \quad 3.6$$

and

$$\bar{u} \frac{\partial \bar{u}}{\partial x} + \bar{v} \frac{\partial \bar{u}}{\partial y} = -\frac{1}{\rho} \frac{\partial \bar{p}}{\partial x} + \nu \frac{\partial^2 \bar{u}}{\partial y^2} - \frac{\partial \overline{u' v'}}{\partial y} - \frac{\partial \overline{u'^2}}{\partial x} \quad 3.7$$

Since the normal mean momentum equation may be written as

$$\bar{p} = \bar{p}_\infty - \frac{\rho \overline{v'^2}}{2} \quad 3.8$$

$$\text{where } \bar{p}_\infty + \frac{\rho u^2}{2} = \text{const}$$

we obtain

$$\bar{u} \frac{\partial \bar{u}}{\partial x} + \bar{v} \frac{\partial \bar{u}}{\partial y} = u_\infty \frac{\partial u_\infty}{\partial x} + \nu \frac{\partial^2 \bar{u}}{\partial y^2} - \frac{\partial \overline{u'v'}}{\partial y} - \frac{\partial}{\partial x} (\overline{u'^2} - \overline{v'^2}) \quad 3.9$$

Thus, we can solve for \bar{u} and \bar{v} only if the turbulence terms are known and/or can be modeled. Normally we may assume that $(\partial/\partial x)(\overline{u'^2} - \overline{v'^2})$ is negligible except near separation.

For turbulence modeling purposes, it is usual to divide the boundary layer into two regions, an outer and inner layer. The outer layer contains 80% of the flow, the inner layer also contains the viscous sub-layer. Mixing length models relate the local shear stress to a mean velocity gradient by means of a turbulence length scale or mixing length

$$-\overline{u'v'} = L^2 \left| \frac{\partial \bar{u}}{\partial y} \right|^2 \quad 3.10$$

where for the inner region $L = K_1 y$ with $K_1 = 0.4$

However, in the viscous sub-layer close to the wall, we must account for turbulence damping so a "damping factor" (A) is included such that

$$L = K_1 y \left[1 - \exp\left(-\frac{y}{A}\right) \right] \quad 3.11$$

where (A) is a strong function of local wall boundary conditions

$$\text{ie. } A = 26 \nu \left(\frac{\tau_w}{\rho} \right)^{\frac{1}{2}} \quad 3.12$$

so that (A) approaches zero outside the sub-layer.

In the outer region it is usual to assume

$$-\overline{u'v'} = K_2 \rho \bar{u}_\infty \delta^* \left| \frac{\partial u}{\partial y} \right| \quad 3.13$$

In locations where boundary layer edge intermittency is present we multiply this expression by an intermittency factor

$$\gamma = \frac{1 - \text{erf} \left[5 \left(\frac{y}{\delta} \right) - 0.78 \right]}{2} \quad 3.14$$

The major objection to the mixing length hypothesis is that it is based on the local mean velocity gradient. But, we know that turbulent length scales and lifetimes are many boundary layer thicknesses, so we cannot assume that turbulence properties are uniquely related to local mean profiles. We must account for mean flow history and turbulence convection.

Other models relate the turbulent shear stress to turbulent kinetic energy ie. $-\overline{u'v'} = kq^2$, where k is taken to be 0.3. This assumed proportionality once again has only limited validity. Along the axis of a pipe, for example, the stress is zero but the turbulence energy is not. In practice, therefore, only external boundary-layer flows can be predicted. It cannot be applied to wakes, wall jets or natural-convection boundary layers since, in these flows the shear stress changes sign whereas the turbulence energy cannot.

Thus we need to determine the types of measurements which will be required to help in turbulence modeling. As a first step, let us determine the mean flow kinetic energy equation in boundary layer form. To achieve this we must use $u = \bar{u} + u'$ and multiply by \bar{u} . So that for the case of zero pressure gradient

$$\bar{u} \frac{\partial \bar{u}}{\partial x} + \bar{v} \frac{\partial \bar{u}}{\partial y} = \nu \frac{\partial^2 \bar{u}}{\partial y^2} \quad 3.15$$

becomes

$$\bar{u} \frac{\partial \frac{1}{2} \bar{u}^2}{\partial x} + \bar{v} \frac{\partial \frac{1}{2} \bar{u}^2}{\partial y} - \overline{u'v'} \frac{\partial \bar{u}}{\partial y} + \frac{\partial}{\partial y} (\overline{u'v' \bar{u}}) = 0 \quad 3.16$$

The first two terms represent the gain due to advection ie. mean energy transport. The third and fourth terms represent the loss due to turbulence production and the gain due to energy flux. In boundary layer flow there is a loss of mean flow kinetic energy over most of the layer except near the wall. The loss in the outer region is due to transfer to the inner layer by means of the Reynolds stress gradient. For flows with pressure gradient the term $\bar{u} \partial(\overline{u'^2}/2)/\partial x$, a term dropped in the above derivation, cannot be neglected. So we can see that, in general, the mean flow energy balance involves expressions for the rate of change of turbulence kinetic energy and shear stress. Derivation of these expressions will give an indication of the required measurements.

To derive the equation for the rate of change of turbulence kinetic energy we insert $u = \bar{u} + u'$ in the boundary layer momentum equation, multiply the result by u' and take the time average. This results in

$$\begin{aligned} \frac{D \frac{1}{2} q^2}{Dt} &= \frac{1}{2} \left(\bar{u} \frac{\partial q^2}{\partial x} + \bar{v} \frac{\partial q^2}{\partial y} \right) \\ &= -\bar{u}'\bar{v}' \frac{\partial \bar{u}}{\partial y} - \left(\frac{\partial}{\partial y} [v'(p' + q^2)] + \epsilon \right) \end{aligned} \quad 3.17$$

where we can see that the convection of turbulence energy by the mean flow is the balance between the turbulence energy produced by the mean motion working against the turbulence shear stress and the turbulence energy diffusion and viscous dissipation (ϵ).

Finally, the rate of change of Reynolds shear stress may be derived by inserting $u = \bar{u} + u'$ into the boundary layer momentum equation, and multiplying the result by v' and taking the time average. Thus we obtain:

$$\begin{aligned} \frac{D \overline{u'v'}}{Dt} &= - \left[\overline{v'^2} \frac{\partial \bar{u}}{\partial y} + \frac{\partial}{\partial y} \overline{u'v'^2} \right] - \frac{1}{\rho} \left[\frac{\partial \overline{p'u'}}{\partial y} + \frac{\partial \overline{p'v'}}{\partial x} \right] \\ &+ \overline{p' \left[\frac{\partial u'}{\partial y} + \frac{\partial v'}{\partial x} \right]} + \nu \left[\overline{u'\nabla^2 v'} + \overline{v'\nabla^2 u'} \right] \end{aligned} \quad 3.18$$

where the rate of change of Reynolds shear stress is the balance between shear stress diffusion, pressure diffusion, pressure scrambling and viscous dissipation.

If heat transfer is present, by analogy with the mean enthalpy equation, we determine that

$$\begin{aligned} \frac{D \frac{1}{2} \overline{\theta'^2}}{Dt} &= \frac{k}{\rho c_p} \overline{\theta'\nabla^2 \theta'} - \left[\overline{u'\theta'} \frac{\partial \bar{\theta}}{\partial x} + \overline{v'\theta'} \frac{\partial \bar{\theta}}{\partial y} \right] \\ &- \frac{1}{2} \left[\frac{\partial \overline{u'\theta'^2}}{\partial x} + \frac{\partial \overline{v'\theta'^2}}{\partial y} \right] \end{aligned} \quad 3.19$$

where we can see that the rate of change of enthalpy function depends on the conductive diffusion, production and turbulent transport respectively.

By analogy with the Reynolds shear stress equation we can derive

$$\begin{aligned} \frac{D\overline{v'\theta'}}{Dt} = & -\frac{1}{\rho} \overline{\theta' \frac{\partial p'}{\partial y}} + \frac{k}{\rho c_p} \overline{v' \nabla^2 \theta'} + \nu \overline{\theta' \nabla^2 v'} \\ & - \left(\overline{u'\theta' \frac{\partial v}{\partial x}} + \overline{v'\theta' \frac{\partial v}{\partial y}} \right) - \left(\overline{u'v'} \frac{\partial \bar{\theta}}{\partial x} + \overline{v'^2} \frac{\partial \bar{\theta}}{\partial y} \right) \\ & - \left(\frac{\partial \overline{u'v'\theta'}}{\partial x} + \frac{\partial \overline{v'^2 \theta'}}{\partial x} \right) \end{aligned} \quad 3.20$$

In this case we have two sets of molecular dissipative terms and two sets of production terms.

Eddy conductivity may be expressed as

$$k_T = -\rho c_p \frac{\overline{v'\theta'}}{\frac{\partial \bar{\theta}}{\partial y}} \quad 3.21$$

so that the turbulent Prandtl number becomes

$$Pr_T = \frac{\epsilon c_p}{k_T} = \frac{\overline{u'v'}}{\overline{v'\theta'}} \frac{\frac{\partial \bar{\theta}}{\partial y}}{\frac{\partial \bar{u}}{\partial y}} \quad 3.22$$

In most cases the turbulent Prandtl number is assumed equal to unity inferring that heat and momentum are transferred by the same processes. However, measurements (ref. 4) indicate significant variations can occur across shear layers. A curve fit to these data suggests the form

$$\text{Pr}_T = 0.95 \left[1 - 0.5 \left(\frac{y}{\delta} \right) \right] \quad 3.23$$

Now, all these previous equations express the rate of change not the magnitude of the turbulence kinetic energy, shear stress and turbulent heat transfer. The local magnitude depends on the integral along the length of a streamline. To get some idea of the length scales of turbulent motion, we can study spatial and space-time correlations.

From the turbulence modeling viewpoint, information on the turbulence scales and lifetimes are also of crucial importance. Since turbulent flows vary not only in time but also in space, their investigation must involve an examination of both the spatial and temporal statistical structure. Space-time correlations can make a contribution to this study since they give evidence of the heredity and structure of turbulence, as well as values of the convection velocities of the vorticity and entropy modes compared with the average mass transport velocities. Examples of both auto and space-time correlations in a compressible turbulent boundary layer are given in figs. 3.1 and 3.2. These data were obtained on a cone-ogive-cylinder model in the Ames 3.5-ft. wind tunnel (ref. 5). Fig. 3.1 shows the auto-correlation of the fluctuating signals on the cylindrical portion of the model 176 cm from the cone apex, at two positions in the turbulent boundary layer and in the far field. It can be seen that there is a marked variation of energy distribution with frequency across the boundary layer and that, as expected, the far field contains proportionately much less energy in the high wave number range than the wall region. The results of a series of filtered (4 kHz)

cross-correlation measurements at several wire separation distances in the boundary layer are shown in fig. 3.2. It can be seen that each cross-correlation curve reaches a maximum at a non-zero value of the time delay, clearly indicating the presence of convection. The amplitude of this maximum is a function of the wire separation distance. A convection velocity of these disturbances may be determined from the time delay at which the maximum of a particular cross-correlation occurs.

The peaks of the cross-correlation obtained for various values of wire separation distance represent the auto-correlation in a reference frame moving with disturbances. They are, therefore, a measure of the lifetime of the disturbance pattern as it is swept along with the mean flow. The long turbulence lifetimes which can be inferred from these space-time correlation measurements (ref. 5) illustrate a major objection to turbulence models based on local mean flow gradients. It cannot be assumed that turbulence is uniquely related to local conditions, and flow history must be considered, especially when attempting to calculate non-equilibrium flows.

To conclude, we can list some of the measurement requirements for the definition of turbulent flow fields. These requirements include:

- 1) Measurements of the spatial and temporal distributions of turbulence, kinetic energy and shear stress.
- 2) Determination of the rates at which these properties are produced, transported and dissipated.
- 3) Determination, from spectra or correlation measurements, of the

contribution of different length scales to the turbulence kinetic energy and shear stresses.

4) The rate at which Reynolds stress and turbulence kinetic energy are transferred from one range of eddy sizes to another.

5) Components of the viscous dissipation from point time histories, assuming Taylor's hypothesis holds, ie.

$$\left(\frac{\partial u}{\partial x}\right)^2 = \frac{1}{\bar{u}^2} \left(\frac{\partial u}{\partial t}\right)^2 \quad 3.24$$

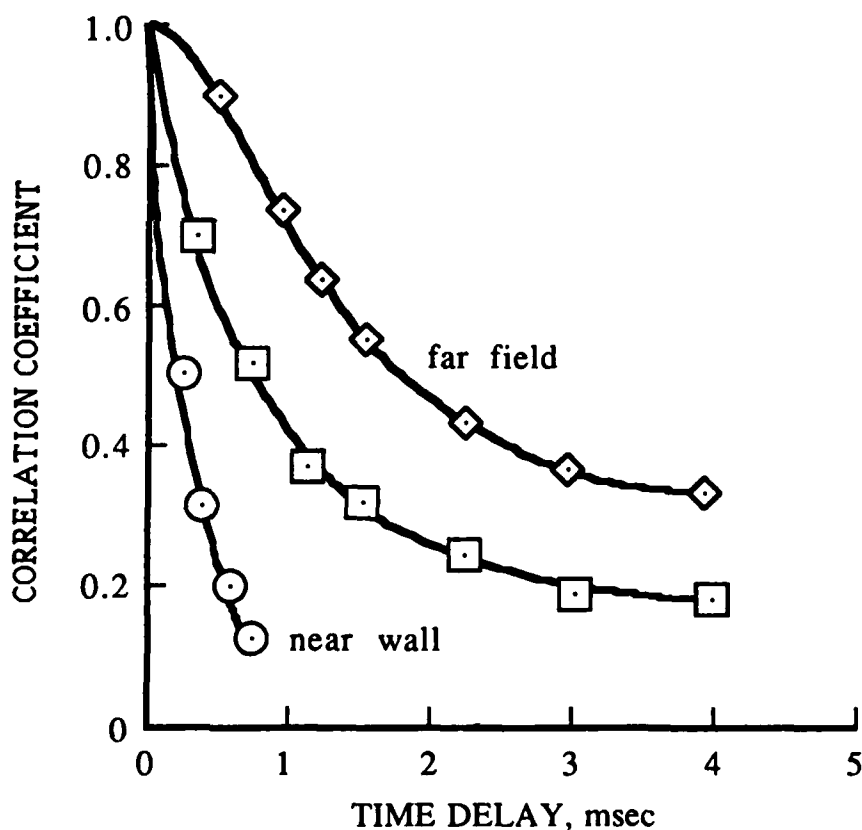


Fig. 3.1 Auto-correlations across a compressible turbulent boundary layer (ref. 5).

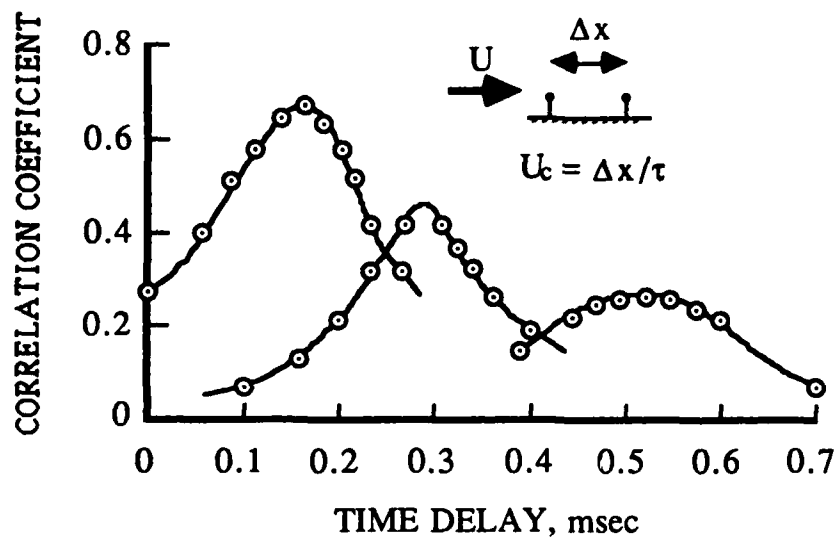


Fig. 3.2 Space-time cross-correlation measurements in a compressible turbulent boundary layer (ref. 5).

Section 4 The Measurement of Turbulent Fluctuations

A hot-wire can be assumed to be a cylinder placed in a flow field for the purpose of making certain types of flow field measurements. The wire is assumed to have length L and a diameter d . Furthermore, we assume that the wire temperature is T_w and if we take a heat balance we note that

$$W - Q_r - Q_c - H_w = 0 \quad 4.1$$

where

- W = the energy (electrical) put into the wire.
- Q_r = Heat loss due to radiation.
- Q_c = Heat loss due to conduction.
- H_w = Heat loss due to convection.

If we assume that there is no heat loss due to radiation, or conduction to the supports, then equation 4.1 can be expressed as $W = H_w$. In incompressible flow numerous hot-wire heat transfer studies show that

$$Nu = \lambda d / k_f = 0.42Pr^{0.2} + 0.57Pr^{0.33}Re^{0.5} \quad 4.2$$

Equation (4.2) is applicable in air and diatomic gases when $0.1 < Re < 1000$, where $Re = \rho_g u d / \mu_g$ and Pr, ρ, μ are evaluated at the film temperature $T_F = (T_w + T_g)/2$. Free convection effects may be neglected if $Gr \times Pr < 10^{-4}$ and $Re > 0.5$. For a 5-micron wire, in high-speed airflows, $Gr \times Pr \approx 10^6$ and the Reynolds number based on wire diameter is generally $\gg 0.5$.

Since, the heat transferred from a wire of length L is $\lambda \pi d L (T_w - T_g) = I^2 R_w$, we may rewrite equation 4.2 as

$$\pi k_f L (T_w - T_g) [0.42 Pr^{0.2} + 0.57 Pr^{0.33} Re^{0.5}] = I^2 R_w \quad 4.3$$

Now, $R_w = R_o [1 + \alpha(T_w - T_o) + \gamma(T_w - T_o)^2 + \dots]$ and neglecting higher order terms, $T_w - T_g = (R_w - R_g)/\alpha R_o$ so that

$$I^2 R_w = \pi k_f L \left(\frac{R_w - R_g}{\alpha R_o} \right) [0.42 Pr^{0.2} + 0.57 Pr^{0.33} Re^{0.5}] \quad 4.4$$

ie

$$\frac{I^2 R_w}{R_w - R_g} = A + B \sqrt{u} \quad 4.5$$

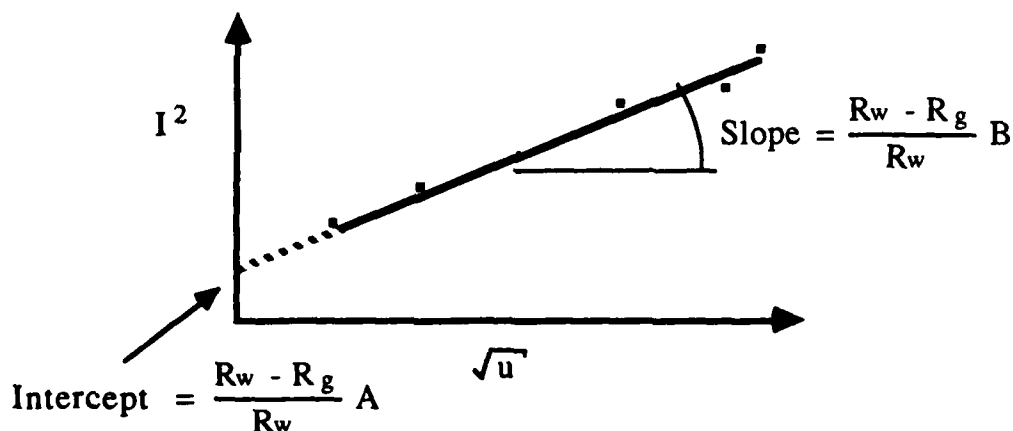
where

$$A = 0.42 \frac{\pi k_f L}{\alpha R_o} Pr^{0.2} \quad 4.6$$

and

$$B = 0.57 \frac{\pi k_f L}{\alpha R_o} Pr^{0.33} \left(\frac{\rho_f d}{\mu} \right)^{0.5} \quad 4.7$$

We can determine A and B experimentally by plotting I^2 vs. \sqrt{u} for constant electrical resistance as shown below.

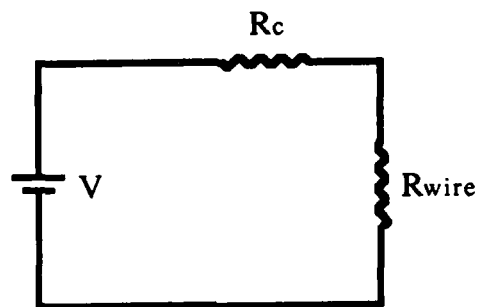


Now let us consider the unsteady heat transfer from a wire in a turbulent flow field where we have $u = \bar{u} + u'$, $R_w = \bar{R}_w + r_w$. If the sensor is made

part of the constant current circuit system shown on the next page. If we assume $u'/u \ll 1$ so that $r_w/(R_w - R_g) \ll 1$ equation 4.5 may then be written as

$$\frac{I^2 R_w}{\bar{R}_w - R_g} \left(1 + \frac{r_w}{\bar{R}_w}\right) \left(1 - \frac{r_w}{R_w - R_g}\right) = A + B \sqrt{u} \left(1 + \frac{1}{2} \frac{u}{\bar{u}}\right) \quad 4.8$$

Constant Current System



$$R_c \gg R_{\text{wire}} \text{ so that } I = \frac{V}{R_c + R_{\text{wire}}} \approx \frac{V}{R_c}$$

or since

$$\frac{I^2 \bar{R}_w}{\bar{R}_w - R_g} = A + B \sqrt{u} \quad 4.9$$

we have

$$-\frac{I^2 \bar{R}_w}{(\bar{R}_w - R_g)^2} \approx B \sqrt{u} \frac{u}{2\bar{u}}$$

so that

$$e = I r_w = -\frac{(\bar{R}_w - R_g)^2}{2I R_g} B \sqrt{u} \frac{u}{\bar{u}} \quad 4.10$$

ie

$$\sqrt{e^2} = s \sqrt{u^2}$$

where

$$s = \frac{(\bar{R}_w - R_g)^2}{2IR_g} \frac{B \sqrt{U}}{U}$$

and $e = -su$. Equation 4.10 applies only in absence of thermal inertia of the wire, cooling effects of the supports and non-uniform velocity distribution along the wire.

Let us first consider the effects of thermal inertia and rewrite the energy balance to account for the heat capacity of the entire wire, C_w , as

$$I^2 R_w = (R_w - R_g)(A + B \sqrt{U}) + \rho_w c_w \frac{\pi d^2}{4} L \frac{dT_w}{dt} \quad 4.11$$

where c_w is the specific heat of the wire.

Perturbing this equation and cancelling the steady state terms gives

$$I^2 r_w = (A + B \sqrt{U}) r_w + (R_w - R_g) B \sqrt{U} \frac{U}{U} + \frac{C_w}{\alpha_g R_g} \frac{dr_w}{dt} \quad 4.12$$

where

$$C_w = \rho_w c_w \frac{\pi d^2}{4} L \quad 4.13$$

or

$$\frac{dr_w}{dt} + \frac{1}{M} r_w = \phi(t) \quad 4.14$$

where

$$M = \frac{C_w}{\alpha_g R_g [(A + B \sqrt{U}) - I^2]} \quad 4.15$$

and

$$\phi(t) = \frac{\alpha_g R_g (R_w - R_g) B \sqrt{u}}{2 C_w} \quad 4.16$$

But from the mean heat balance

$$A + B\sqrt{U} - I^2 = \frac{R_g}{R_w - R_g} I^2 \quad 4.17$$

therefore

$$M = \frac{C_w (R_w - R_g)}{I^2 \alpha_g R_g} \quad 4.18$$

The solution of equation 4.14 is obtained as follows. Let $(\rho r_w) = \lambda(t)$ and

$$\beta r_w = \int_{-\infty}^t \lambda(t) dt$$

$$\therefore \beta \frac{dr_w}{dt} + r_w \frac{d\beta}{dt} = \lambda(t) \quad 4.19$$

$$\therefore \frac{1}{\beta} \frac{d\beta}{dt} = \frac{1}{M} \quad \lambda(t) = \phi(t)\beta \quad \log \beta = \frac{t}{M}$$

$$\therefore \beta = e^{\left(\frac{t}{M}\right)}$$

$$\therefore r_w = \int_{-\infty}^t e^{-\left(\frac{t}{M}\right)} \phi(\tau) e^{-\left(\frac{\tau}{M}\right)} d\tau \quad 4.20$$

$$= \int_{-\infty}^t \phi(\tau) \exp\left[-\frac{1}{M}(t-\tau)\right] d\tau$$

Thus if $u(t) = u^* e^{i\omega t}$ where u^* represents a velocity amplitude, then

$$\phi(t) = \phi^* e^{i(\omega t - \pi)} \quad 4.21$$

where

$$\phi^* = \frac{\alpha R_o (\bar{R}_w - R_g) B \sqrt{u}}{C_w} \frac{u^*}{2\bar{u}} = \frac{(\bar{R}_w - R_g)^2 B \sqrt{u}}{M I^2 R_g} \frac{u^*}{2\bar{u}} \quad 4.22$$

Equation 4.20 then gives

$$r_w = -\phi^* M \frac{e^{i\omega t}}{1 + i\omega M} = r_w^* e^{i(\omega t - \psi)} \quad 4.23$$

where

$$r_w^* = \frac{-\phi^* M}{\sqrt{1 + \omega^2 M^2}}$$

and

$$\psi = \tan^{-1}(\omega M)$$

If we take $e = -su$ where s is the velocity sensitivity then we can see that thermal inertia affects both the amplitude and phase of the hot-wire response ie.

$$s = \frac{e^{-i\psi}}{\sqrt{1 + \omega^2 M^2}} s_{NTI} \quad 4.24$$

where NTI denotes no thermal inertia. This shows that both phase shifts and amplitude variations are functions of the frequency of the velocity fluctuation. M is defined as the time constant and $\omega_0 = 1/M$ is called the roll-off frequency. The time constant is a strong function of wire diameter and mass flux. Take, for example, a 5 micron tungsten wire in a turbulent flow of 30 m/sec, with $T_w - T_g = 115^\circ\text{C}$, $T_g = 288^\circ\text{K}$, and $I \approx 76$ mA, the wire time constant is approximately 3×10^{-4} sec and the signal amplitude at 250 Hz is

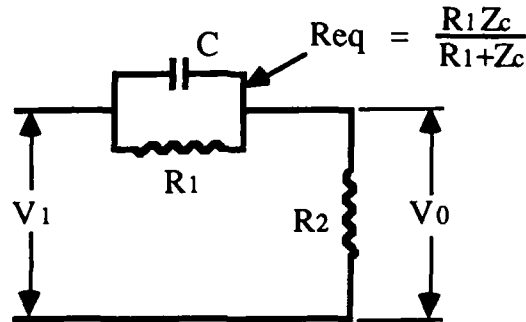
$$\frac{s}{s_{NTI}} = \frac{1}{\sqrt{1 + 9 \times 10^{-8} (2\pi \times 250)^2}} = \frac{1}{\sqrt{1 + 2.2}} = \frac{1}{1.1055}$$

so that the signal has already dropped down 10% at very low frequencies. The signal phase angle, which may be calculated from

$$\phi = \tan^{-1}(-\omega M) = \tan^{-1}(2\pi \times 250 \times 3 \times 10^{-4}) = \tan^{-1}(0.47) \quad 4.25$$

shows that there is a 25-deg. phase lag at 250 Hz. Thus it is crucial that we compensate for these effects.

A typical compensation circuit is shown below



An analysis of this circuit gives

$$I = \frac{V_1}{R_{eq} + R_2} \quad 4.26$$

$$\therefore V_0 = \frac{V_1 R_2}{R_{eq} + R_2} = \frac{V_1}{1 + \frac{R_{eq}}{R_2}} = \frac{V_1}{\left(1 + \frac{R_1 Z_c}{R_1 R_2 + R_2 Z_c}\right)} \quad 4.27$$

Now again assume $u = \bar{u} + u'$, $R_w = \bar{R}_w + r_w$, $T_w = \bar{T}_w + t_w$ and since

$$T_w - T_g = \frac{R_w - R_g}{\alpha_g R_g} \quad 4.28$$

so that $r_w = R_0 \alpha t_w$. On substitution in equation 4.11 we obtain

$$I^2 \bar{R}_w + I^2 r_w = (R_w + r_w - R_g) \left[A + B \sqrt{\bar{u}} \left(1 + \frac{1}{2} \frac{u}{\bar{u}} \right) \right] + \frac{C_w}{\alpha_g R_g} \frac{dr_w}{dt} \quad 4.29$$

Since

$$I^2 \bar{R}_w = (A + B \sqrt{\bar{u}}) (R_w - R_g) \quad 4.30$$

neglecting higher order terms we obtain

$$I^2 r_w = (A + B\sqrt{u}) r_w + (R_w - R_g) B\sqrt{u} \frac{u}{2\bar{u}} + \frac{C_w}{\alpha_g R_g} \frac{dr_w}{dt} \quad 4.31$$

where the wire phase and amplitude characteristics may be written as

$$\phi(t) = \frac{-\alpha R_o (\bar{R}_w - R_g) B\sqrt{u} u}{C_w 2\bar{u}} \quad 4.32$$

and

$$M = \frac{C_w}{\alpha R_o [I^2 + (A + B\sqrt{u})]} \quad 4.33$$

Or, since

$$A + B\sqrt{u} - I^2 = \frac{R_g}{\bar{R}_w - R_g} I^2$$

$$M = \frac{C_w (\bar{R}_w - R_g)}{\alpha I^2 R_o R_g} \quad 4.34$$

Now the relationship between the circuit input and output voltages may be expressed as

$$\begin{aligned} \frac{V_o}{V_i} &= \frac{R_1 R_2 + R_2 Z_c}{R_1 R_2 + R_2 Z_c + R_1 Z_c} = \frac{R_2}{R_1} \left[\frac{R_1 + Z_c}{Z_c + R_2 + \frac{R_2}{R_1} Z_c} \right] \\ &= \frac{R_2}{R_1} \left[\frac{1 + \frac{R_1}{Z_c}}{1 + \frac{R_2}{R_1} + \frac{R_2}{Z_c}} \right] = \frac{R_2}{R_1} \left[\frac{1 + j\omega R_1 C}{\left(1 + \frac{R_2}{R_1}\right) + j\omega R_2 C} \right] \\ &= \frac{R_2}{R_1} \frac{\sqrt{1 + \omega^2 R_1^2 C^2} e^{j \tan^{-1}(\omega R_1 C)}}{\sqrt{\left(1 + \frac{R_2}{R_1}\right)^2 + \omega^2 R_2^2 C^2} e^{j \tan^{-1}\left(\frac{\omega R_2 C}{1 + \frac{R_2}{R_1}}\right)}} \quad 4.35 \end{aligned}$$

so that

$$\frac{V_0}{V_1} = \frac{R_2}{R_1} \sqrt{\frac{1 + \omega^2 R_1^2 C^2}{\left(1 + \frac{R_2}{R_1}\right)^2 + \omega^2 R_2^2 C^2}} e^{j \tan^{-1} \psi'} \quad 4.36$$

Clearly then we can match for the hot-wire amplitude roll off if,

$$\sqrt{1 + \omega^2 M^2} = \sqrt{\frac{1 + \omega^2 R_1^2 C^2}{\left(1 + \frac{R_2}{R_1}\right)^2 + \omega^2 R_2^2 C^2}} \quad 4.37$$

Now defining $\omega'_0 = 1/R_1 C$ and $\omega_0 = 1/M$ for the hot-wire, for amplitude compensation we have

$$1 + \left(\frac{\omega}{\omega_0}\right)^2 = \frac{1 + \left(\frac{\omega}{\omega'_0}\right)^2}{\left(1 + \frac{R_2}{R_1}\right)^2 + \left(\frac{R_2}{R_1}\right)^2 \left(\frac{\omega}{\omega'_0}\right)^2} \quad 4.38$$

and the circuit phase angle

$$\psi' = \frac{\frac{\omega}{\omega_0} - \left(\frac{\frac{R_2}{R_1} \frac{\omega}{\omega_0}}{1 + \frac{R_2}{R_1}}\right)}{1 + \left(\frac{\omega}{\omega_0}\right) \left(\frac{\frac{R_2}{R_1} \frac{\omega}{\omega_0}}{1 + \frac{R_2}{R_1}}\right)} = \frac{\frac{\omega}{\omega_0}}{1 + \left(\frac{R_2}{R_1}\right) \left[1 + \left(\frac{\omega}{\omega'_0}\right)^2\right]} = \phi \quad 4.39$$

for hot-wire phase correction.

In an actual compensating circuit, the capacitance must be a variable as the wire time constant depends on both overheat and mass flow (ρu).

Usually $R_2 \ll R_1$ (say 1/1000) so that

$$\begin{aligned} \text{at } \omega = 0 \quad \frac{V_0}{V_1} &\approx \frac{R_2}{R_1} \\ \text{and for } \omega \rightarrow \infty \quad \frac{V_0}{V_1} &\rightarrow 1 \end{aligned} \quad 4.40$$

The point on the curve where V_0/V_1 flattens off is $\omega/\omega_0 = R_2/R_1$ or $\omega = 1/CR_2$ so that variable capacitance provides for adjustable limiting frequency compensation but the overall gain is fixed at R_2/R_1 . For variable R_1 , the frequency at which compensation is correct is fixed at $\omega_{\text{comp}} = 1/CR_2$ and the overall gain changes with R_1 . Since it can be shown that

$$\frac{d\psi'}{d\left(\frac{\omega}{\omega_0}\right)} \propto 1 + \frac{R_2}{R_1} \left(1 + \left(\frac{\omega}{\omega_0}\right)^2\right)$$

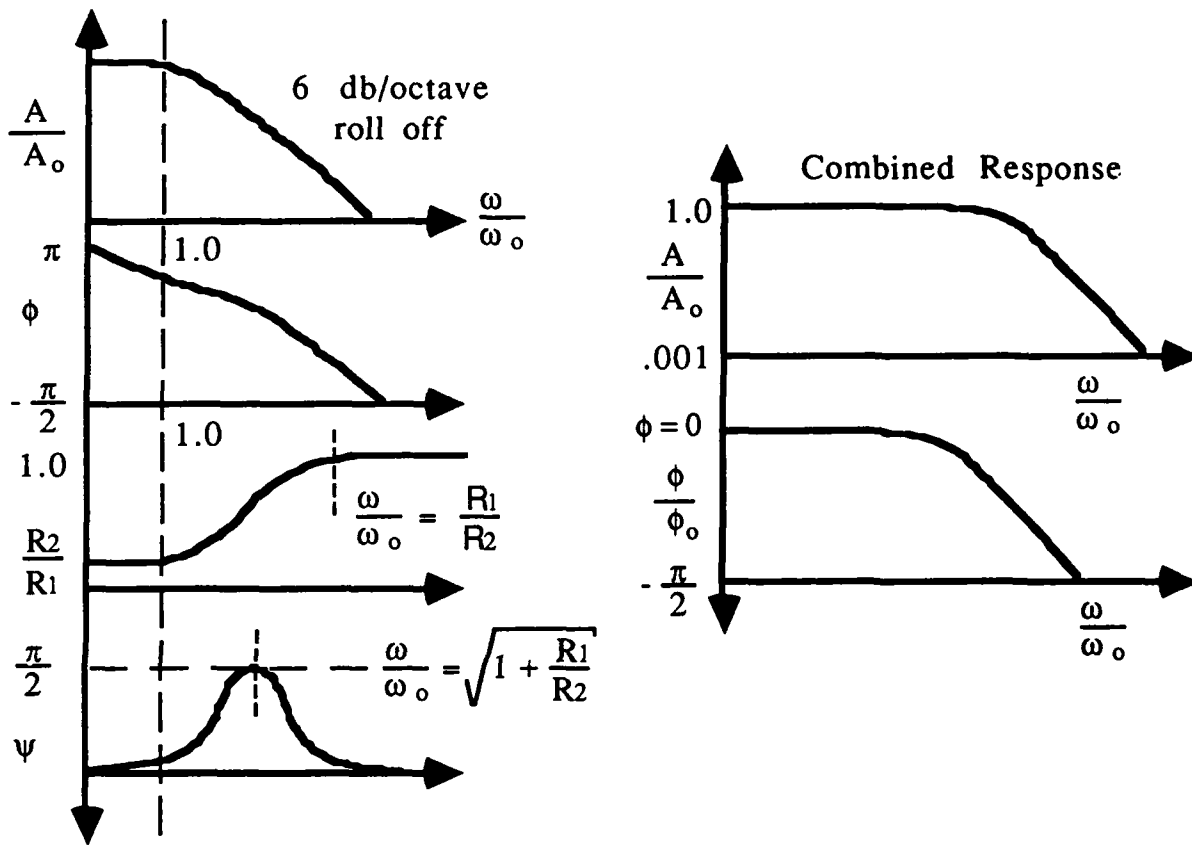
ψ' is maximum when

$$1 + \frac{R_2}{R_1} - \frac{R_2}{R_1} \left(\frac{\omega}{\omega_0}\right)^2 = 0 \quad 4.41$$

That is when

$$\frac{\omega}{\omega_0} = \sqrt{1 + \frac{R_1}{R_2}} \quad 4.42$$

Typical circuit response curves for $R_2/R_1 = 1/1000$ are shown below along with the wire circuit output.



We note that it is possible to correct amplitude to higher frequency than phase. The effect of time-constant error on the hot-wire output can also be determined. For the circuit we may write

$$\frac{V_o}{V_i} = G \sqrt{1 + \left(\frac{\omega}{\omega_A}\right)^2} \quad 4.43$$

G = gain factor and ω_A = set for M_A

Since the wire output may be written as

$$\frac{V_w}{V_{fluid}} = \frac{1}{\sqrt{1 + \left(\frac{\omega}{\omega_0}\right)^2}} \quad 4.44$$

where $M_0 = 1/\omega_0$

$$\therefore \frac{V_o}{V_f} = G \frac{\sqrt{1 + \left(\frac{\omega}{\omega_A}\right)^2}}{\sqrt{1 + \left(\frac{\omega}{\omega_0}\right)^2}} \quad 4.45$$

$$\text{for } \omega \rightarrow 0 \quad V_o/V_f \rightarrow G$$

$$\omega \rightarrow \infty \quad V_o/V_f \rightarrow G \omega_0/\omega_A$$

We can see from figure 4.1, that as long as ω_0/ω_A is within $\pm 30\%$ of unity, the response is flat above $\omega/\omega_0 \approx 5$. So, apart from signals of frequencies less than $5\omega_0$, we can account for errors due to incorrect circuit time-constant settings (ω_A) by multiplying the signal by ω_A/ω_0 .

Alternatively, we can write

$$e_o^2 = \int_0^\infty F(f) df \quad 4.46$$

where e_o is the uncompensated wire output and $F(f)$ is the power spectrum ie. the signal amplitude squared vs. frequency. The compensated signal is then

$$e_{comp}^2 = \int_0^\infty F(f)(1 + \omega^2 + M_e^2) df = e_o^2 + M_e^2 \int_0^\infty \omega^2 F(f) df \quad 4.47$$

The true signal would therefore be

$$e_T^2 = \int_0^\infty F(f)(1 + \omega^2 + M_T^2) df = e_o^2 + M_T^2 \int_0^\infty \omega^2 F(f) df \quad 4.48$$

eliminating

$$\int_0^\infty \omega^2 F(f) df$$

we have

$$\frac{e_{\text{comp}}^2 - e_o^2}{e_T^2 - e_o^2} \frac{M_T^2}{M_c^2} = 1 \quad 4.49$$

which may be rewritten as

$$\frac{e_T}{e_{\text{comp}}} = \frac{M_T}{M_c} \sqrt{1 - \frac{e_o^2 (e_T^2 - e_{\text{comp}}^2)}{e_{\text{comp}}^2 (e_T^2 - e_o^2)}} \quad 4.50$$

This correction is acceptable when M_T and M_c differ by less than 30 percent.

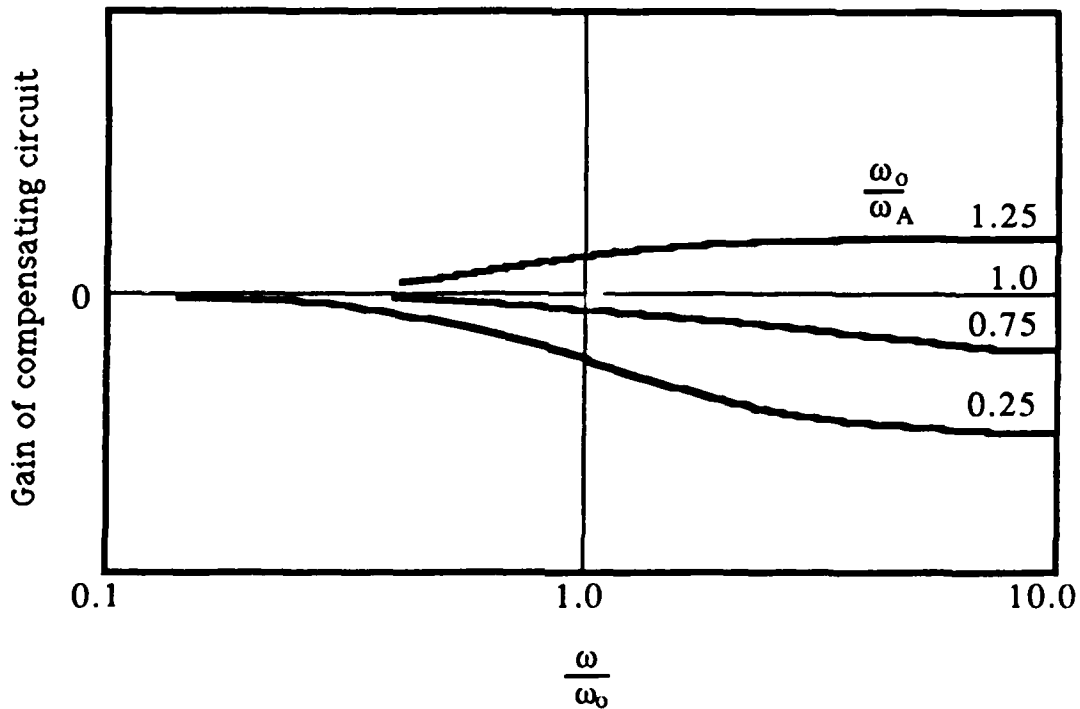
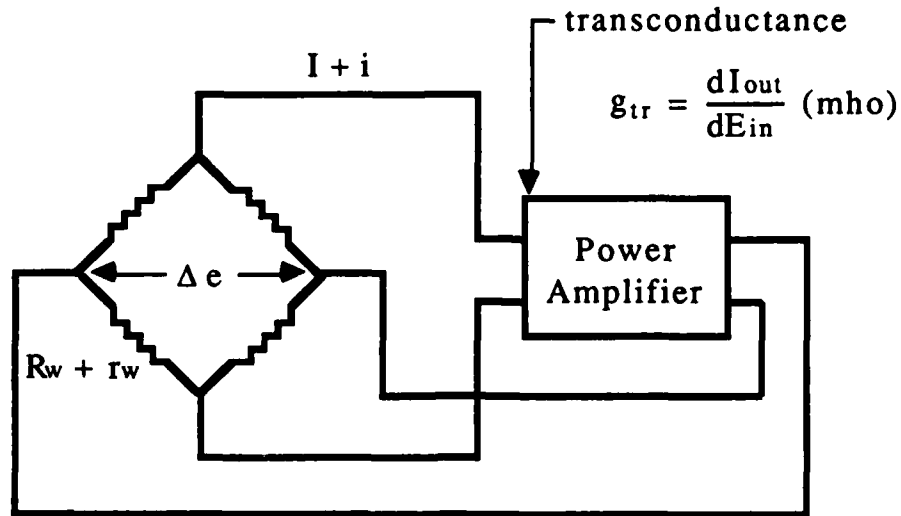


Fig. 4.1 Hot-wire compensating circuit response.

Now let us turn our attention to the constant temperature method ($r_w \rightarrow 0$) and consider a hot-wire probe in the circuit shown below.



$$dI = i = -g_{tr} dE = -g_{tr} I r_w$$

Now assuming $I = \bar{I} + i$, $u = \bar{u} + u'$ and substituting in equation 4.5, neglecting terms in r_w , we obtain

$$I^2 \bar{R} + 2iI\bar{R}_w = (\bar{R}_w - R_g)(A + B\sqrt{\bar{u}}) + (R_w - R_g)B\sqrt{\bar{u}} \frac{u}{2\bar{u}} \quad 4.51$$

so that

$$i = \frac{\bar{R}_w - R_g}{4I\bar{R}_w} B\sqrt{\bar{u}} \frac{u}{\bar{u}} \quad 4.52$$

and $e = iR_w = s_{ct} u$. Where the constant temperature sensitivity is given by

$$s_{ct} = \frac{(\bar{R}_w - R_g)B\sqrt{\bar{u}}}{4I\bar{u}} \quad 4.53$$

We also see that the constant temperature sensitivity is related to the constant current sensitivity (s) by

$$s_{ct} = \frac{R_g}{2(\bar{R}_w - R_g)} s \quad 4.54$$

so that for $R_w/R_g > 3/2$, $s_{ct} < s$, ie. at low overheats, constant temperature operation is less sensitive than constant current.

In order to study dynamic behavior, we must consider small changes (lags) in $R_w = \bar{R}_w + r_w$. Neglecting higher order terms in i , r_w and u' , we see from the thermal equilibrium equation that

$$\bar{I}^2 r_w + 2i\bar{I}\bar{R}_w = (A + B\sqrt{\bar{u}})r_w + (\bar{R}_w - R_g) B\sqrt{\bar{u}} \frac{u}{2\bar{u}} + C_w \frac{dT_w}{dt} \quad 4.55$$

using $T_w = r_w/\alpha R_o$ and substituting for g_{tr} we obtain

$$\frac{di}{dt} + \frac{\alpha R_o}{C_w} (A + B\sqrt{\bar{u}} - \bar{I}^2 + 2\bar{I}^2 \bar{R}_w g_{tr}) i = \frac{\alpha g_{tr} \bar{I} R_o (\bar{R}_w - R_g)}{C_w} B\sqrt{\bar{u}} \frac{u}{2\bar{u}} \quad 4.56$$

solving this equation as previously, we determine that

$$M_{ct} = \frac{C_w}{\alpha R_o (A + B\sqrt{\bar{u}} - \bar{I}^2 + 2\bar{I}^2 \bar{R}_w g_{tr})} \quad 4.57$$

or

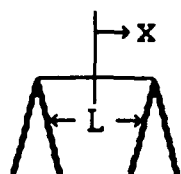
$$M_{ct} = \frac{M}{1 + 2 \left[\frac{\bar{R}_w - R_g}{R_g} \right] \bar{R}_w g_{tr}} \quad 4.58$$

ie. $M_{ct} \ll M$.

Typically, $R_w/R_g = 2$, $R_w = 10 \Omega$ and $g_{tr} = 10$ mhos, so that $M_{ct} = 1/200 M$. However, we also note that the response depends on $(R_w - R_g)/R_g$, so that when $R_w - R_g \rightarrow 0$ $M_{ct} \rightarrow M$. Thus, the constant temperature anemometer frequency response is poor at low overheat (ref. 6).

The phase shift is also a strong function of overheat and mass flow rate. At low overheat, phase shifts in the feed back amplifier can lead to large bridge oscillations. To avoid this we need flat amplifier response to at least twice the desired compensation frequency. Bridge stability also depends on the amount of out of balance which is a function of $R_w - R_g$. Typically for a $5\mu\text{m}$ tungsten wire at high overheat, -3db relative amplitude can exceed 100 kHz, but with a phase lag of 60 deg.

Now let us consider the effects of conduction to the wire supports. Generally, hot-wire supports are much thicker than the wire itself for reasons of strength so that, since their relative resistance is low, they will not be heated appreciably by the electric current. We can determine the hot-wire temperature distribution and determine the effects of heat conduction to the supports by rewriting the energy balance as



$$I^2 R_w = (R_w - R_g)(A + B\sqrt{u}) - \frac{\pi d^2}{4} k_w \frac{d^2 T_w}{dx^2} \quad 4.59$$

where k_w is the thermal conductivity of the wire. Now since $R_w - R_g = \alpha R_o (T_w - T_g)$ we obtain

$$\frac{d^2 (T_w - T_g)}{dx^2} - \frac{\alpha R_o [A + B\sqrt{u} - I^2]}{\frac{\pi d^2}{4} k_w} (T_w - T_g) + \frac{I^2 R_g}{\frac{\pi d^2}{4} k_w} = 0 \quad 4.60$$

where

$$T_w - T_g = 0 \quad \text{for} \quad x = \pm \frac{L}{2}$$

$$\frac{d(T_w - T_g)}{dx} = 0 \quad \text{at} \quad x = 0$$

The solution of this equation is

$$T_w - T_g = \frac{I^2 \frac{R_g}{R_o}}{\alpha (A + B\sqrt{U} - I^2)} \left[1 - \frac{\cosh (x/L_c)}{\cosh (x/2L_c)} \right] \quad 4.61$$

where L_c , the cold length ie. the length effectively cooled by the end supports, is a function of wire diameter $f(d)$ and may be written as

$$L_c = \frac{d}{2} \sqrt{\frac{\pi k_w}{\alpha (A + B\sqrt{U} - I^2)}} \quad 4.62$$

and the effective wire length is equal to $l - 2(L_c)$. With some approximations equation 4.61 may be written as

$$\frac{T_w - T_g}{T_{w_\infty} - T_g} = 1 - \frac{\cosh x/L_c}{\cosh L/2L_c} \quad 4.63$$

and examples are shown below.

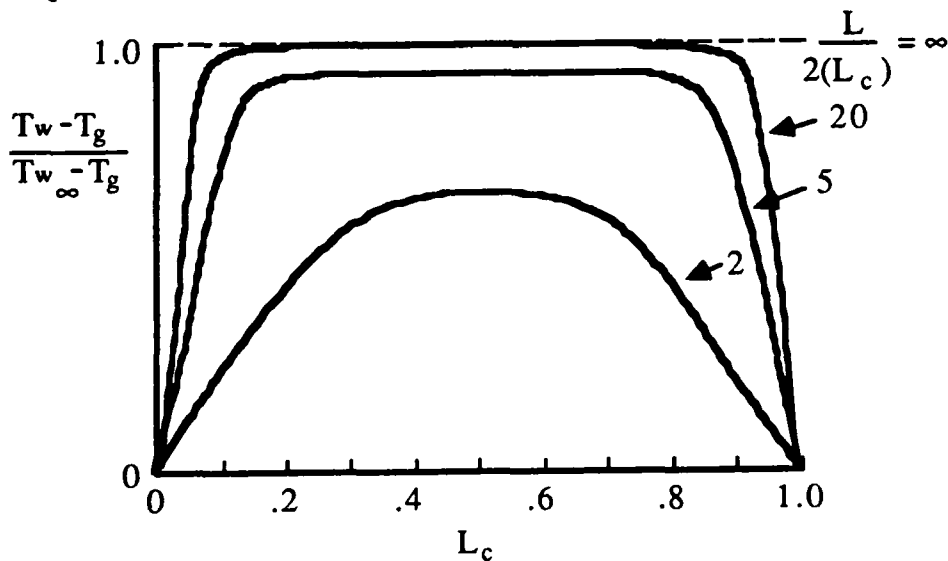


Fig. 4.2 Hot-wire temperature distributions.

From this figure we can see that we must keep $L/2(L_c) \geq 5$ ie. no more than about 20 percent of the wire cooled, no more than 10 percent at

each end. For typical operating conditions this means $L/d \approx 100$ to 200 for platinum-rhodium wires and still higher for tungsten since $k_w(\text{tungsten}) = 2.5 k_w(\text{platinum})$.

The effects of end losses on dynamic response are very complex. They may be summarized as follows. It is impossible to correctly compensate with simple RC circuits since the phase shift is not constant along the wire. However deviations are small (within 2 percent for $L/2(L_c) > 3$) if compensation is correct for $\omega = 0$ and ∞ . The wire time constant decreases as L/d increases, but there is a limit to L/d due to strength and non-uniform velocity distribution along the wire which we will consider next.

Consider the case of uniform flow \bar{u} and turbulence intensity u_1 . Since the wire voltage

$$e = K \int_0^L u_1(x_2) dx_2 \quad 4.64$$

then if $u_1 = \text{constant}$,

$$\overline{e^2} = K^2 L^2 \overline{u_1^2} \quad 4.65$$

This would also be the case in non-uniform flow if we measure a true "point" value. Now if $R_2(x_2)$ is the lateral correlation coefficient distribution along the wire then, when the two rms levels $u'_1(x_2)$ and $u'_1(x_2 + a)$ are equal,

$$R_2(x_2) = \frac{u_1(x_2) u_1(x_2+a)}{u_1'(x_2) u_1'(x_2+a)} = \frac{u_1(x_2) u_1(x_2+a)}{u_1'(x_2)^2} \quad 4.66$$

But if $u_1'(x_2)$ is not constant, the measured mean square voltage output is

$$\overline{e_m^2} = K^2 \left[\int_0^L u_1(x_2) dx_2 \right]^2 \quad 4.67$$

which, if $\overline{f(x_2)} = \overline{f(x_2)}$ can be written as

$$e_m^2 = K^2 \int_0^L \int_0^L \overline{u_1(x_2) u_1(x_2')} dx_2 dx_2' \quad 4.68$$

In homogeneous turbulence

$$\overline{u_1^2} = \overline{u_1^2(x_2)} = \overline{u_1^2(x_2')}$$

so we have

$$e_m^2 = K^2 \overline{u_1^2} \int_0^L \int_0^L R_2(x)(x_2 - x_2') dx_2 dx_2' \quad 4.69$$

ie

$$\overline{u_1(x_2')} = \frac{R_2(x) \overline{u_1^2}}{\overline{u_1(x_2)}} \quad 4.70$$

Now, substituting in equation 4.68, and defining $s = (x_2 - x_2')$ we obtain

$$\overline{e_m^2} = 2K^2 \overline{u_1^2} \int_0^L (L-s) R_2 ds \quad 4.71$$

comparing $\overline{e^2}$ and $\overline{e_m^2}$ given by both equation 4.65 and 4.71 we see that

$$\frac{\overline{e^2}}{\overline{e_m^2}} = I_m^2 \quad 4.72$$

where

$$\frac{1}{I_m^2} = \frac{2}{L^2} \int_0^L (L-s) R_2 ds \quad 4.73$$

Since $R_2 \leq 1.0$, the turbulent energy measured with a long wire is always smaller than the true point value. So, to correct $\overline{e_m^2}$, we need to know the lateral cross-correlation coefficient. Now, if the wire length far exceeds the lateral integral scale,

$$\Lambda = \int_0^{\infty} R_2 dx_2 \quad 4.74$$

then

$$\overline{e_m^2} = 2K^2 \overline{u_1^2} (\Lambda \Lambda_2 - \Lambda_2') \quad 4.75$$

where

$$\Lambda_2' = \int_0^{\infty} x_2 R_2 dx_2$$

(the first moment of R_2) so that

$$\frac{1}{I_m^2} = \frac{\overline{e_m^2}}{e^2} = \frac{2}{L^2} (\Lambda \Lambda_2 - \Lambda_2') = 2 \left[\frac{\Lambda_2}{L} - \frac{\Lambda_2'}{(\Lambda_2)^2} \frac{\Lambda_2^2}{L^2} \right] \quad 4.76$$

where

$$\frac{\Lambda_2'}{(\Lambda_2)^2}$$

depends on the shape of the correlation curve. When

$$\frac{L}{\Lambda_2} \rightarrow \infty \quad \frac{1}{I_m^2} \rightarrow 0 \quad \text{so that} \quad \overline{e_m^2} \rightarrow 0$$

ie. no turbulence would be measured at all if $L = \infty$.

The effects of L , d , and L/d can be summarized as follows. For a small time-constant, ie. high-frequency compensation, we require a small wire diameter. For a long uniform wire temperature and high-frequency

response, we require $L/d > 200$. Decreased wire diameter increases signal/noise ratio, but decreases strength and large L/d probes give poor response in a variable field. However, small L/d probes lead to adverse aerodynamic interference effects. So we can see that probe design must be a compromise.

The effects of mean fluid temperature changes can be assessed as follows. Consider the energy balance

$$\frac{I^2 R_w}{R_w - R_g} = A(T_g) + B\sqrt{u} \quad 4.77$$

where $A = f(T_g)$ whereas B is generally constant provided T_w is adjusted to keep T_w/T_g constant. But the turbulence measurements are independent of A since

$$\frac{I^2 R_w r_w}{(R_w - R_g)} \approx B\sqrt{u} \frac{u}{2u} \quad 4.78$$

so that mean temperature changes do not effect hot-wire turbulence measurements. The primary effect of mean flow temperature changes on the wire calibrations are shown in fig. 4.3.

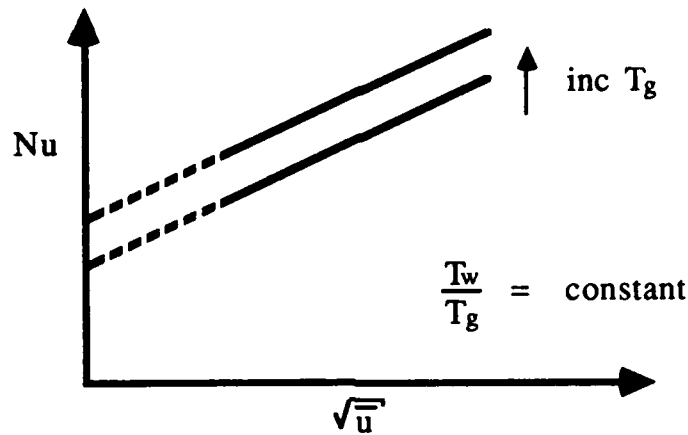


Fig. 4.3 Effect of ambient temperature change on hot-wire calibration

Finally, let us consider the effects of large turbulence fluctuations and the limitations they impose on our earlier assumptions. In such cases the effective velocity may be written as

$$\sqrt{u_{\text{eff}}} = \sqrt{\bar{u}} \left[1 + \frac{1}{2} \frac{u_1}{\bar{u}} - \frac{1}{8} \frac{u_1^2}{\bar{u}^2} + \frac{1}{16} \frac{u_1^3}{\bar{u}^3} + \frac{1}{4} \frac{u_2^2}{\bar{u}^2} - \frac{3}{8} \frac{u_1 u_2^2}{\bar{u}^3} + \dots \right] \quad 4.79$$

If we time average, then the measured velocity is given by

$$\sqrt{\bar{u}_{\text{meas}}} = \sqrt{u_{\text{eff}}} = \sqrt{\bar{u}} \left[1 - \frac{1}{8} \frac{\overline{u_1^2}}{\bar{u}^2} + \frac{1}{4} \frac{\overline{u_2^2}}{\bar{u}^2} + \frac{1}{16} \frac{\overline{u_1^3}}{\bar{u}^3} - \frac{3}{8} \frac{\overline{u_1 u_2^2}}{\bar{u}^3} + \dots \right] \quad 4.80$$

$$\therefore \bar{u}_{\text{meas}} = \bar{u} \left[1 - \frac{1}{4} \frac{\overline{u_1^2}}{\bar{u}^2} + \frac{1}{2} \frac{\overline{u_2^2}}{\bar{u}^2} + \frac{1}{8} \frac{\overline{u_1^3}}{\bar{u}^3} - \frac{3}{4} \frac{\overline{u_1 u_2^2}}{\bar{u}^3} + \dots \right] \quad 4.81$$

So if the fluctuations are large, the measurement is a function of u_1 , u_2 and $\overline{u_1 u_2}$ plus higher order terms. So we must correct the mean measurements. Neglecting higher order terms we have

$$u_{\text{meas}} \approx \bar{u} \left[1 - \frac{1}{4} \frac{\overline{u_1^2}}{\bar{u}^2} + \frac{1}{2} \frac{\overline{u_2^2}}{\bar{u}^2} \right]$$

In isotropic flows $\overline{u_1^2} \approx \overline{u_2^2}$ so that $\overline{u}_{meas} > \overline{u}_{actual}$. Now the hot-wire response to turbulent fluctuations may be written as

$$\frac{I^2 R_w}{R_w - R_g} = A + B\sqrt{\overline{u}} \left[1 + \frac{1}{2} \frac{u_1}{\overline{u}} - \frac{1}{8} \frac{u_1^2}{\overline{u}^2} + \dots \right] \quad 4.82$$

putting $R_w = \overline{R}_w + r_w$ where r_w is not « \overline{R}_w . We obtain

$$I^2(\overline{R}_w + r_w) = (A + B\sqrt{\overline{u}})(\overline{R}_w - R_g + r_w) + B\sqrt{\overline{u}}(\overline{R}_w - R_g + r_w)u^* \quad 4.83$$

where

$$u^* = \frac{1}{2} \frac{u_1}{\overline{u}} - \frac{1}{8} \frac{u_1^2}{\overline{u}^2} + \frac{1}{4} \frac{u_2^2}{\overline{u}^2} + \frac{1}{16} \frac{u_1^3}{\overline{u}^3} - \frac{3}{8} \frac{u_1 u_2^2}{\overline{u}^3} + \dots \quad 4.84$$

averaging we obtain

$$I^2 \overline{R}_w = (A + B\sqrt{\overline{u}})(\overline{R}_w - R_g) + B\sqrt{\overline{u}}(\overline{R}_w - R_g)u^* + B\sqrt{\overline{u}} \overline{u^* r_w} \quad 4.85$$

Now for linearized theory

$$I^2 \overline{R}_{w_{lin}} = (A + B\sqrt{\overline{u}})(\overline{R}_{w_{lin}} - R_g) \quad 4.86$$

so that from equations 4.83, 4.85 and 4.86 we obtain

$$\overline{e^2} = I^2 \overline{r_w^2} = (\overline{R}_w - R_g)^2 \frac{(\overline{R}_{w_{lin}} - R_g)^2}{I^2 R_g^2} B^2 \overline{u} \frac{\overline{u_1^2}}{4 \overline{u}^2} [1 - \varphi(u_1, u_2)] \quad 4.87$$

According to linearized theory, equation 4.10, we determine that

$$\overline{e^2} = \frac{\overline{R}_{w_{lin}} - R_g}{I^2 R_g^2} B^2 \overline{u} \left(\frac{\overline{u_1^2}}{4 \overline{u}^2} \right)_{lin} \quad 4.88$$

$$\therefore \left(\frac{\overline{u_1^2}}{4 \overline{u}^2} \right)_{lin} = \left(\frac{\overline{u_1^2}}{4 \overline{u}^2} \right)_{act} \left(\frac{\overline{R}_{w_{lin}} - R_g}{R_w - R_g} \right)^2 [1 - \varphi(u_1, u_2)] \quad 4.89$$

or after further calculation

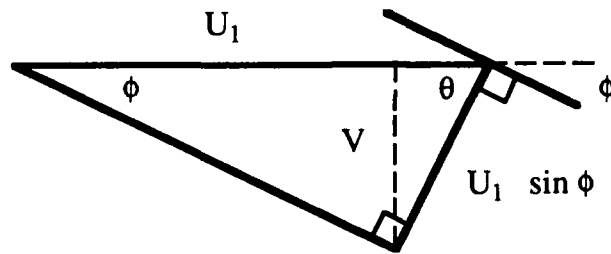
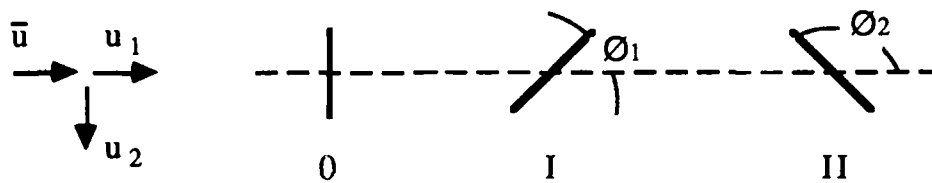
$$\left(\frac{\overline{u_1^2}}{\overline{u}^2} \right)_{lin} = \left(\frac{\overline{u_1^2}}{\overline{u}^2} \right)_{act} [1 - \varphi(u_1, u_2)] \quad 4.90$$

where $\psi(u_1, u_2)$ is a function of $u_1^n, u_2^m, u_1^n u_2^m$. So that, in highly turbulent environments, what is actually measured is not the u_1 component alone but a mixture. To measure u_1 we must not only know u_2 but also the higher order correlations which are not usually known for non isotropic turbulent flows. We may conclude that the correct measurement of turbulence of high intensity is practically impossible with a hot-wire. But, if errors of 10-20% are accepted, it is permissible to use linearized theory up to turbulence intensities of 20-25%. This covers a large range of flows as the table below indicates. Errors due to high turbulence and resulting directional intermittency are discussed in ref. 7.

Table 1

Flow Type	Turbulence Intensity
Wind Tunnel (poor)	0.1 - 0.5%
Wind Tunnel (good)	< 0.05%
Turbulent Jet	30 - 60%
Kármán Vortex Street	5 - 15%
Turbulent Boundary Layer	4 - 10%
Turbulent Wake	2 - 5%
Screen Turbulence (nearly isentropic)	0.3 - 2%

The measurement of turbulence characteristics with a hot-wire anemometer may be achieved as follows. Consider the response of the hot wires designated 0, I and II shown in the flow on the following page.



$$V = U_1 \sin \phi \sin \theta$$

For thermal equilibrium we may write

$$e_0 = - (s_1)_0 u_1 \quad 4.91$$

$$e_I = - (s_1)_I u_1 - (s_2)_I u_2 \quad 4.92$$

$$e_{II} = - (s_1)_{II} u_1 + (s_2)_{II} u_2 \quad 4.93$$

Now, if we use an X array with identical wires or make the sensitivities equal by adjusting the individual currents, we get

$$(s_1)_I = (s_1)_{II} \text{ and } (s_2)_I = (s_1)_{II}$$

if $\phi_1 = \phi_2 = 45$ deg. then $s_1 = s_2 = s$, so that u_1 , u_2 and $\bar{u}_1 \bar{u}_2$ may be obtained from

$$\begin{aligned} \bar{e}_S^2 &= (\bar{e}_I + \bar{e}_{II})^2 = 4 s^2 \bar{u}_1^2 = 4 s_1^2 \bar{u}_1^2 \\ \bar{e}_D^2 &= (\bar{e}_I - \bar{e}_{II})^2 = 4 s^2 \bar{u}_2^2 = 4 s_2^2 \bar{u}_2^2 \end{aligned} \quad 4.94$$

$$\text{and } \bar{e}_I^2 - \bar{e}_{II}^2 = 4 s^2 \bar{u}_1 \bar{u}_2 = 4 s_1 s_2 \bar{u}_1 \bar{u}_2$$

where

$$s_1 = \left. \frac{\partial E}{\partial U_1} \right|_{\phi = \text{const}, V = \text{const}} \quad 4.95$$

and

$$s_2 = \left. \frac{\partial E}{\partial V} \right|_U \quad 4.96$$

The calibration sensitivities can be determined as follows. Since

$$\frac{\partial E}{\partial V} = \frac{\partial E}{\partial \phi} / \frac{\partial V}{\partial \phi} \quad 4.97$$

and velocity component resolution shows that

$$\frac{\partial V}{\partial \phi} = U_1 [\sin \phi \cos \Theta \frac{d\Theta}{d\phi} + \cos \phi \sin \Theta] \quad 4.98$$

If the wire is at 45 deg. to the flow then

$$\frac{\partial V}{\partial \phi} = U_1 \quad 4.99$$

and

$$s_2 = \left. \frac{\partial E}{\partial V} \right|_U = \frac{1}{U_1} \left. \frac{\partial E}{\partial \phi} \right|_{U_1 = \text{const}} \quad 4.100$$

so calibration is relatively straightforward.

Alternatively, $\overline{u_1 u_2}$ may be obtained by measuring the correlation factor between e_S and e_D ie.

$$R_{AB} = R_{AB(\text{meas})} G_A G_B = G_A G_B \overline{e_S e_D} = 4s^2 \overline{u_1 u_2}$$

where G_A and G_B are the anemometer gains. So that

$$\overline{u_1 u_2} = \frac{R_{AB}}{4s^2} \quad 4.101$$

To determine the cross-correlation coefficient of u_1 we put two wires at points A and B, so we have

$$e_A = (s_1)_A (u_1)_A \quad 4.102$$

and

$$e_B = (s_1)_B (u_1)_B \quad 4.103$$

The cross-correlation of u_1 can then be calculated from

$$\frac{(\overline{e_A + e_B})^2 - (\overline{e_A - e_B})^2}{(\overline{e_A + e_B})^2 + (\overline{e_A - e_B})^2} = \frac{4 \overline{e_A e_B}}{2(\overline{e_A^2} + \overline{e_B^2})} = \frac{2(s_1)_A (s_1)_B \overline{(u_1)_A (u_1)_B}}{(s_1)_A^2 \overline{(u_1)_A^2} + (s_1)_B^2 \overline{(u_1)_B^2}} \quad 4.104$$

If we adjust $\overline{e_A^2} = \overline{e_B^2}$ ie. $e_A' e_B' = \overline{e_A^2} = \overline{e_B^2}$, then the cross-correlation coefficient reduces to

$$\frac{2 \overline{e_A e_B}}{e_A' e_B'} = \frac{2 \overline{e_A e_B}}{\overline{e_A^2}} = \frac{2 \overline{e_A e_B}}{\overline{e_B^2}}$$

where ' denotes RMS values ie.

$$Re_A e_B = \frac{\overline{(u_1)_A (u_1)_B}}{\overline{(u_1)_A} \overline{(u_1)_B}} = \frac{\overline{(u_1)_A (u_1)_B}}{\overline{(u_1)_A^2}} = \frac{\overline{(u_1)_A (u_1)_B}}{\overline{(u_1)_B^2}} \quad 4.105$$

We can determine the Reynolds shear stress coefficient

$$\frac{\overline{u_1 u_2}}{u_1' u_2'}$$

from

$$\frac{\overline{e_I^2} - \overline{e_{II}^2}}{\sqrt{\overline{e_s^2}} \sqrt{\overline{e_D^2}}} = \frac{4s^2 \overline{u_1 u_2}}{4s^2 u_1' u_2'} = \frac{\overline{u_1 u_2}}{u_1' u_2'} \quad 4.106$$

So we do not need to calibrate the probes.

To determine the space-time correlation of the Reynolds shear stress

$$\overline{(u_{1A} u_{2A})(u_{1B} u_{2B})} = \overline{u_{12A} u_{12B}} \quad 4.107$$

we can use two hot-wire X probes and measure the correlation function between

$$\begin{aligned} e_{DA} &= (e_{IA} - e_{IIA}) = 2s_A u_{12A} \\ e_{DB} &= (e_{IB} - e_{IIB}) = 2s_B u_{12B} \end{aligned} \quad 4.108$$

ie.

$$\frac{\overline{(e_{DA} + e_{DB})^2} - \overline{(e_{DA} - e_{DB})^2}}{\overline{(e_{DA} + e_{DB})^2} + \overline{(e_{DA} - e_{DB})^2}}} = \frac{4 \overline{e_{DA} e_{DB}}}{2 \overline{(e_{DA} + e_{DB})^2}} = \frac{2s_A s_B \overline{u_{12A} u_{12B}}}{s_A \overline{u_{12A}^2} + s_B \overline{u_{12B}^2}} \quad 4.109$$

If we adjust $\overline{e_{DA}^2} = \overline{e_{DB}^2}$ ie $e_{DA}' e_{DB}' = \overline{e_{DA}^2} = \overline{e_{DB}^2}$ then

$$R u_{12A} u_{12B} = \frac{\overline{e_{DA} e_{DB}}}{\overline{e_{DA}^2}} = \frac{\overline{e_{DA} e_{DB}}}{\overline{e_{DB}^2}} = \frac{\overline{e_{DA} e_{DB}}}{e_{DA}' e_{DB}'} \quad 4.110$$

so that

$$R u_{12A} u_{12B} = \frac{\overline{u_{12A} u_{12B}}}{\overline{u_{12A}^2}} = \frac{\overline{u_{12A} u_{12B}}}{\overline{u_{12B}^2}} = \frac{\overline{u_{12A} u_{12B}}}{u_{12A}' u_{12B}'} \quad 4.111$$

Triple-point correlation measurements determine the kinematic diffusion of turbulent energy. Terms such as

$$\overline{u_1^2 u_2}$$

may be obtained from an X wire when $s_1 = s_2 = s$ as follows, with

$$A^2 = (e_I + e_{II})^2 = 4s^2 u_1^2 \quad \text{and} \quad B = e_I - e_{II} = 2su^2$$

then

$$\frac{\overline{(A^2 + B)^2} - \overline{(A^2 - B)^2}}{\overline{(A^2 + B)^2} + \overline{(A^2 - B)^2}} = \frac{4\overline{A^2 B}}{2(\overline{A^4 + B^2})} = \frac{2s^3 \overline{u_1^2 u_2}}{s^4 \overline{u_1^4} + s^2 \overline{u_2^2}} \quad 4.112$$

If we adjust $\overline{A^4} = \overline{B^2}$, then $\overline{A^2 B} = \overline{A^4} = \overline{B^2}$, so that

$$R = \frac{\overline{u_1^2 u_2}}{\overline{u_1^2 u_2}} \quad 4.113$$

or we can measure the correlation factor

$$\overline{(e_A + e_B)^2} - \overline{(e_A - e_B)^2}$$

so that

$$2s^3 \overline{AB} = G_A G_B R_{AB(mess)} = R_{AB}, \quad \therefore \overline{AB} = \frac{R_{AB}}{2s^3} \quad 4.114$$

Then divide by say $s^3 \overline{u^3}$ to remove the wire sensitivity. Other components eg.

$$\overline{u_2^3} \quad \& \quad \overline{u_2 u_3^2}$$

may be obtained in a similar manner.

The space-time triple point correlations can be obtained from two X wires at two different points in the flow. Defining A and B as

$$A = e_A^2 = e_{I_A}^2 - e_{II_A}^2 = s_A^2 u_{1_A} u_{2_A} \quad 4.115$$

$$B = e_B^2 = e_{I_B}^2 - e_{II_B}^2 = s_B^2 u_{1_B} u_{2_B}$$

then

$$R(x,t) = \frac{\overline{(u_1^2)_A (u_1)_B}}{\overline{(u_1)_A^2 (u_1)_B}}, \quad \overline{(u_2^2)_A (u_1)_B} \quad \text{and} \quad \overline{(u_2)_A (u_1)_A (u_1)_B} \quad 4.116$$

Flatness factors, which give an indication of the extent of turbulent intermittency, are defined as

$$\frac{\overline{u^4}}{\overline{u^2}^2} = T_u$$

$$\frac{\overline{v^4}}{\overline{v^2}^2} = T_v \quad \& \quad \frac{\overline{w^4}}{\overline{w^2}^2} = T_w$$

The turbulence intermittency may be determined from

$$\gamma = \frac{4}{T_u} = \frac{3.5}{T_v} = \frac{3.5}{T_w}$$

Longitudinal microscale may be defined, using the auto-correlation R_{11} , as

$$\lambda_{x_1}^2 = \frac{\overline{2u_1^2}}{\left(\frac{\partial u_1}{\partial x_1}\right)^2} = - \frac{2}{\left[\frac{\partial^2}{\partial x_1^2} R_{11}(x_1, 0, 0, 0)\right]_{x_1=0}} \quad 4.117$$

$$\left(\frac{\partial u_1}{\partial x_1}\right)^2 = - \overline{u_1^2} \left[\frac{\partial^2}{\partial x_1^2} R_{11}(x_1, 0, 0, 0)\right]_{x_1=0} \quad 4.118$$

for steady homogeneous turbulence only. Since for steady homogeneous turbulence

$$R_{11}(x_1, 0, 0, 0) \rightarrow 1 - x_1^2/\lambda_1^2 \quad \text{as } r \rightarrow 0$$

Now invoking Taylor's hypothesis $x = u_c t$

$$\lambda_t = \lambda_1/u_c$$

where λ_t is defined by

$$R_{11}(0,0,0,t) \rightarrow 1 - \frac{t^2}{\lambda_1^2} \text{ as } t \rightarrow 0$$

$$\text{ie. } \lambda_1^2 = \frac{2 \overline{u_1^2}}{\left(\frac{\partial u_1}{\partial t}\right)^2} \quad 4.119$$

Similarly, we may measure the lateral microscales defined as

$$\lambda_{x_2}^2 = \frac{2 \overline{u_1^2}}{\left(\frac{\partial u_1}{\partial x_2}\right)^2} \quad 4.120$$

and

$$\lambda_{x_3}^2 = \frac{2 \overline{u_1^2}}{\left(\frac{\partial u_1}{\partial x_3}\right)^2} \quad 4.121$$

We can also measure terms such as

$$\overline{\left(\frac{\partial u_1}{\partial x_2}\right)^2}$$

which appear in the equation for the turbulent dissipation (ϵ), by placing two wires a distance x_2 apart to obtain

$$[(u_1)_A - (u_1)_B]^2$$

With a differentiation circuit, which will be described later, we can also obtain

$$\overline{\left(\frac{\partial u}{\partial t}\right)^2}$$

and in a similar manner we may measure

$$\overline{\left(\frac{\partial^2 u}{\partial t^2}\right)^2} \quad \& \quad \overline{\left(\frac{\partial u}{\partial t}\right)^3}$$

When the electronic noise is large enough to influence measurements made with a hot-wire anemometer, the noise must be subtracted from the anemometer output to obtain the correct net result. To make this correction, the hot-wire equation can be expressed (ref. 8) as

$$\frac{(e' + e'_n)}{GE} = S \frac{(u' + u'_n)}{\bar{u}} \quad 4.122$$

where the gain is G and the noise is denoted by the subscript n . The level of the electronic noise can be approximately obtained by covering the hot-wire probe and measuring e'_n and E_n . Under this condition, equation 4.122 can be expressed as

$$\frac{e'_n}{G_n E_n} = S \left(\frac{u'_n}{\bar{u}} \right) \quad 4.123$$

Forming the mean square of equation 4.122 and assuming that there is no correlation between the electronic noise and the velocity fluctuations we have

$$\overline{\frac{(e' + e'_n)^2}{G^2 E^2}} = S^2 \left[\overline{\left(\frac{u'}{\bar{u}}\right)^2} + \overline{\left(\frac{u'_n}{\bar{u}}\right)^2} \right] \quad 4.124$$

So that, the velocity fluctuation in the flow is

$$\overline{\left(\frac{u'}{\bar{u}}\right)^2} = \frac{\overline{(e' + e'_n)^2}}{S^2 G^2 E^2} - \overline{\left(\frac{u'_n}{\bar{u}}\right)^2} \quad 4.125$$

Substituting equation 4.123 into 4.125 results in

$$\overline{\left(\frac{u'}{\bar{u}}\right)^2} = \frac{\overline{(e' + e'_n)^2}}{S^2 G^2 E^2} - \left(\frac{\bar{u}_n}{\bar{u}}\right)^2 \frac{\overline{e_n'^2}}{S^2 G_n^2 E_n^2} \quad 4.126$$

A value is now required for the quantity u_n^2/u^2 in equation 4.126. From the calibration of the hot-wire, we have

$$\log E = A \log \bar{u} + \log B \quad 4.127$$

which can be written as follows by noting that $A = S$

$$\bar{u} = \left(\frac{E}{B}\right)^{\frac{1}{S}} \quad 4.128$$

Then using equation 4.128 u_n/u becomes

$$\frac{\bar{u}_n}{\bar{u}} = \left(\frac{E_n}{E}\right)^{\frac{1}{S}} \quad 4.129$$

Substituting equation 4.129 into 4.126 gives the final result

$$\overline{\left(\frac{u'}{\bar{u}}\right)^2} = \frac{\overline{(e' + e'_n)^2}}{S^2 G^2 E^2} - \left(\frac{E_n}{E}\right)^{\frac{2}{S}} \frac{\overline{e_n'^2}}{S^2 G_n^2 E_n^2} \quad 4.130$$

or in terms of the rms voltages measured with an rms meter

$$\overline{\left(\frac{u'}{\bar{u}}\right)^2} = \frac{\tilde{e}_T'^2}{S^2 G^2 E^2} - \left(\frac{E_n}{E}\right)^{\frac{2}{S}} \frac{\tilde{e}_n'^2}{S^2 G_n^2 E_n^2} \quad 4.131$$

where the subscript T refers to the total rms measurement.

The effect of noise on correlation measurements may be assessed as follows. Let the noise be a and b on two anemometer outputs v_1 and v_2 , then the cross-correlation function may be written as

$$R = \frac{\overline{(v_1 + a)(v_2 + b)}}{\left(\overline{(v_1 + a)^2}\right)^{\frac{1}{2}} \left(\overline{(v_2 + b)^2}\right)^{\frac{1}{2}}} = \frac{\overline{v_1 v_2}}{\left(\overline{v_1^2 + a^2}\right)^{\frac{1}{2}} \left(\overline{v_2^2 + b^2}\right)^{\frac{1}{2}}} \quad 4.132$$

since $\overline{v_1 a} = \overline{v_2 b} = \overline{v_1 b} = \overline{v_2 a} = \overline{ab} = 0$

If we write $\frac{\overline{v_1^2}}{a^2} = E_1$ & $\frac{\overline{v_2^2}}{b^2} = E_2$ then

$$\frac{R_{\text{True}}}{R_{\text{meas}}} = [(1 + E_1)(1 + E_2)]^{\frac{1}{2}} \quad 4.133$$

So we can see that the measured correlation increases with increased signal to noise ratio.

Section 5 The Hot-Wire in Compressible Flow

We shall see that hot-wire fluctuation measurements require detailed knowledge of the steady-state heat loss laws. Wire response to mean flow is well defined for the incompressible case. For isothermal, incompressible flow, a hot-wire responds only to velocity changes and the output can be correlated quite well over a wide range of Reynolds numbers. Fig. 5.1 is a summary plot of heat transfer measurements for circular cylinders in subsonic, continuum flow.

However, at high speeds, wire response is more complex since wire recovery factor is a function of both Mach number and Knudsen number. Fig. 5.2 was prepared as a guide to the experimental variation of Nusselt number as a function of Reynolds number and Mach number. The sensor output is reasonably well behaved for supersonic Mach numbers as indicated by the lower curve of fig. 5.2. However, the output is Mach number dependent in the transonic range particularly at low Reynolds number. It will be seen that the slope of the Nu vs. Re relationship is of particular concern in turbulence measurements. Fig. 5.3 shows the measured exponents as a function of Reynolds and Mach numbers for several investigations. At high Mach numbers, the exponent is seen to vary monotonically between the free molecular and continuum values. For an insulated wire, the slope begins to deviate from the continuum value at wire Reynolds numbers below 200. In continuum flow, wire recovery temperature is a function of Mach number since there is a changing relationship between frictional and compression effects. But, as

Mach number increases, these effects cancel so that the recovery temperature ratio becomes approximately constant at supersonic Mach numbers (fig. 5.4). In the transitional regime, measurements indicate that at Knudsen numbers of about 0.1 the recovery temperature begins to rise above the high Reynolds number value. Thus the recovery temperature can range from below to above total temperature. Measurements have been made over the complete range range from continuum to free molecular Knudsen numbers. These results are summarized in fig. 5.5. The direct effect of wire Reynolds number on wire recovery temperature in supersonic flow can be determined from fig. 5.6.

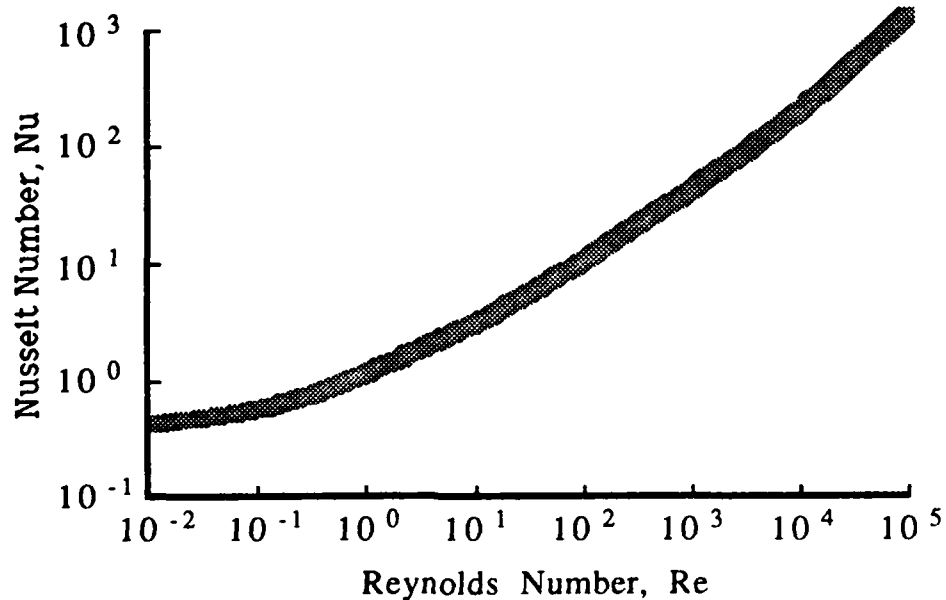


Fig. 5.1 Summary of heat loss from circular cylinders in cross-flow

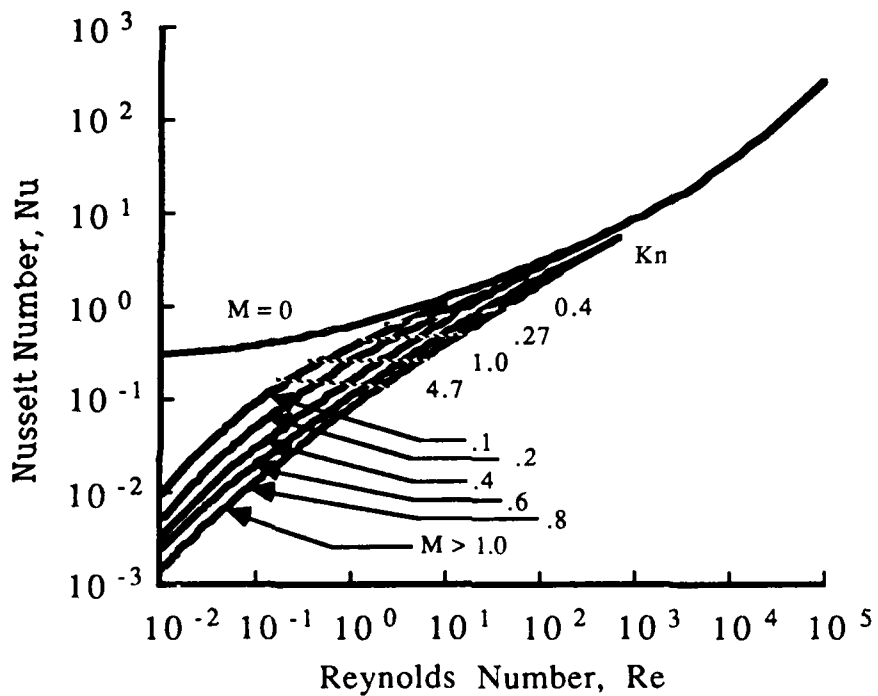


Fig. 5.2 Empirical correlations of hot-wire heat transfer at low Reynolds number.

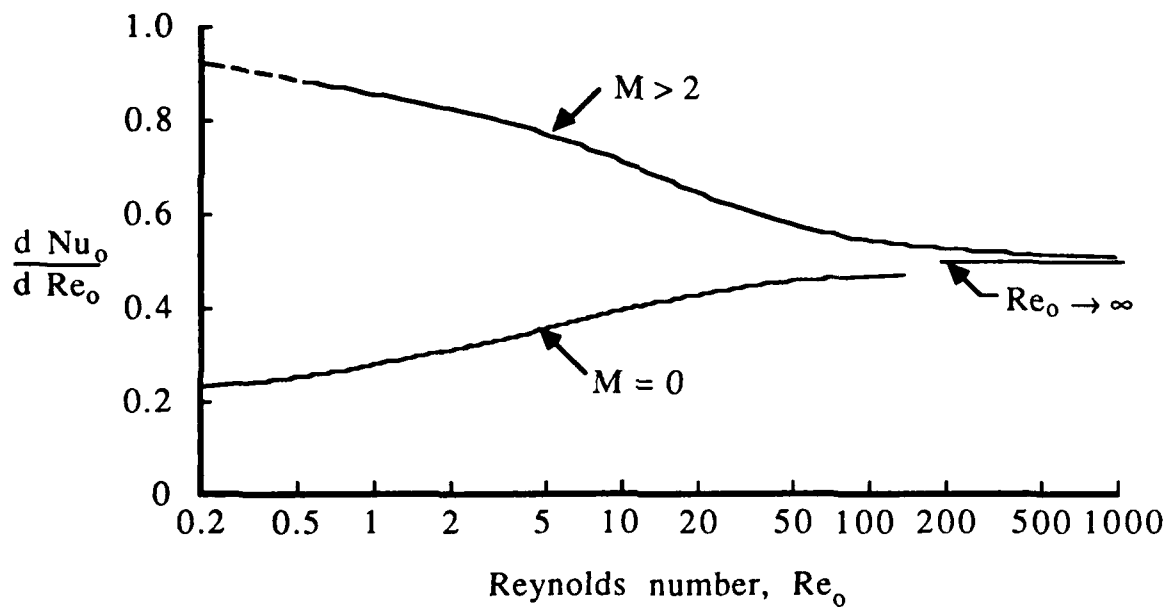


Fig. 5.3 Slope of Nusselt number - Reynolds number relation

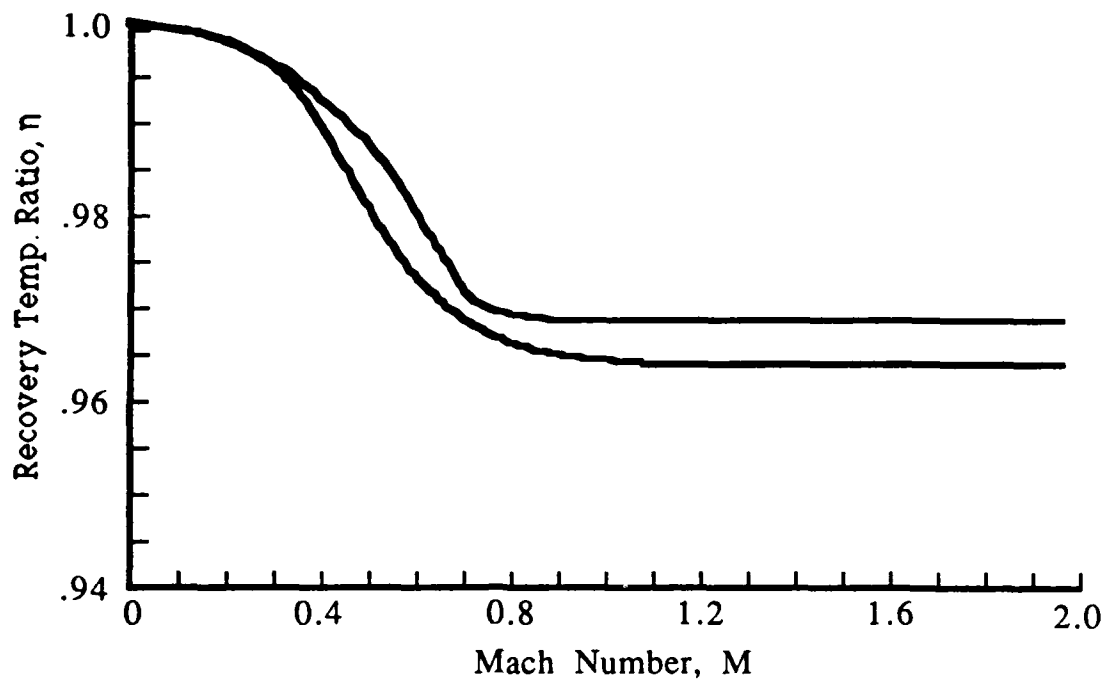


Fig. 5.4 Recovery temperature variations.

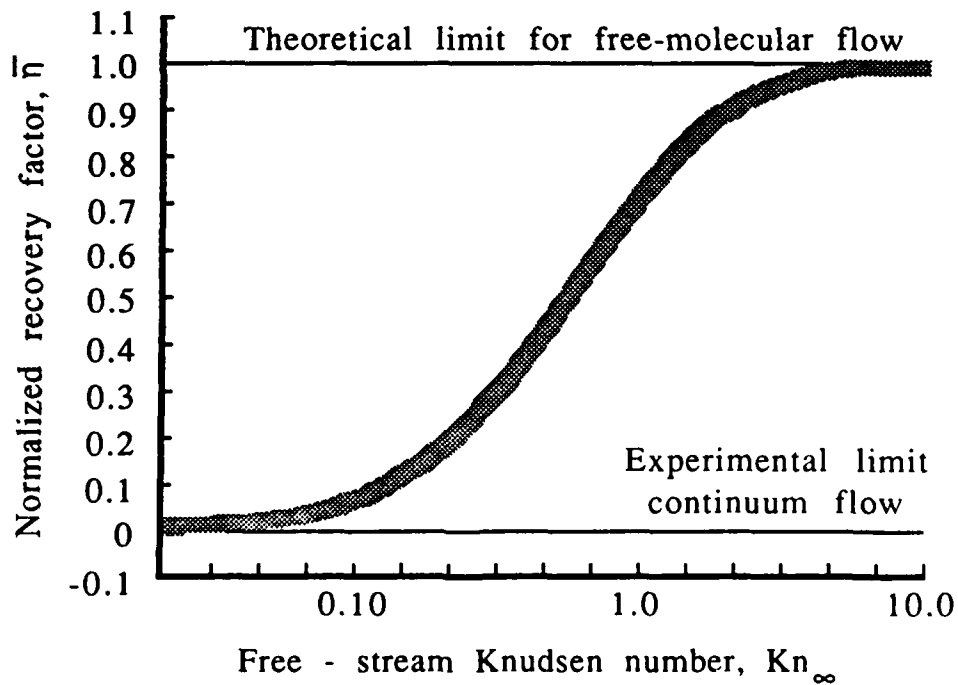


Fig. 5.5 Normalized variation of recovery temperature with Knudsen number.

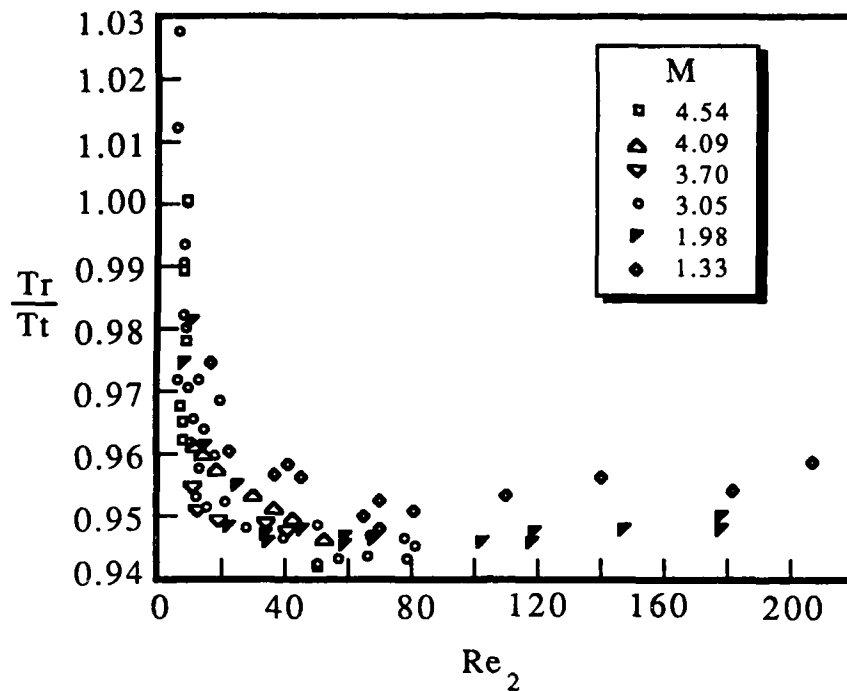


Fig. 5.6 Variations of recovery temperature in supersonic flow (ref. 1).

The derivation of the general fluctuation sensitivities of a hot-wire anemometer involves the perturbation of the steady-state heat transfer law and expressing the result in measurable electrical and fluid flow properties. In compressible flow, dimensional analysis and test data imply that

$$Nu = \lambda d/k = f(Re, M, \theta) \quad \theta = T_w/T_t \quad 5.1$$

and, assuming that the electrical energy input to the wire equals the heat loss due to convection, we may write

$$W = I^2 R = Nu_t \pi k_t L (T_w - \eta T_t) \quad 5.2$$

Consider first the electrical properties where

$$dW/W = 2 d \ln I + d \ln R_w \quad 5.3$$

But, since the wire current does change with wire resistance, we, in fact, have

$$\frac{dW}{W} = \frac{2 d \ln I}{d \ln R_w} d \ln R_w + d \ln R_w \quad 5.4$$

Now if we define the finite circuit parameter $\epsilon = (d \ln I)/(d \ln R_w)$ we obtain

$$d \ln W = (1 - 2\epsilon) d \ln R_w \quad 5.5$$

or

$$d \ln W = (1 - 2\epsilon)(d \ln R_w/d \ln T_w)d \ln T_w = (1 - 2\epsilon)K d \ln T_w \quad 5.6$$

where $K = d \ln R_w/d \ln T_w$. Now

$$\begin{aligned} d \ln e &= d \ln I R_w \\ &= d \ln I + d \ln R_w \\ &= \left(1 + \frac{d \ln I}{d \ln R_w}\right) = (1 - \epsilon) \end{aligned} \quad 5.7$$

Since

$$d \ln e = (1 - \epsilon) \frac{d \ln R_w}{d \ln T_w} d \ln T_w = (1 - \epsilon)K d \ln T_w \quad 5.8$$

then

$$d \ln e = \frac{(1 - \epsilon)}{(1 - 2\epsilon)} d \ln W \quad 5.9$$

Also, combining equations 5.6 and 5.9, we determine that

$$d \ln T_w = d \ln e / K(1 - \epsilon) \quad 5.10$$

These are important relationships between wire heat transfer and measurable wire properties, which will be used later.

Now we need to determine similar logarithmic variations in heat loss. To do this we write

$$H = \pi L k_t (T_w - \eta T_t) Nu_t Re_t \quad 5.11$$

$$H = \pi L k_t (T_w - \eta T_t) Nu_t Re_t \quad 5.11$$

Now, using the chain rule

$$dH = dk_t \frac{\partial H}{\partial k_t} + dT_w \frac{\partial H}{\partial T_w} + dNu \frac{\partial H}{\partial Nu} + d\eta \frac{\partial H}{\partial \eta} + dT_t \frac{\partial H}{\partial T_t} \quad 5.12$$

If we divide by H, the first term on the RHS of equation 5.12 becomes

$$\frac{1}{H} \frac{\partial H}{\partial k_t} dk_t = \frac{Nu(T_w - \eta T_t)}{k_t Nu(T_w - \eta T_t)} dk_t = \frac{dk_t}{k_t} = d \ln k_t = n_t d \ln T_t$$

the second term becomes

$$\frac{k_t Nu}{k_t Nu(T_w - \eta T_t)} dT_w = \frac{dT_w}{(T_w - \eta T_t)} = \frac{T_w/T_t}{(T_w/T_t - \eta)} d \ln T_w = \frac{\Theta}{(\Theta - \eta)} d \ln T_w$$

the third term becomes

$$\frac{k_t (T_w - \eta T_t)}{k_t Nu(T_w - \eta T_t)} dNu = \frac{dNu}{Nu} = d \ln Nu$$

the fourth term becomes

$$-\frac{T_t k_t Nu}{k_t Nu(T_w - \eta T_t)} d\eta = -\frac{d\eta}{(T_w/T_t - \eta)} = -\frac{\eta}{(\Theta - \eta)} d \ln \eta$$

and finally the fifth term becomes

$$\begin{aligned} -\frac{\eta k_t Nu}{k_t Nu(T_w - \eta T_t)} dT_t &= -\frac{\eta}{(\Theta - \eta)} d \ln T_t \\ &= -\left(\frac{\Theta - \eta - \Theta}{(\Theta - \eta)}\right) d \ln T_t \\ &= -\left(1 + \frac{\eta}{(\Theta - \eta)}\right) d \ln T_t \end{aligned}$$

Now defining the overheat parameter as

$$\zeta_{wr} = \frac{T_w - T_r}{T_r} = \frac{(\Theta - \eta)}{\eta} \quad 5.13$$

and collecting terms we obtain

$$d \ln H = \frac{\theta}{\theta - \eta} d \ln T_w + \left[n_t - 1 - \frac{1}{\tau_{wr}} \right] d \ln T_t - \frac{1}{\tau_{wr}} d \ln \eta + d \ln Nu \quad 5.14$$

Now, compressible flow measurements suggest that $Nu = f(Re_t, M, \theta, \rho, \phi)$ and $\eta = f(Re_t, M, \theta, \rho, \phi)$. Thus, as a first step, we must determine the auxiliary dependence of M and Re_t on the sensing variables. Accordingly, we may write $Re_t = \rho u d / \mu_t$ as

$$d \ln Re_t = d \ln \rho + d \ln u - d \ln \mu_t \quad 5.15$$

if $\mu \cong T_t^{m_t}$ then

$$d \ln Re_t = d \ln \rho + d \ln u - m_t d \ln T_t \quad 5.16$$

Now the iso-energetic compressible relation gives

$$M^2 = \frac{u^2}{\gamma RT} \left(1 + \frac{\gamma-1}{2} \frac{u^2}{\gamma RT} \right)^{-1} = \frac{u^2}{\gamma RT} \quad 5.17$$

so that

$$d \ln M = \alpha^{-1} (d \ln u - 1/2 (d \ln T_t)) \quad 5.18$$

$$\text{where } \alpha = \left(1 + \frac{\gamma-1}{2} M^2 \right)^{-1}$$

Now, using the chain rule once again, we may write

$$d \eta = \frac{\partial \eta}{\partial Re_t} d Re_t + \frac{\partial \eta}{\partial M} d M + \frac{\partial \eta}{\partial \rho} d \rho + \frac{\partial \eta}{\partial \phi} d \phi \quad 5.19$$

dividing by η , we may write the first term as

$$\left(\frac{\partial \eta}{\eta} / \frac{\partial Re_t}{Re_t} \right) \frac{d Re_t}{Re_t} = \frac{\partial \ln \eta}{\partial \ln Re_t} d \ln Re_t$$

and, treating successive terms, we obtain

$$d \ln \eta = \frac{\partial \ln \eta}{\partial \ln Re_t} d \ln Re_t + \frac{\partial \ln \eta}{\partial \ln M} d \ln M + \frac{\partial \ln \eta}{\partial \ln \rho} d \ln \rho$$

$$+ \frac{\partial \ln \eta}{\partial \ln \phi} d \ln \phi$$

which may be rewritten, using equations 5.16 and 5.18, as

$$d \ln \eta = \frac{\partial \ln \eta}{\partial \ln Re_t} (d \ln u + d \ln \rho - m_t d \ln T_t)$$

$$+ \frac{\partial \ln \eta}{\partial \ln M} \left(\frac{d \ln u}{\alpha} - \frac{d \ln T_t}{2\alpha} \right) + \frac{\partial \ln \eta}{\partial \ln \rho} d \ln \rho$$

$$+ \frac{\partial \ln \eta}{\partial \ln \phi} d \ln \phi \quad 5.20$$

In a similar manner we determine that

$$d \ln Nu = \frac{\partial \ln Nu}{\partial \ln Re_t} d \ln Re_t + \frac{\partial \ln Nu}{\partial \ln M} d \ln M + \frac{\partial \ln Nu}{\partial \ln \rho} d \ln \rho$$

$$+ \frac{\partial \ln Nu}{\partial \ln \Theta} d \ln \Theta + \frac{\partial \ln Nu}{\partial \ln \phi} d \ln \phi \quad 5.21$$

Now, since

$$d \ln \Theta = d \ln T_w - d \ln T_t \quad \left(\Theta = \frac{T_w}{T_t} \right) \quad 5.22$$

We may rewrite equation 5.21 as

$$d \ln Nu = \frac{\partial \ln Nu}{\partial \ln Re_t} (d \ln u + d \ln \rho - m_t d \ln T_t)$$

$$+ \frac{\partial \ln Nu}{\partial \ln \Theta} (d \ln T_w - d \ln T_t) + \frac{\partial \ln Nu}{\partial \ln \rho} d \ln \rho$$

$$+ \frac{\partial \ln Nu}{\partial \ln \phi} d \ln \phi \quad 5.23$$

Substituting for $d \ln \eta$ and $d \ln Nu$ in equation 5.14 and collecting like terms, we determine that:

$$\begin{aligned}
d \ln H = & \left[n_t - m_t \frac{Re_t}{Nu_t} \frac{\partial Nu_t}{\partial Re_t} - \frac{\Theta}{Nu_t} \frac{\partial Nu_t}{\partial \Theta} \right. \\
& \left. - \frac{1}{\tau_{wr}} \left\{ 1 - \frac{1}{2\alpha} \frac{M}{\eta} \frac{\partial \eta}{\partial M} - m_t \frac{Re_t}{\eta} \frac{\partial \eta}{\partial Re_t} \right\} - \frac{1}{2\alpha} \frac{M}{Nu_t} \frac{\partial Nu_t}{\partial M} \right] d \ln T_t \\
+ & \left[\frac{Re_t}{Nu_t} \frac{\partial Nu_t}{\partial Re_t} + \frac{1}{\alpha} \frac{M}{Nu_t} \frac{\partial Nu_t}{\partial M} - \frac{1}{\tau_{wr}} \left\{ \frac{1}{\alpha} \frac{M}{\eta} \frac{\partial \eta}{\partial M} + \frac{Re_t}{\eta} \frac{\partial \eta}{\partial Re_t} \right\} \right] d \ln u \\
+ & \left[\frac{Re_t}{Nu_t} \frac{\partial Nu_t}{\partial Re_t} - \frac{1}{\tau_{wr}} \frac{Re_t}{\eta} \frac{\partial \eta}{\partial Re_t} \right] d \ln \rho + \left[\frac{\Theta}{Nu_t} \frac{\partial Nu_t}{\partial \Theta} + \frac{\Theta}{\Theta - \eta} \right] d \ln Tw \\
+ & \left[\frac{\phi}{Nu_t} \frac{\partial Nu_t}{\partial \phi} - \frac{1}{\tau_{wr}} \frac{\phi}{\eta} \frac{\partial \eta}{\partial \phi} \right] d \ln \phi \qquad 5.24
\end{aligned}$$

Since we have previously shown that

$$d \ln W = d \ln H = \left(\frac{1 - 2\epsilon}{1 - \epsilon} \right) d \ln e \quad \text{and} \quad d \ln Tw = \frac{d \ln e}{K(1 - \epsilon)}$$

we can rewrite equation 5.24 as

$$\begin{aligned}
& \left(\frac{1 - 2\epsilon}{1 - \epsilon} \right) d \ln e - \left[\frac{d \ln Nu}{d \ln \Theta} + \frac{\Theta}{\Theta - \eta} \right] \frac{d \ln e}{K(1 - \epsilon)} \\
& = \left[n_t - m_t \frac{Re_t}{Nu_t} \frac{\partial Nu_t}{\partial Re_t} - \frac{\Theta}{Nu_t} \frac{\partial Nu_t}{\partial \Theta} \right. \\
& \quad \left. - \frac{1}{\tau_{wr}} \left\{ 1 - \frac{1}{2\alpha} \frac{M}{\eta} \frac{\partial \eta}{\partial M} - m_t \frac{Re_t}{\eta} \frac{\partial \eta}{\partial Re_t} \right\} - \frac{1}{2\alpha} \frac{M}{Nu_t} \frac{\partial Nu_t}{\partial M} \right] d \ln T_t \\
& + \left[\frac{Re_t}{Nu_t} \frac{\partial Nu_t}{\partial Re_t} + \frac{1}{\alpha} \frac{M}{Nu_t} \frac{\partial Nu_t}{\partial M} - \frac{1}{\tau_{wr}} \left\{ \frac{1}{\alpha} \frac{M}{\eta} \frac{\partial \eta}{\partial M} + \frac{Re_t}{\eta} \frac{\partial \eta}{\partial Re_t} \right\} \right] d \ln u \\
& + \left[\frac{Re_t}{Nu_t} \frac{\partial Nu_t}{\partial Re_t} - \frac{1}{\tau_{wr}} \frac{Re_t}{\eta} \frac{\partial \eta}{\partial Re_t} \right] d \ln \rho \\
& + \left[\frac{\phi}{Nu_t} \frac{\partial Nu_t}{\partial \phi} - \frac{1}{\tau_{wr}} \frac{\phi}{\eta} \frac{\partial \eta}{\partial \phi} \right] d \ln \phi \qquad 5.25
\end{aligned}$$

Now

$$d \ln W = d \ln I^2 R_w = \frac{\partial \ln R_w}{\partial \ln I} d \ln I + 2(d \ln I) \qquad 5.26$$

and, for fixed flow conditions, equation 5.14 gives

$$d \ln H = \left[\frac{d \ln Nu}{d \ln \Theta} + \frac{\Theta}{\Theta - \eta} \right] d \ln T_w \quad 5.27$$

So that, introducing $A_w' = 1/2(\partial \ln R_w / \partial \ln I)$ and equating $W = H$, we obtain

$$(2A_w' + 2) d \ln I = \left[\frac{d \ln Nu}{d \ln \Theta} + \frac{\Theta}{\Theta - \eta} \right] \frac{2A_w'}{K} d \ln I \quad 5.28$$

so that

$$K \left[1 + \frac{1}{A_w'} \right] = \left[\frac{d \ln Nu}{d \ln \Theta} + \frac{\Theta}{\Theta - \eta} \right] \quad 5.29$$

and so the LHS of equation 5.25 reduces to

$$\left(\frac{1 - 2\epsilon}{1 - \epsilon} \right) d \ln e - K \left[1 + \frac{1}{A_w'} \right] \frac{d \ln e}{K(1 - \epsilon)} = \frac{1}{A_w'} \left(\frac{1 - 2\epsilon A_w'}{1 - \epsilon} \right) d \ln e$$

If we define $E' = (1 - \epsilon)/(1 - 2\epsilon A_w')$, then we determine that

$$\begin{aligned} d \ln e = E' A_w' & \left[\left[n_t - m_t \frac{Re_t}{Nu_t} \frac{\partial Nu_t}{\partial Re_t} - \frac{\Theta}{Nu_t} \frac{\partial Nu_t}{\partial \Theta} \right. \right. \\ & \left. \left. - \frac{1}{\tau_{wr}} \left\{ 1 - \frac{1}{2\alpha} \frac{M}{\eta} \frac{\partial \eta}{\partial M} - m_t \frac{Re_t}{\eta} \frac{\partial \eta}{\partial Re_t} \right\} - \frac{1}{2\alpha} \frac{M}{Nu_t} \frac{\partial Nu_t}{\partial M} \right] d \ln T_t \right. \\ & + \left[\frac{Re_t}{Nu_t} \frac{\partial Nu_t}{\partial Re_t} + \frac{1}{\alpha} \frac{M}{Nu_t} \frac{\partial Nu_t}{\partial M} - \frac{1}{\tau_{wr}} \left\{ \frac{1}{\alpha} \frac{M}{\eta} \frac{\partial \eta}{\partial M} + \frac{Re_t}{\eta} \frac{\partial \eta}{\partial Re_t} \right\} \right] d \ln u \\ & + \left[\frac{Re_t}{Nu_t} \frac{\partial Nu_t}{\partial Re_t} - \frac{1}{\tau_{wr}} \frac{Re_t}{\eta} \frac{\partial \eta}{\partial Re_t} \right] d \ln \rho \\ & \left. + \left[\frac{\phi}{Nu_t} \frac{\partial Nu_t}{\partial \phi} - \frac{1}{\tau_{wr}} \frac{\phi}{\eta} \frac{\partial \eta}{\partial \phi} \right] d \ln \phi \right] \quad 5.30 \end{aligned}$$

where the last term in equation 5.30 may be rewritten as

$$\left[\frac{1}{\tau_{wr}} \frac{\partial \ln \eta}{\partial \phi} - \frac{\partial \ln Nu_t}{\partial \phi} \right] d \phi$$

Now, following Kovaszny (ref. 9), the basic equation for a hot-wire

inclined to the flow may be written as

$$\frac{e'}{e} = \Delta e_{\rho} \frac{\rho'}{\bar{\rho}} + \Delta e_{u} \frac{u'}{\bar{u}} + \Delta e_{T_r} \frac{T_r'}{T_r} \pm \Delta e_{\phi} \frac{v'}{\bar{u}} \quad 5.31$$

where the sign conventions must be determined separately for constant current and constant temperature operation as will be shown in section 6. Replacing the logarithmic variables by fractional perturbations and approximating $d\phi$ by v'/\bar{u} , the hot-wire sensitivities in equation 5.31 may be finally written as

$$\Delta e_{T_r} \equiv \frac{E'}{100} \left[n_t - m_t \left(\frac{\partial \ln Nu}{\partial \ln Re_t} \right) - \left(\frac{\partial \ln Nu}{\partial \ln \Theta} \right) - \frac{1}{\tau_{wr}} \left\{ 1 - \frac{1}{2\alpha} \frac{M}{n} \frac{\partial n}{\partial M} - m_t \frac{Re_t}{n} \frac{\partial n}{\partial Re_t} \right\} - \frac{1}{2\alpha} \left(\frac{\partial \ln Nu}{\partial \ln M} \right) \right] \quad 5.32$$

$$\Delta e_u \equiv \frac{E'}{100} \left[\left(\frac{\partial \ln Nu}{\partial \ln Re_t} \right) + \frac{1}{\alpha} \left(\frac{\partial \ln Nu}{\partial \ln M} \right) - \frac{1}{\tau_{wr}} \left\{ \frac{1}{\alpha} \left(\frac{\partial \ln n}{\partial \ln M} \right) + \left(\frac{\partial \ln n}{\partial \ln Re_t} \right) \right\} \right] \quad 5.33$$

$$\Delta e_{\rho} \equiv \frac{E'}{100} \left[\left(\frac{\partial \ln Nu}{\partial \ln Re_t} \right) - \frac{1}{\tau_{wr}} \left(\frac{\partial \ln n}{\partial \ln Re_t} \right) \right] \quad 5.34$$

and

$$\Delta e_v \equiv \frac{E'}{100} \left[\frac{1}{\tau_{wr}} \left(\frac{\partial \ln n}{\partial \phi} \right) - \left(\frac{\partial \ln Nu}{\partial \phi} \right) \right] \quad 5.35$$

We shall see that the proportionality constants are related to the particular electrical system and are different for constant current and constant temperature applications. However, these hot-wire sensitivities apply to all flows whether subsonic, supersonic, incompressible or compressible whether continuum or free molecular. For supersonic Mach numbers ie. $M \sin \phi > 1.2$ we have seen that all derivatives with respect to

Mach number are negligible so that $\Delta e_p = \Delta e_u$. Now, since

$$\frac{\partial(\rho u)}{\partial \bar{u}} = \frac{\partial \rho}{\partial \bar{u}} + \bar{u} \quad 5.36$$

equation 5.31 may be rewritten as

$$e' = \Delta e_{T_r} \frac{T_r'}{T_r} + \Delta e_{\rho u} \frac{(\rho u)'}{\rho u} \pm \Delta e_{\phi} \frac{v'}{u} \quad 5.37$$

Now let us consider how to evaluate various fluctuating terms for the case of a normal hot-wire, where we can rewrite equation 5.37 as

$$e' = \Delta e_{T_r} \frac{T_r'}{T_r} + \Delta e_{\rho u} \frac{(\rho u)'}{\rho u} \quad 5.38$$

We start by taking into consideration the so called Kovaszny diagram (ref. 9) as follows. Squaring both sides of equation 5.38 we get

$$\overline{e'^2} = \Delta e_{T_r}^2 \frac{\overline{T_r'^2}}{T_r^2} + 2(\Delta e_{T_r})(\Delta e_{\rho u}) \frac{(\overline{\rho u})' \overline{T_r'}}{(\overline{\rho u}) \overline{T_r}} + \Delta e_{\rho u}^2 \frac{(\overline{\rho u})'^2}{(\overline{\rho u})^2} \quad 5.39$$

Dividing through by $(\Delta e_{T_r})^2$ the above expression becomes

$$\frac{\overline{e'^2}}{(\Delta e_{T_r})^2} = \frac{(\overline{\rho u})'^2}{(\overline{\rho u})^2} \left(\frac{\Delta e_{\rho u}}{\Delta e_{T_r}} \right)^2 + 2 \frac{(\overline{\rho u})' \overline{T_r'}}{(\overline{\rho u}) \overline{T_r}} \left(\frac{\Delta e_{\rho u}}{\Delta e_{T_r}} \right) + \frac{\overline{T_r'^2}}{T_r^2} \quad 5.40$$

If we now define

$$\frac{\overline{e'^2}}{(\Delta e_{T_r})^2} = s^2 \quad \text{and} \quad \frac{\Delta e_{\rho u}}{\Delta e_{T_r}} = r$$

then our expression can be rewritten as

$$s^2 = \frac{(\overline{\rho u})'^2}{(\overline{\rho u})^2} r^2 + 2 \frac{(\overline{\rho u})' \overline{T_r'}}{(\overline{\rho u}) \overline{T_r}} r + \frac{\overline{T_r'^2}}{T_r^2} \quad 5.41$$

Kovaszny then suggests we plot s^2 versus r . This is a second order curve in r and the coefficients

$$\frac{\overline{(\rho u)^2}}{\overline{(\rho u)^2}}, \quad \frac{\overline{(\rho u) \overline{T_t}}}{\overline{(\rho u \overline{T_t})}}, \quad \frac{\overline{T_t^2}}{\overline{T_t^2}}$$

are obtained by a least square fit of the function $s^2 = f(r)$. These coefficients then become

$$2 \frac{\overline{(\rho u) \overline{T_t}}}{\overline{(\rho u \overline{T_t})}} = \frac{1}{D} \begin{vmatrix} N & \sum_{i=1}^N s_i^2 & \sum_{i=1}^N r_i^2 \\ \sum_{i=1}^N r_i & \sum_{i=1}^N r_i s_i^2 & \sum_{i=1}^N r_i^3 \\ \sum_{i=1}^N r_i^2 & \sum_{i=1}^N r_i^2 s_i^2 & \sum_{i=1}^N r_i^4 \end{vmatrix}$$

and

$$\frac{\overline{T_t^2}}{\overline{T_t^2}} = \frac{1}{D} \begin{vmatrix} \sum_{i=1}^N s_i^2 & \sum_{i=1}^N r_i & \sum_{i=1}^N r_i^2 \\ \sum_{i=1}^N r_i s_i^2 & \sum_{i=1}^N r_i^2 & \sum_{i=1}^N r_i^3 \\ \sum_{i=1}^N r_i^2 s_i^2 & \sum_{i=1}^N r_i^3 & \sum_{i=1}^N r_i^4 \end{vmatrix}$$

where

$$D \equiv \begin{vmatrix} N & \sum_{i=1}^N r_i & \sum_{i=1}^N r_i^2 \\ \sum_{i=1}^N r_i & \sum_{i=1}^N r_i^2 & \sum_{i=1}^N r_i^3 \\ \sum_{i=1}^N r_i^2 & \sum_{i=1}^N r_i^3 & \sum_{i=1}^N r_i^4 \end{vmatrix}$$

and N is the total number of points used.

In order to obtain other terms which appear directly in the turbulent

momentum and energy equations, we assume that we have an isentropic flow field. This permits us to write the energy equation in its differential form as

$$\frac{1}{\alpha} \frac{\partial T_t}{T_t} = (\gamma - 1) M^2 \frac{\partial u}{u} + \frac{\partial p}{p} - \frac{\partial \rho}{\rho} \quad 5.42$$

$$\text{where } \alpha = 1 / \left(1 + \frac{\gamma - 1}{2} M^2 \right)$$

Next let us consider the equation for the mass flow per unit area and time in its differential form

$$\frac{\partial m}{m} = \frac{\partial u}{u} + \frac{\partial \rho}{\rho} \quad 5.43$$

Substituting for $\partial \rho / \rho$ in equation 5.42 gives

$$\frac{1}{\alpha} \frac{\partial T_t}{T_t} = (\gamma - 1) M^2 \frac{\partial u}{u} + \frac{\partial p}{p} - \frac{\partial m}{m} + \frac{\partial u}{u} \quad 5.44$$

or, collecting terms, we obtain

$$\frac{\partial u}{u} = \frac{1}{\alpha [1 + (\gamma - 1) M^2]} \frac{\partial T_t}{T_t} - \frac{1}{[1 + (\gamma - 1) M^2]} \left[\frac{\partial p}{p} - \frac{\partial m}{m} \right] \quad 5.45$$

Which, defining $\beta = \alpha(\gamma - 1)M^2$, can be written as

$$\frac{\partial u}{u} = \left(\frac{1}{\alpha + \beta} \right) \frac{\partial T_t}{T_t} - \left(\frac{\alpha}{\alpha + \beta} \right) \left[\frac{\partial p}{p} - \frac{\partial m}{m} \right] \quad 5.46$$

so that, since $p'/\bar{p} \leq 1.0$

$$\frac{u'}{\bar{u}} = \left(\frac{1}{\alpha + \beta} \right) \frac{T_t'}{\bar{T}_t} + \left(\frac{\alpha}{\alpha + \beta} \right) \frac{(\rho u)'}{(\bar{\rho} \bar{u})} \quad 5.47$$

Squaring both sides of this equation leads to the expression for the streamwise turbulence intensity

$$\frac{\overline{u'^2}}{\overline{u}^2} = \left(\frac{1}{\alpha + \beta}\right)^2 \frac{\overline{T_t'^2}}{\overline{T_t}^2} + \left(\frac{2\alpha}{\alpha + \beta}\right) \frac{\overline{(\rho u)' T_t'}}{\overline{(\rho u) T_t}} + \left(\frac{\alpha}{\alpha + \beta}\right)^2 \frac{\overline{(\rho u)'^2}}{\overline{(\rho u)}^2} \quad 5.48$$

In order to obtain an expression for the density fluctuation, we consider the mass flow equation in the form

$$\frac{\partial \rho}{\rho} = \frac{\partial m}{m} - \frac{\partial u}{u} \quad 5.49$$

Substituting in equation 5.46 and again neglecting pressure fluctuations we obtain

$$\frac{\partial \rho}{\rho} = \left[1 - \frac{\alpha}{\alpha + \beta}\right] \frac{\partial m}{m} - \left(\frac{1}{\alpha + \beta}\right) \frac{\partial T_t}{T_t} \quad 5.50$$

which may be written as

$$\frac{\partial \rho}{\rho} = \left(\frac{\beta}{\alpha + \beta}\right) \frac{\partial(\rho u)}{\rho u} - \left(\frac{1}{\alpha + \beta}\right) \frac{\partial T_t}{T_t} \quad 5.51$$

ie.

$$\frac{\rho'}{\rho} = \left(\frac{\beta}{\alpha + \beta}\right) \frac{(\rho u)'}{\rho u} - \left(\frac{1}{\alpha + \beta}\right) \frac{T_t'}{T_t} \quad 5.52$$

while the squared term may be written as

$$\frac{\overline{\rho'^2}}{\overline{\rho}^2} = \left(\frac{\beta}{\alpha + \beta}\right)^2 \frac{\overline{(\rho u)'^2}}{\overline{(\rho u)}^2} - \left(\frac{2\beta}{\alpha + \beta}\right) \frac{\overline{(\rho u)' T_t'}}{\overline{(\rho u) T_t}} + \left(\frac{1}{\alpha + \beta}\right)^2 \frac{\overline{T_t'^2}}{\overline{T_t}^2} \quad 5.53$$

The mass fluctuation can now be derived by setting

$$\begin{aligned} \frac{\rho' u'}{\rho u} &= \frac{\rho'}{\rho} \times \frac{u'}{u} = \left[\left(\frac{\beta}{\alpha + \beta}\right) \frac{(\rho u)'}{\rho u} - \left(\frac{1}{\alpha + \beta}\right) \frac{T_t'}{T_t} \right] \\ &\quad \times \left[\left(\frac{\alpha}{\alpha + \beta}\right) \frac{(\rho u)'}{\rho u} + \left(\frac{1}{\alpha + \beta}\right) \frac{T_t'}{T_t} \right] \end{aligned} \quad 5.54$$

time averaging we obtain

$$\frac{\overline{\rho' u'}}{\overline{\rho u}} = \frac{\alpha \beta}{(\alpha + \beta)^2} \frac{\overline{(\rho u)'^2}}{\overline{(\rho u)}^2} + \frac{(\beta - \alpha)}{(\alpha + \beta)^2} \frac{\overline{(\rho u)' T_t'}}{\overline{(\rho u) T_t}} - \left(\frac{1}{\alpha + \beta}\right)^2 \frac{\overline{T_t'^2}}{\overline{T_t}^2} \quad 5.55$$

We can also determine expressions for the static temperature fluctuation and the term $\overline{u'T'}$ which is obtained by considering the perfect gas law

$$p = R(\rho T) \quad 5.56$$

or

$$\frac{\partial T}{T} = \frac{\partial p}{p} - \frac{\partial \rho}{\rho} \quad 5.57$$

Neglecting $\partial p/p$ because it is small compared to the other terms, we see that

$$\frac{\partial T}{T} = - \frac{\partial \rho}{\rho} \quad \text{or} \quad \frac{T'}{T} = - \frac{\rho'}{\rho} \quad 5.58$$

then from equation 5.53 we see that

$$\frac{T'}{T} = - \left[\left(\frac{\beta}{\alpha + \beta} \right) \frac{(\rho u)'}{\rho \bar{u}} - \left(\frac{1}{\alpha + \beta} \right) \frac{T_t'}{T_t} \right] \quad 5.59$$

so that

$$\begin{aligned} \frac{u'T'}{\bar{u}\bar{T}} &= \frac{u'}{\bar{u}} \times \frac{T'}{T} = \left[\left(\frac{\alpha}{\alpha + \beta} \right) \frac{(\rho u)'}{\rho \bar{u}} + \left(\frac{1}{\alpha + \beta} \right) \frac{T_t'}{T_t} \right] \\ &\quad \times - \left[\left(\frac{\beta}{\alpha + \beta} \right) \frac{(\rho u)'}{\rho \bar{u}} - \left(\frac{1}{\alpha + \beta} \right) \frac{T_t'}{T_t} \right] \end{aligned} \quad 5.60$$

which may be rewritten as

$$\frac{\overline{u'T'}}{\bar{u}\bar{T}} = - \left[\frac{(\alpha - \beta)}{(\alpha + \beta)^2} \frac{\overline{(\rho u)'T_t'}}{\rho \bar{u} T_t} - \frac{\alpha \beta}{(\alpha + \beta)^2} \frac{\overline{(\rho u)'^2}}{(\rho \bar{u})^2} + \frac{1}{(\alpha + \beta)^2} \frac{\overline{T_t'^2}}{T_t^2} \right] \quad 5.61$$

The relationship between $\overline{\rho'u'}$ and $\overline{u'T'}$ can be determined using equation 5.58 since

$$\frac{\rho'}{\rho} \times \frac{u'}{\bar{u}} = - \frac{T'}{T} \times \frac{u'}{\bar{u}} \quad 5.62$$

so that

$$\overline{\rho u'} = -\frac{\bar{\rho}}{\bar{T}} (\overline{u'T'}) \quad 5.63$$

Other useful relationships between the measured and derived normal hot-wire parameters may also be obtained. Previously, we showed that

$$\frac{T'}{\bar{T}} = -\left[\left(\frac{\beta}{\alpha + \beta} \right) \frac{(\rho u)'}{\bar{\rho u}} - \left(\frac{1}{\alpha + \beta} \right) \frac{T'_t}{\bar{T}_t} \right] \quad 5.59$$

and

$$\frac{u'}{\bar{u}} = \left(\frac{1}{\alpha + \beta} \right) \frac{T'_t}{\bar{T}_t} + \left(\frac{\alpha}{\alpha + \beta} \right) \frac{(\rho u)'}{(\bar{\rho u})} \quad 5.47$$

Solving both equations for $(\rho u)' / (\bar{\rho u})$ leads to

$$\frac{(\rho u)'}{(\bar{\rho u})} = \left(\frac{\alpha + \beta}{\alpha} \right) \left[\frac{u'}{\bar{u}} - \left(\frac{1}{\alpha + \beta} \right) \frac{T'_t}{\bar{T}_t} \right] = \left(\frac{\alpha + \beta}{\beta} \right) \left[\left(\frac{1}{\alpha + \beta} \right) \frac{T'_t}{\bar{T}_t} - \frac{T'}{\bar{T}} \right] \quad 5.64$$

so that

$$\left(\frac{\alpha + \beta}{\alpha} \right) \frac{u'}{\bar{u}} - \frac{1}{\alpha} \frac{T'_t}{\bar{T}_t} = \frac{1}{\beta} \frac{T'_t}{\bar{T}_t} - \left(\frac{\alpha + \beta}{\beta} \right) \frac{T'}{\bar{T}} \quad 5.65$$

then

$$\left(\frac{\alpha + \beta}{\alpha \beta} \right) \frac{T'_t}{\bar{T}_t} = \left(\frac{\alpha + \beta}{\alpha} \right) \frac{u'}{\bar{u}} + \left(\frac{\alpha + \beta}{\beta} \right) \frac{T'}{\bar{T}} \quad 5.66$$

multiplying through by $\alpha\beta/(\alpha + \beta)$ we get

$$\frac{T'_t}{\bar{T}_t} = \beta \frac{u'}{\bar{u}} + \alpha \frac{T'}{\bar{T}} \quad 5.67$$

Now, since

$$\frac{T'_t}{\bar{T}_t} = \beta \frac{u'}{\bar{u}} + \alpha \frac{T'}{\bar{T}} = (\alpha + \beta) \frac{T'}{\bar{T}} + \beta \frac{(\rho u)'}{(\bar{\rho u})} \quad 5.68$$

then

$$\frac{(\rho u)'}{(\bar{\rho u})} = \frac{1}{\beta} \left[\beta \frac{u'}{\bar{u}} + \alpha \frac{T'}{\bar{T}} - (\alpha + \beta) \frac{T'}{\bar{T}} \right] \quad 5.69$$

so that

$$\frac{(\rho u)'}{(\overline{\rho u})} = \frac{u'}{\bar{u}} - \frac{T'}{\bar{T}} \quad 5.70$$

It should be noted that this last expression can also be derived from the fact that $m = \rho u$ and $p = R\rho T$ provided the assumption is made that the p'/\bar{p} is negligible.

It is important to recall that all the above relationships can be derived from single normal hot-wire measurements. However, other turbulent terms which appear in the momentum and energy equations require inclined hot-wire measurements.

Let us now consider the case of a yawed hot-wire. If we return to the hot-wire equation 5.37 and square it we see that

$$\overline{e'^2} = \left[\Delta e_{T_r} \frac{T'}{\bar{T}_t} + \Delta e_{\rho u} \frac{(\rho u)'}{(\overline{\rho u})} + \Delta e_v \frac{v'}{\bar{u}} \right]^2 \quad 5.71$$

expanding and collecting like terms we obtain

$$\begin{aligned} \overline{e'^2} = & (\Delta e_{\rho u})^2 \frac{\overline{(\rho u)'^2}}{(\overline{\rho u})^2} + (\Delta e_{T_r})^2 \frac{\overline{T_t'^2}}{\bar{T}_t^2} + (\Delta e_v)^2 \frac{\overline{v'^2}}{\bar{u}^2} + 2 (\Delta e_{T_r})(\Delta e_{\rho u}) \frac{\overline{(\rho u)'} T_t'}{(\overline{\rho u}) \bar{T}_t} \\ & + 2 (\Delta e_{T_r})(\Delta e_v) \frac{\overline{T_t' v'}}{\bar{u} \bar{T}_t} + 2 (\Delta e_{\rho u})(\Delta e_v) \frac{\overline{(\rho u)' v'}}{(\overline{\rho u}) \bar{u}} \end{aligned} \quad 5.72$$

Now we run the test twice at each point, once with the hot-wire at $\phi = 0^\circ$ and a second time with the wire at $\phi = 180^\circ$, then we can write that

$$\overline{e'^2}_{\phi=0^\circ} - \overline{e'^2}_{\phi=180^\circ} = \pm 4 (\Delta e_v) \left[(\Delta e_{T_r}) \frac{\overline{T_t' v'}}{\bar{u} \bar{T}_t} + (\Delta e_{\rho u}) \frac{\overline{(\rho u)' v'}}{(\overline{\rho u}) \bar{u}} \right] \quad 5.73$$

since

$$\left[(\Delta e_{T_r})(\Delta e_{\rho u}) \frac{(\overline{\rho u})' \overline{T_t}'}{(\overline{\rho u}) \overline{T_t}'} \right]_{\phi=0^\circ} = \left[(\Delta e_{T_r})(\Delta e_{\rho u}) \frac{(\overline{\rho u})' \overline{T_t}'}{(\overline{\rho u}) \overline{T_t}'} \right]_{\phi=180^\circ}$$

$$\left[(\Delta e_{T_r})(\Delta e_v) \frac{\overline{T_t} \overline{v}}{\overline{u} \overline{T_t}} \right]_{\phi=0^\circ} = - \left[(\Delta e_{T_r})(\Delta e_v) \frac{\overline{T_t} \overline{v}}{\overline{u} \overline{T_t}} \right]_{\phi=180^\circ}$$

and

$$\left[(\Delta e_{\rho u})(\Delta e_v) \frac{(\overline{\rho u})' \overline{v}'}{(\overline{\rho u}) \overline{u}} \right]_{\phi=0^\circ} = - \left[(\Delta e_{\rho u})(\Delta e_v) \frac{(\overline{\rho u})' \overline{v}'}{(\overline{\rho u}) \overline{u}} \right]_{\phi=180^\circ}$$

Dividing through by

$$\pm 4 (\Delta e_{T_r})(\Delta e_v)$$

we obtain

$$\frac{\overline{e}_{\phi=0^\circ}^2 - \overline{e}_{\phi=180^\circ}^2}{\pm 4 (\Delta e_{T_r})(\Delta e_v)} = \left(\frac{\Delta e_{\rho u}}{\Delta e_{T_r}} \right) \frac{(\overline{\rho u})' \overline{v}'}{(\overline{\rho u}) \overline{u}} + \frac{\overline{T_t} \overline{v}}{\overline{u} \overline{T_t}} \quad 5.74$$

However, if we define

$$s^* \equiv \frac{\overline{e}_{\phi=0^\circ}^2 - \overline{e}_{\phi=180^\circ}^2}{\pm 4 (\Delta e_{T_r})(\Delta e_v)} \quad 5.75$$

and

$$r \equiv \frac{\Delta e_{\rho u}}{\Delta e_{T_r}} \quad 5.76$$

then equation 5.74 can be rewritten as follows

$$s^* = \frac{(\overline{\rho u})' \overline{v}'}{(\overline{\rho u}) \overline{u}} r + \frac{\overline{T_t} \overline{v}}{\overline{u} \overline{T_t}} \quad 5.77$$

If we now plot s^* versus r we see that the function is linear with a slope of

$$\frac{(\overline{\rho u})'v'}{(\overline{\rho u})\bar{u}}$$

and an intercept of

$$\frac{\overline{T_t}'v'}{\bar{u}\overline{T_t}}$$

These values can also be obtained if we perform a least square fit to the data. It can be shown that, if we have N number of data points, this method gives

$$\frac{(\overline{\rho u})'v'}{(\overline{\rho u})\bar{u}} = \frac{N \sum_{i=1}^N r_i s_i^{*2} - \sum_{i=1}^N r_i \sum_{i=1}^N s_i^{*2}}{N \sum_{i=1}^N r_i^2 - \left(\sum_{i=1}^N r_i \right)^2} \quad 5.78$$

and

$$\frac{\overline{T_t}'v'}{\bar{u}\overline{T_t}} = \frac{\sum_{i=1}^N r_i \sum_{i=1}^N s_i^{*2} - \sum_{i=1}^N r_i \sum_{i=1}^N r_i s_i^{*2}}{N \sum_{i=1}^N r_i^2 - \left(\sum_{i=1}^N r_i \right)^2} \quad 5.79$$

At this point it should be noted that from the normal hot-wire measurements we have values for

$$\frac{(\overline{\rho u})^2}{(\overline{\rho u})}, \frac{(\overline{\rho u})'\overline{T_t}'}{(\overline{\rho u})\overline{T_t}}, \text{ and } \frac{\overline{T_t}'^2}{\overline{T_t}^2}$$

and from the yawed wire measurements we now know

$$\frac{(\overline{\rho u})'v'}{(\overline{\rho u})\bar{u}} \text{ and } \frac{\overline{T_t}'v'}{\bar{u}\overline{T_t}}$$

Since $e'^2_{\phi=0}$ will also have been recorded we can obtain the value of $\overline{v'^2}/\bar{u}^2$ from the following expression

$$\frac{\overline{v'^2}}{\overline{u^2}} = \frac{1}{(\Delta e_v)^2} \left[\overline{e'^2}_{\phi=0^\circ} - \left\{ \Delta e_{\rho u}^2 \frac{\overline{(\rho u)'^2}}{(\overline{\rho u})\overline{u}} + \Delta e_{T_r}^2 \frac{\overline{T_r'^2}}{\overline{T_r}^2} - 2(\Delta e_{T_r})(\Delta e_{\rho u}) \frac{\overline{(\rho u)'T_r'}}{(\overline{\rho u})\overline{T_r}} \right. \right. \\ \left. \left. \pm 2(\Delta e_{T_r})(\Delta e_v) \frac{\overline{T_r'v'}}{\overline{u}\overline{T_r}} \pm 2(\Delta e_{\rho u})(\Delta e_v) \frac{\overline{(\rho u)'v'}}{(\overline{\rho u})\overline{u}} \right\} \right] \quad 5.80$$

We can now determine the Reynolds shear stress term $\overline{u'v'}$ by multiplying equation 5.47 by v'/\overline{u} to obtain:

$$\frac{\overline{u'v'}}{\overline{u^2}} = \left(\frac{1}{\alpha + \beta} \right) \frac{\overline{T_r'v'}}{\overline{u}\overline{T_r}} + \left(\frac{\alpha}{\alpha + \beta} \right) \frac{\overline{(\rho u)'v'}}{(\overline{\rho u})\overline{u}} \quad 5.81$$

The term $\overline{v'T'}$ which appears in the turbulent Prandtl number formulation, equation 3.22, is obtained by multiplying equation 5.59 by v'/\overline{u} to obtain:

$$\frac{\overline{v'T'}}{\overline{u}\overline{T'}} = - \left[\left(\frac{\beta}{\alpha + \beta} \right) \frac{\overline{(\rho u)'v'}}{(\overline{\rho u})\overline{u}} - \left(\frac{1}{\alpha + \beta} \right) \frac{\overline{T_r'v'}}{\overline{u}\overline{T_r}} \right] \quad 5.82$$

Two other useful relationships may also be derived. Multiplying equation 5.67 by v'/\overline{u} gives

$$\frac{\overline{T_r'v'}}{\overline{u}\overline{T_r}} = \beta \frac{\overline{u'v'}}{\overline{u^2}} + \alpha \frac{\overline{v'T'}}{\overline{u}\overline{T'}} \quad 5.83$$

Similarly, from equation 5.70 we obtain

$$\frac{\overline{(\rho u)'v'}}{(\overline{\rho u})\overline{u}} = \frac{\overline{u'v'}}{\overline{u^2}} - \frac{\overline{v'T'}}{\overline{u}\overline{T'}} \quad 5.84$$

The triple correlation $\overline{\rho'u'v'}$ which appears in the compressible shear stress formulation (see section 1) can be determined from equation 5.47, 5.52 and the rms measurement of equation 5.80. So, at this point we know, in principle, how to obtain the turbulent flow properties and correlations which appear in the momentum and energy equations from variables determined directly by the hot-wire.

Although many years of effort have been expended in hot-wire anemometry research, it is still clearly an inexact science. We have seen that numerous assumptions must be made to estimate the fluctuating flow variables from the measured hot-wire quantities. Now let us turn our attention to some of the practical aspects of hot-wire anemometry.

**Section 6 Practical Procedures for Turbulence
Measurements**

We have seen in section 4 that, with appropriate electrical compensation, the time constant can be restored to frequencies sufficient to assume essentially instantaneous response. Imposing this constraint, we may rewrite the general expressions for wire sensitivity (ref. 1) for constant current as

$$\begin{aligned} \Delta e = & -\Delta e_{\rho} \left(100 \frac{\Delta \rho}{\rho}\right) - \Delta e_{u} \left(100 \frac{\Delta u}{U}\right) \\ & + \Delta e_{T.} \left(100 \frac{\Delta \bar{T}_o}{\bar{T}_o}\right) + \Delta e_{\phi} \left(100 \frac{\Delta v}{U}\right) \end{aligned} \quad 6.1$$

with

$$\Delta e_{\rho} = \frac{\bar{\epsilon} E'}{100} \left[A_w \frac{\partial \ln Nu_o}{\partial \ln Re_o} - \frac{A_w}{\tau_{wr}} \frac{\partial \ln \eta}{\partial \ln Re_o} \right] \quad 6.2$$

$$\begin{aligned} \Delta e_u = & \frac{\bar{\epsilon} E'}{100} \left[A_w \left\{ \frac{\partial \ln Nu_o}{\partial \ln Re_o} + \frac{1}{\alpha} \frac{\partial \ln Nu_o}{\partial \ln M} \right\} \right. \\ & \left. - \frac{A_w}{\tau_{wr}} \left\{ \frac{1}{\alpha} \frac{\partial \ln \eta}{\partial \ln M} + \frac{\partial \ln \eta}{\partial \ln Re_o} \right\} \right] \end{aligned} \quad 6.3$$

$$\begin{aligned} \Delta e_{T.} = & \frac{\bar{\epsilon} E'}{100} \left[K + A_w \left\{ K - 1 - n_t - m_t \frac{\partial \ln Nu_o}{\partial \ln Re_o} + \frac{1}{2\alpha} \frac{\partial \ln Nu_o}{\partial \ln M} \right\} \right. \\ & \left. - \frac{A_w}{\tau_{wr}} \left\{ \frac{1}{2\alpha} \frac{\partial \ln \eta}{\partial \ln M} + m_t \frac{\partial \ln \eta}{\partial \ln Re_o} \right\} \right] \end{aligned} \quad 6.4$$

and

$$\Delta e_{\phi} = -\frac{\bar{\epsilon} E' A_w}{100} \left[\frac{\partial \ln H}{\partial \phi} \right] = \frac{\bar{\epsilon} E' A_w}{100} \left[\frac{1}{\tau_{wr}} \frac{\partial \ln \eta}{\partial \phi} - \frac{\partial \ln Nu_o}{\partial \phi} \right] \quad 6.5$$

$$\text{where } E' = (1 - \epsilon)/(1 + 2A_w \epsilon) \quad 6.6$$

For constant temperature systems, the sensitivities are usually defined with respect to a fluctuating current, so we may write

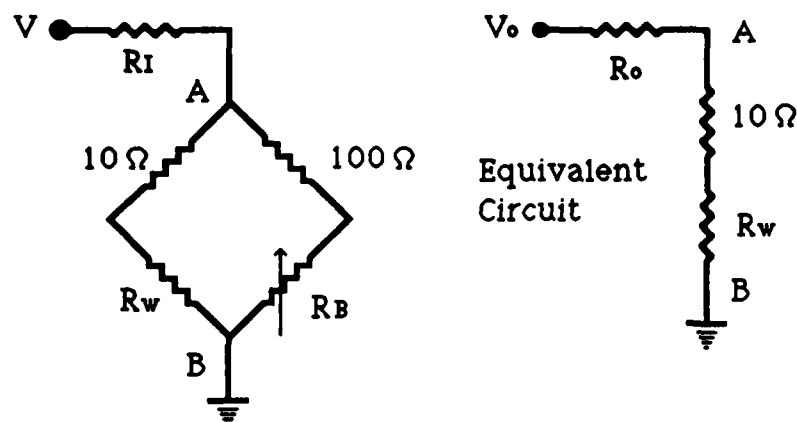
$$\begin{aligned} \Delta I = & \Delta I_{\rho} \left(100 \frac{\Delta \rho}{\rho} \right) + \Delta I_{\alpha} \left(100 \frac{\Delta u}{U} \right) \\ & - \Delta I_{T_0} \left(100 \frac{\Delta \bar{T}_0}{T_0} \right) + \Delta I_{\phi} \left(100 \frac{\Delta \phi}{U} \right) \end{aligned} \quad 6.7$$

We can obtain the sensitivities for ΔI from those for Δe by replacing $\bar{e}E'$ by IE'' , where E'' is the feed-back reduction factor defined in (ref. 10) as

$$E'' = - \frac{1}{2A\dot{w} + \frac{1}{\epsilon}} \quad 6.8$$

Thus, for the correct interpretation of the electrical signal from a hot-wire, we must consider the response of the electrical system, the variation of wire resistance with operating temperature and the fluid dynamic calibration.

Let us first consider the electrical system. We can see that an important term in any hot-wire anemometer measurement is the feedback parameter (ϵ) which relates wire power loss to measured wire voltage. Consider then the constant-current circuit shown on the next page where $\epsilon = -(d \log I_w)/(d \log R_w)$ and its equivalent circuit derived using Thevenin's theorem.



Now the open-circuit voltage across AB is

$$V_o = \frac{V(100 + R_B)}{(R_I + R_B + 100)} \quad 6.9$$

and the resistance in series with AB when V is shorted is

$$\begin{aligned} R_o &= \left(\frac{1}{100 + R_B} + \frac{1}{R_I} \right)^{-1} \\ &= \frac{R_I(R_B + 100)}{(R_I + R_B + 100)} \end{aligned} \quad 6.10$$

so that the wire current is

$$\begin{aligned} I_w &= \frac{V_o}{R_o + R_w + 10} = \frac{V(100 + R_B)(R_I + R_B + 100)}{(R_I + R_B + 100)(R_I(R_B + 100) + (10 + R_w)(R_I + R_B + 100))} \\ &= \frac{V(100 + R_B)}{R_I(R_B + R_w + 110) + (10 + R_w)(R_B + 100)} \end{aligned} \quad 6.11$$

Since

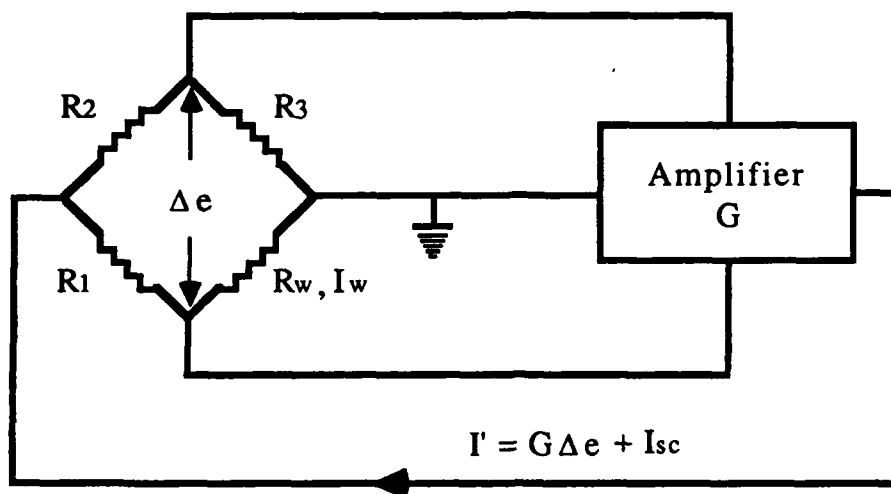
$$\frac{d \log I_w}{d \log R_w} = \frac{-R_w(R_I + R_B + 100)}{R_I(R_B + R_w + 110) + (10 + R_w)(R_B + 100)} \quad 6.12$$

then

$$\epsilon = \frac{R_w(R_I + R_B + 100)}{R_I(R_B + R_w + 110) + (10 + R_w)(R_B + 100)} \quad 6.13$$

Now consider the constant temperature system shown in the figure below where the amplifier is characterized by its transconductance, G, and its

short circuit current I_{sc} .



Now $I' = G\Delta e + I_{sc}$ and the relationship between the current I' supplied to the bridge and wire current I_w , is

$$I_w = I'\alpha' \quad \text{where} \quad \alpha' = \frac{R_2 + R_3}{R_1 + R_2 + R_3 + R_w} \quad 6.14$$

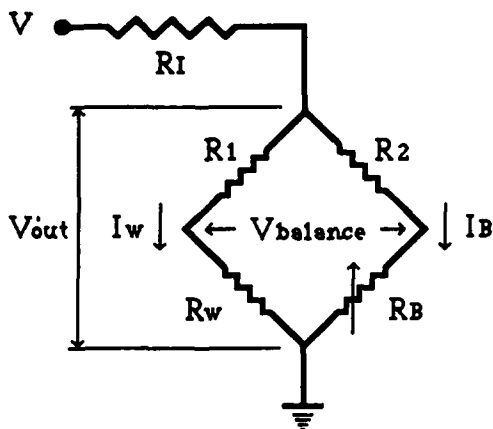
The unbalanced voltage is proportional to the bridge unbalance $R_b - R_w$ so that

$$\Delta e = \alpha'I'(R_b - R_w) \quad 6.15$$

Perturbing these equations leads to

$$\epsilon = -\frac{\partial \log I'}{\partial \log R_w} = -\frac{\partial \log I_w}{\partial \log R_w} = \frac{R_w G \alpha'}{1 - G \alpha' (R_b - R_w)} \quad 6.16$$

Thus we can relate wire voltage to the wire input power for both constant current and constant temperature anemometer systems. Next we need to determine the relationship between the measured output voltage and actual wire voltage as shown on the next page



$$V_{out} = e + R_1 I_w$$

$$V_{out} = e' + R_1 \frac{\partial I_w}{\partial R_w} R_w$$

$$V_{out} = e' + R_1 R_w \frac{I_w}{R_w} \frac{\partial I_w}{\partial R_w}$$

$$V_{out} = e' - R_1 R_w \frac{I_w}{R_w} \epsilon \quad 6.17$$

$$e = I_w R_w$$

$$e' = I_w' R_w + R_w I_w$$

$$e' = \frac{\partial I_w}{\partial R_w} R_w R_w + R_w I_w \quad 6.18$$

so that

$$V_{out} = e' - \frac{R_1}{R_w} e' \frac{\epsilon}{1 - \epsilon} = e' \left[1 - \frac{R_1}{R_w} \frac{\epsilon}{1 - \epsilon} \right] \quad 6.19$$

or

$$\text{RMS } V_{out} = \text{RMS } e' \left[1 - \frac{R_1}{R_w} \frac{\epsilon}{1 - \epsilon} \right] \quad 6.20$$

Now let us look at the parameters which govern the relationship between wire resistance and operating temperature. First consider the resistance-temperature relation and some wire properties given below.

Wire Properties

	Platinum	Platinum/10%Rhodium	Units
c_p	.032 @ 500°R .037 @ 850°R	slightly higher	cal/g°C
ρ	21.37	20.48	gm/cc
k	.17	.072	cal/sec cm °C
α_r	3.8×10^{-3}	1.6×10^{-3}	1/°C
γ_r	-.045	-.06	1/°C

The resistance-temperature relationship may be expressed as

$$R_w = R_f \{ 1 + \alpha_f (T_w - T_f) + \gamma_f [\alpha_f (T_w - T_f)]^2 \} \quad 6.21$$

where f is some reference condition. The parameter K which relates wire power input and temperature can be calculated from

$$\begin{aligned} K &\approx \frac{1}{1 + a_w} (\alpha_r T_r + a_w) = \frac{d \log R_w}{d \log T_w} \\ &= \frac{R_f}{R_w} T_w [\alpha_f + 2\gamma_f \alpha_f^2 (T_w - T_f)] \\ &= \frac{R_f}{R_w} \alpha_f T_w [1 + 2\gamma_f \alpha_f (T_w - T_f)] \end{aligned} \quad 6.22$$

Plots of K and wire temperature versus wire resistance ratios are shown in figures 6.1 and 6.2.

Wire overheat parameters may be determined as follows

$$a_w' = (R_w - R_r) / R_r \quad 6.23$$

where R_r is the recovery resistance of the wire. The recovery factor T_r/T_w varies between 0.96 and 1.1, but is essentially constant (0.96) for Mach numbers greater than 2.0 and Reynolds numbers greater than 20. Typically, $A_w' > a_w'$ by up to 20% at high overheat ratios and there are several ways to compute its value. A method which eliminates the differentiation of experimental data with a steep slope is detailed below. Experimentally it is easier to determine A_w' beginning with a plot of

$$\frac{I_w^2 R_w}{a_w} \text{ vs } a_w' = \frac{R_w - R_r}{R_r}$$

Now, defining C as the slope of $(I_w^2 R_w)/a_w'$ vs a_w' at high overheat,

$$\text{ie. } C = \frac{\left(\frac{I_w^2 R_w}{a_w}\right) a_w = 0 - \frac{I_w^2 R_w}{a_w}}{a_w \left(\frac{I_w^2 R_w}{a_w}\right)} \quad 6.24$$

then

$$A_w = \frac{a_w}{1 - (1 - a_w) \frac{C a_w}{1 - C a_w}} \quad 6.25$$

We are now in a position to determine the finite circuit parameter E' . The remaining terms in the sensitivity equations are defined as follows

\bar{e} = mean voltage across the wire H = total power to the wire

$$\tau_{wr} = \frac{T_w}{T_r} = \frac{a_w}{\alpha r T_r} (1 - a_w \gamma_r) \quad 6.26$$

$$\alpha = \frac{1}{1 + \frac{\gamma - 1}{2} M^2} \quad 6.27$$

$$m_t = \frac{\partial \log \mu}{\partial \log T_t} = .65 \quad \text{and} \quad n_t = \frac{\partial \log k}{\partial \log T_t} = .75$$

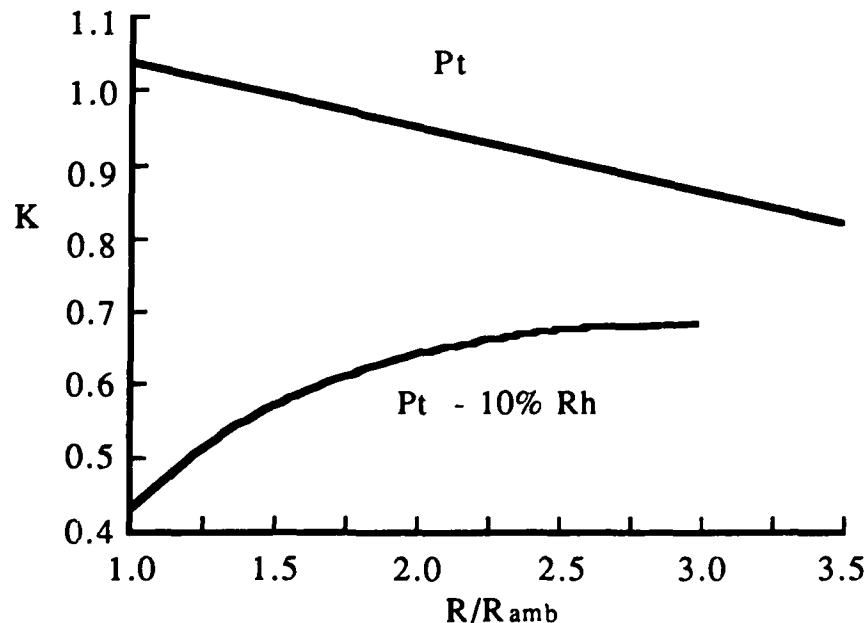


Fig. 6.1 Variation of parameter K with wire temperature

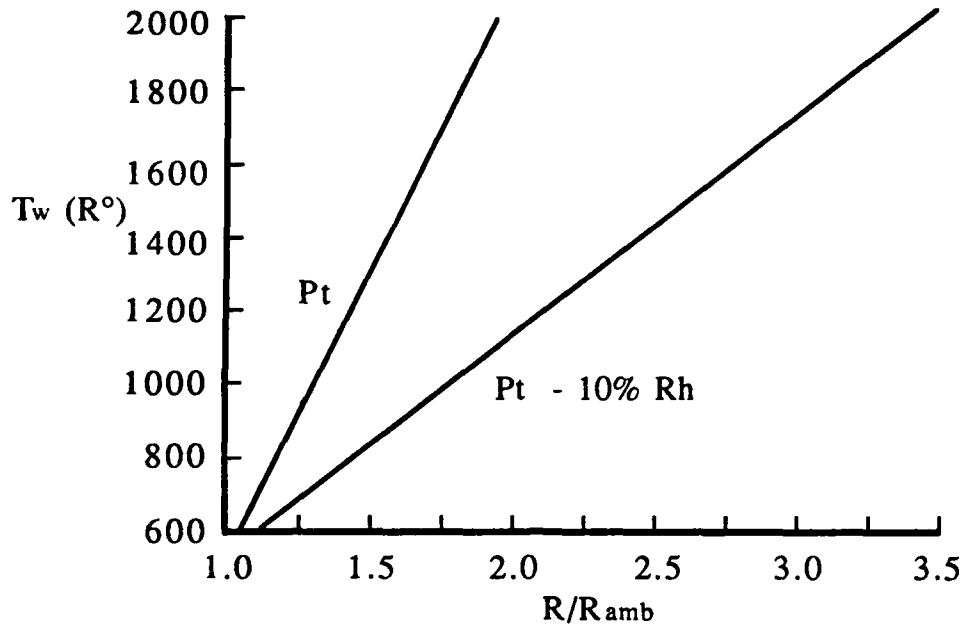


Fig. 6.2 Variation of wire temperature with wire resistance

For constant current operation we also need to determine the wire time constant from ref. 1 as

$$\mu = \frac{C_{pw} \rho_w d^2}{4 Nu_{om} k_{oair}} \frac{R_w}{R_r} \quad 6.28$$

A plot of Nu_o versus Re_o is given below. But we should use measured values of Nusselt number (Nu_{om}). Typical comparisons between measured and theoretical values are shown in figure 6.3. Figure 6.4 shows the effects of the wire dimensions and thermal properties. If we know C_{pw} , ρ_w , d^2 , Nu_{om} , k_o , and R_w/R_r , we may calculate the true time-constant and correct the measured wire voltage as follows

$$\frac{\Delta e}{\Delta e_m} = \frac{\mu}{\mu_{set}} \sqrt{1 - \frac{\Delta e^2}{\Delta e_m^2} \left(\frac{\Delta e^2 - \Delta e_m^2}{\Delta e^2 - \Delta e_o^2} \right)} \quad 6.29$$

where Δe_o is uncompensated wire voltage which is small for usual values of

μ . Thus,

$$\frac{\Delta e}{\Delta e_m} \approx \frac{\mu}{\mu_{set}}$$

where μ_{set} is the compensating amplifier time constant. So we are now in a position to account for the effects of the electrical system and wire resistance variations on the measured electrical signal.

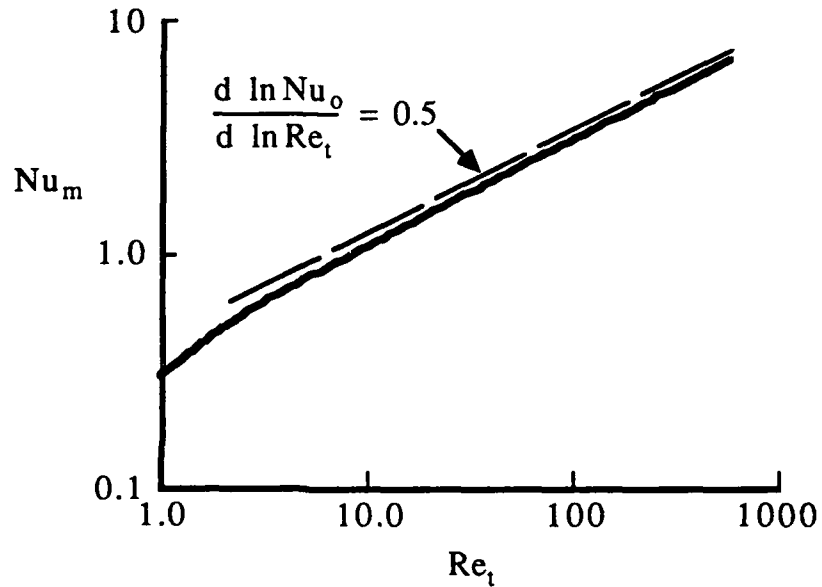


Fig. 6.3 Comparison of measured and theoretical heat loss.

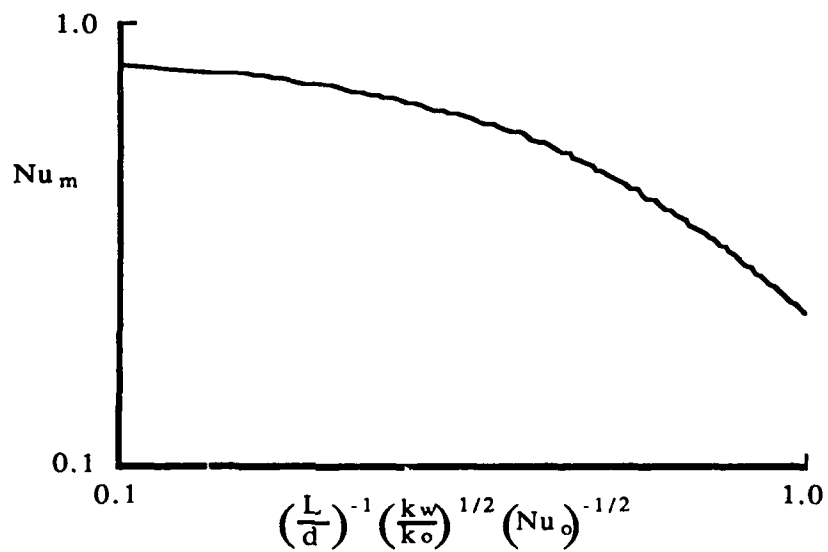


Fig. 6.4 Effect of wire properties on heat transfer.

AD-A174 806

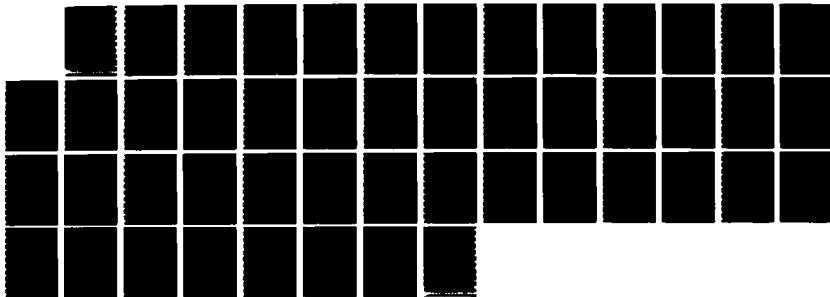
TURBULENT BOUNDARY LAYER MEASUREMENT TECHNIQUES(U)
COMPLERE INC PALO ALTO CA F K OWEN ET AL AUG 86
AFWAL-TR-86-3031 F33615-82-C-3022

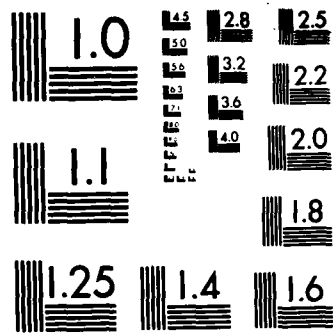
2/2

UNCLASSIFIED

F/G 20/4

NL





MICROCOPY RESOLUTION TEST CHART
NATIONAL BUREAU OF STANDARDS-1963-A

Now let us direct our attention to the remaining terms in the sensitivity equations. Following the results of section 5, we may make the following high Mach number approximations for $M \sin \phi > 1.2$ and $(\partial \ln Nu_o / \partial \ln M) \approx 0$.

$$\frac{\partial \ln Nu_o}{\partial \ln Re_o} = \frac{0.5}{1 - \sqrt{\frac{Re_{om}^*}{Re_o \sin \phi}}} \quad 6.30$$

where

$$Re_{om}^* = [1.1 - .82\psi(\sqrt{Re_o} - 1.1) \cdot 5]^2 \quad 6.31$$

with

$$\psi = \frac{d}{L} \sqrt{\frac{k_w}{k_{o,air}}} \quad 6.32$$

$$\eta = 0.95 + 0.0963/Re_o \quad 6.33$$

$$\frac{\partial \eta}{\partial Re_o} = \frac{-0.0963}{Re_o^2} \quad \text{or} \quad \frac{\partial \ln \eta}{\partial \ln Re_o} = -\frac{1}{1 + 10 Re_o} \quad 6.34$$

Normally we assume that for $Re_o > 40$

$$\frac{\partial \ln \eta}{\partial \ln Re_o} = 0 \quad 6.35$$

Finally for $M \sin \phi > 1.2$

$$\frac{\partial \ln \eta}{\partial \ln M} \approx 0$$

so that for high M_∞ ie. $M_\infty \sin \phi > 1.2$

$$\Delta e_p = \Delta e_u = \Delta e_{pu}$$

and we may rewrite the sensitivity equations as

$$\Delta e_{\rho u} = \frac{\bar{\epsilon} E'}{100} \left[A \dot{w} \frac{\partial \ln Nu_o}{\partial \ln Re_o} - \frac{A \dot{w}}{\tau_{wr}} \frac{\partial \ln \eta}{\partial \ln Re_o} \right] \quad 6.36$$

$$\Delta e_{T_r} = \frac{\bar{\epsilon} E'}{100} \left[K + A \dot{w} \left\{ K - 1.75 + 0.65 \frac{\partial \ln Nu_o}{\partial \ln Re_o} - \frac{0.65}{\tau_{wr}} \frac{\partial \ln \eta}{\partial \ln Re_o} \right\} \right] \quad 6.37$$

$$\Delta e_{\phi} = - \frac{\bar{\epsilon} E' A \dot{w}}{100} \left[\frac{\partial \ln H}{\partial \phi} \right] \quad 6.38$$

Thus, for $M \sin \phi > 1.2$ and $Re_o > 40$, it is possible to calibrate a wire directly in a flow with varying mean mass flow distribution such as a boundary layer or by varying the freestream total pressure. With

$$Re_o = \frac{\rho u d}{\mu} \quad \text{and} \quad Nu_o = \frac{I^2 R_w}{\pi l k_T (T_w - T_r)} = \frac{I^2 R_w R_r \alpha_r}{\pi l k_T (R_w - R_r)} \quad 6.39$$

the term

$$\begin{aligned} \frac{\partial \ln Nu_o}{\partial \ln Re_o} &= \frac{Re_o}{Nu_o} \frac{\partial Nu_o}{\partial Re_o} \\ &= \left(\frac{\rho u / \mu}{I^2 R_w R_r / (R_w - R_r)} \right) \left(\frac{\partial I^2 R_w R_r / k_T (R_w - R_r)}{\partial \rho u / \mu} \right) \end{aligned} \quad 6.40$$

So that if we measure

$$\frac{I^2 R_w R_r}{k_T (R_w - R_r)}$$

at several different values of $\rho u / \mu$ and differentiate the data we can determine

$$\frac{\partial \ln Nu_o}{\partial \ln Re_o}$$

directly. It helps to plot

$$\frac{I^2 R_w R_r}{k_T (R_w - R_r)}$$

against the square root of $\rho u/\mu$ since, for $Re > 40$, this plot is usually linear and may be smoothed before differentiation.

Other forms of the sensitivity equations can be introduced which also allow for direct, in-situ calibration. If we put a normal wire into a uniform free-stream, equation 6.1 reduces to

$$e' = \Delta e_{T_r} \left(100 \frac{T_r}{T_t} \right) = \frac{\bar{E}}{100} \left[\frac{\partial \ln \bar{E}}{\partial \ln T_r} \right] \quad 6.41$$

Similarly, holding other terms constant, we can show that

$$\Delta e_{\rho u} = \frac{\bar{E}}{100} \left[\frac{\partial \ln \bar{E}}{\partial \ln \rho u} \right] \quad 6.42$$

and

$$\Delta e_v = \frac{\bar{E}}{100} \left[\frac{\partial \ln \bar{E}}{\partial \phi} \right] \quad 6.43$$

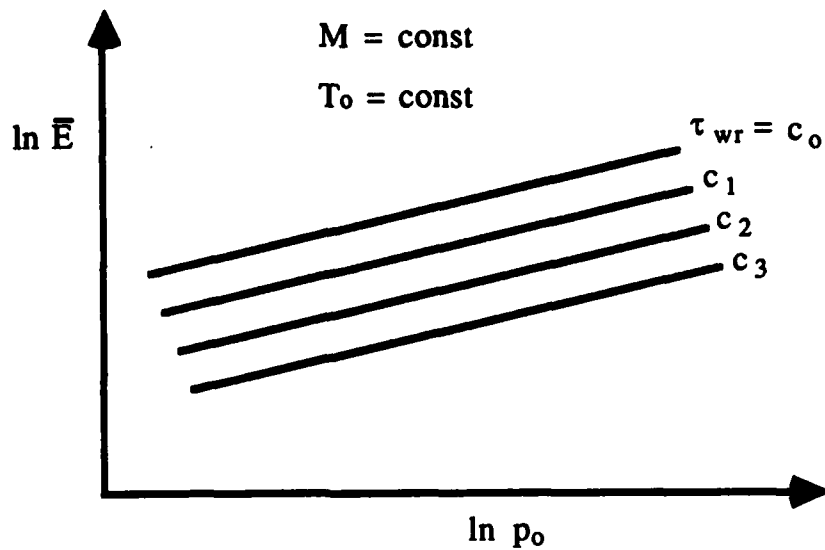
Now, if total temperature and Mach number are held constant, we may write

$$\partial \ln \rho u = \partial \ln p_o \quad 6.44$$

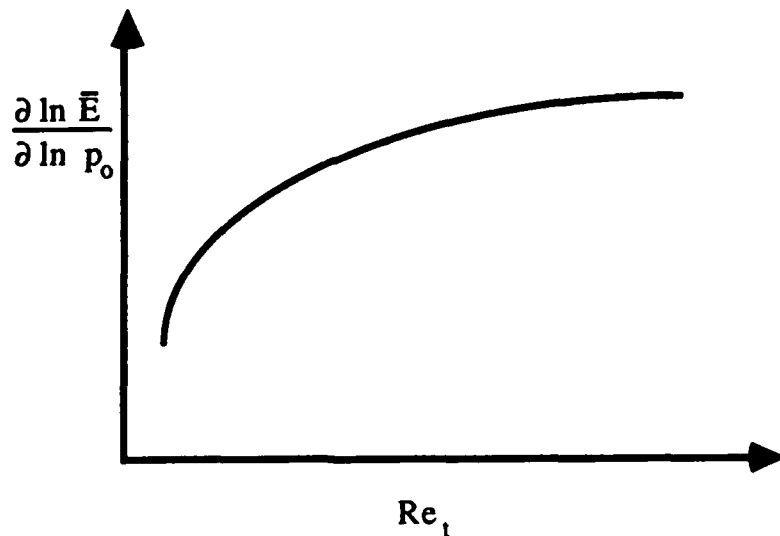
so that equation 6.42 may be rewritten as

$$\Delta e_{\rho u} = \frac{\bar{E}}{100} \left[\frac{\partial \ln \bar{E}}{\partial \ln p_o} \right] \quad 6.45$$

The sensitivity $\Delta e_{\rho u}$ can then be evaluated from the wind tunnel calibration of a wire on the tunnel center-line by varying p_o for constant M and T_o . We also must hold the overheat constant at various values. If we record values of \bar{E} versus p_o at various constant overheats and plot $\ln \bar{E}$ versus $\ln p_o$ as shown on the next page,

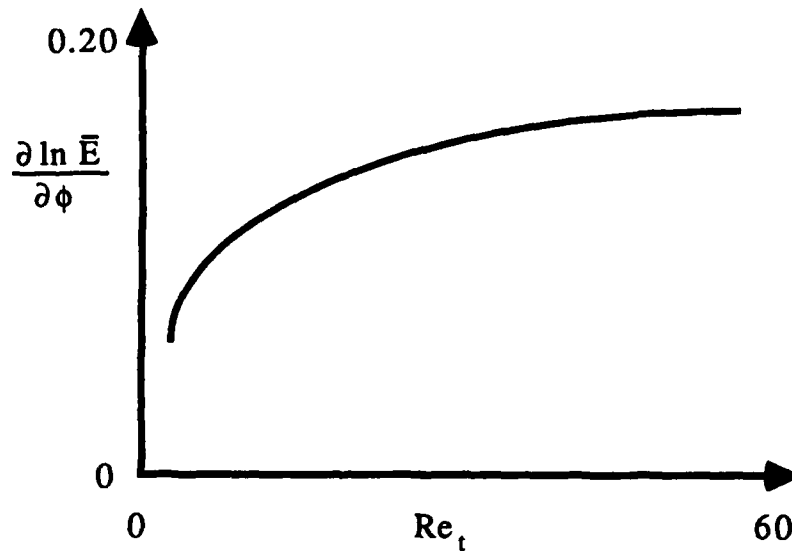


we can obtain the slopes $\partial \ln \bar{E} / \partial \ln p_0$. These slopes are independent of M and τ_{wr} . In fact, $\partial \ln \bar{E} / \partial \ln p_0$ is only a function of Re_t as shown below.



It is recommended that Δe_ϕ is obtained by changing wire angle at constant overheat in a fixed free-stream flow. We note that this calibration should be conducted at a variety of tunnel total pressures with Mach number and total temperature held constant. The sensitivity varies non-linearly with Reynolds number but is independent of Mach

number. A typical calibration is shown below.



The sensitivity Δe_{T_t} presents a slight problem since it cannot normally be determined in-situ using the simplified equation 6.41 as it requires a tunnel center-line calibration in which M and p_o are held constant as total temperature is changed. This is generally not feasible, since changing T_o will usually change p_o as well as $\bar{p}u$. However, for $M \sin \phi > 1.2$ and $Re_o > 40$ we can rewrite equation 6.37 as

$$\Delta e_{T_t} = \frac{\bar{e}E'}{100} [K + A\dot{w} (K - 1.75) - m_t \Delta e_{\rho u}] \quad 6.46$$

so that the total temperature sensitivity can be calculated using the in-situ determination of mass flux sensitivity and equation 6.22.

Once the hot-wire has been calibrated, the usual test procedure is as follows. First we record I_w , V_w , V'_{out} (compensated), $V'_{balance}$ (uncompensated), R_B , R_I (setting for overheat), R_w cold and μ_{set} for each

overheat setting. Next we plot R_w vs I_w and calculate A'_w vs R_w . Then, for each R_w , we calculate the following terms

- | | | |
|--|--|-------------------------------------|
| 1. ϵ | 8. $\frac{\partial \ln \eta}{\partial \ln Re}$ | 15. μ |
| 2. A'_w | 9. \bar{e} - wire voltage (V_w) | 16. V'_{out} |
| 3. T_w | 10. E' | 17. $\frac{V'_{out}}{e'}$ |
| 4. K | 11. Δe_m | 18. \bar{e}' |
| 5. a'_w | 12. Δe_{T_0} | 19. \bar{e}'_{corr} |
| 6. τ_{wr} | 13. I_w | 20. r the sensitivity ratio |
| 7. $\frac{\partial \ln Nu}{\partial \ln Re}$ | 14. C_w | $\frac{\Delta e_m}{\Delta e_{T_0}}$ |

If we now take the root-mean-square hot-wire signal and divide by Δe_{T_0} we obtain

$$v^2 = \left(\frac{e'}{\Delta e_{T_0}} \right)^2 = \overline{T_0'^2} + r^2 \overline{(\rho u)'^2} - 2r \overline{\rho u' T_0'} \quad 6.47$$

and we may determine the three unknowns

$$\overline{T_0'^2}, \overline{(\rho u)'^2} \text{ and } \overline{(\rho u)' T_0'}$$

In principle, only three overheat settings are required. But, in practice, at least three times that number should be made in order to provide consistency checks and reduce the scatter. The results can also be determined from the so-called Kovaszny diagram (ref. 9) or by regression. The Kovaszny diagram can be obtained by plotting $v = e'/\Delta e_{T_0}$ against the sensitivity ratio (r). Typical curves showing the dependence on the relative magnitude of the three unknown quantities are presented in figure 6.5. If only mass flow fluctuations are present the diagram will be a straight line from the origin with the slope

proportional to the mass flow fluctuation level. If only total temperature fluctuations are present, the diagram is a horizontal line at the total temperature fluctuation level. If both fluctuations are present, the plot varies according to the correlation coefficient between the two fluctuations. For perfectly correlated or anti-correlated fluctuations, the curve becomes a straight line, and when there is zero correlation it is a hyperbola. In these cases, the two fluctuation levels can be determined as indicated in figure 6.5.

For a yawed wire we have

$$e' = \Delta e_{\rho u} \frac{(\rho u)'}{\rho u} + \Delta e_{T_t} \frac{T_t'}{T_t} \pm \Delta e_{\phi} \frac{v'}{u} \quad 6.48$$

so that, when we difference the mean square of two readings taken 180 deg. apart, we obtain

$$\overline{e'^2} = \overline{e'^2_{0^\circ}} - \overline{e'^2_{180^\circ}} = 4 \left[\Delta e_{\rho u} \Delta e_{\phi} \overline{(\rho u)' v'} + \Delta e_{\phi} \Delta e_{T_t} \overline{v' T_t'} \right] \quad 6.49$$

which we may write as

$$s^* = \frac{\overline{e'^2}}{4 \Delta e_{\phi} \Delta e_{T_t}} = 4 \left[\overline{v' T_t'} + r^* \overline{(\rho u)' v'} \right] \quad 6.50$$

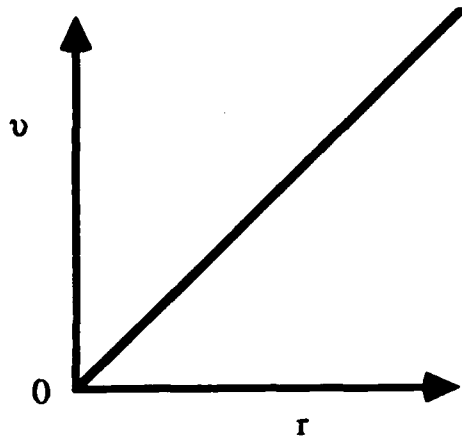
where

$$r^* = \frac{\Delta e_{\rho u} \Delta e_{\phi}}{\Delta e_{\phi} \Delta e_{T_t}} \quad 6.51$$

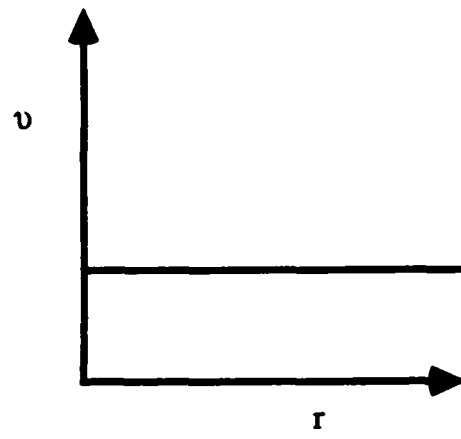
If we plot s^* against r^* we obtain

$$\overline{(\rho u)' v'} \quad \text{and} \quad \overline{v' T_t'}$$

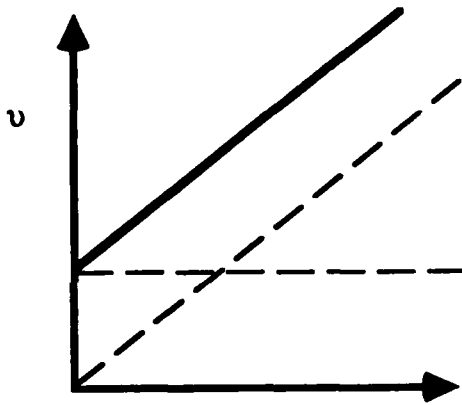
from the intercept and slope respectively.



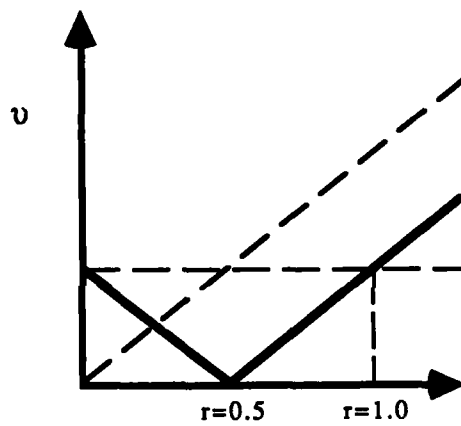
a) velocity fluctuation alone



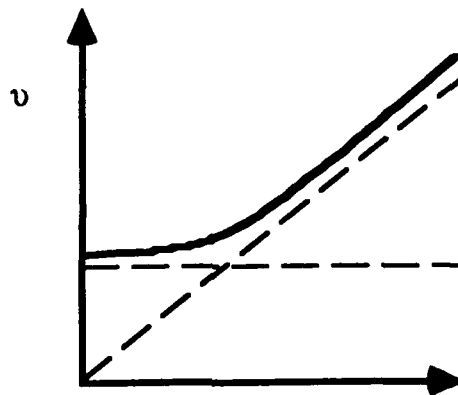
b) temperature fluctuation alone



c) $R = -1$



d) $R = +1$



e) $R = 0$

Fig. 6.5 Typical mode fluctuation diagrams

Now, having obtained the rms values

$$\frac{(\rho u)'}{\rho u}, \frac{T_1'}{T_1} \quad \text{and the correlation } \overline{(\rho u)' T_1'}$$

from a normal wire, and

$$\overline{(\rho u)' v'} \quad \text{and} \quad \overline{v' T_1'}$$

from a yawed wire, we are in a position to determine the fluctuating flow variables outlined in section 5.

Unfortunately, the mass flow and total temperature fluctuations are not the sole characteristic parameters of an unsteady supersonic flow field. We must also consider the vorticity τ , entropy σ , and sound π modes.

If the fluctuation levels are low, as in the free stream, these modes satisfy separate linear differential equations and the hot-wire equation becomes (ref. 1)

$$\Delta e = \sigma \Delta e_\sigma + \tau \Delta e_\tau + \pi \Delta e_\pi \quad 6.52$$

where

$$\Delta e_\sigma = \Delta e_\rho + \alpha \Delta e_T \quad 6.53$$

$$\Delta e_\tau = \beta \Delta e_T - \Delta e_u = \beta \Delta e_T - \Delta e_\rho \quad (M > 1.2) \quad 6.54$$

$$\begin{aligned} \Delta e_\pi &= \alpha(\gamma - 1)(1 - n_x M) \Delta e_T - \frac{n_x}{M} \Delta e_u - \Delta e_\rho \\ &= \alpha(\gamma - 1)(1 - n_x M) \Delta e_T - \left(\frac{n_x}{M} + 1\right) \Delta e_\rho \quad (M > 1.2) \quad 6.55 \end{aligned}$$

where

$$\alpha = 1 / \left(1 + \frac{\gamma - 1}{2} M^2\right) = (1 + 0.2M^2)$$

and

$$\beta = \alpha(\gamma - 1)M^2 = 0.4\alpha M$$

for air and n_x is the direction cosine defined as $n_x = -1/M$.

The fluctuation variables are given in ref. 1 as

$$\frac{\Delta T}{T} = \sigma + (\gamma - 1)\pi \quad 6.56$$

$$\frac{\Delta \rho}{\rho} = -\sigma + \pi \quad 6.57$$

$$\frac{\Delta u}{u} = \tau + \frac{n_x \pi}{M} \quad 6.58$$

$$\frac{\Delta p}{p} = \gamma \pi \quad 6.59$$

$$\frac{\Delta T_t}{T_t} = \alpha\sigma + \beta\tau + \left[(\gamma - 1)\alpha + \frac{\beta n_x}{M} \right] \pi \quad 6.60$$

$$\frac{\Delta m}{m} = -\sigma + \tau + \left(1 - \frac{n_x}{M} \right) \pi = \frac{\Delta \rho}{\rho} + \frac{\Delta u}{u} \quad 6.61$$

But we cannot determine all these variables directly from hot-wire measurements. A usual compromise is to plot $\Delta e/\Delta e_\sigma$ against $\Delta e_\pi/\Delta e_\sigma$ to determine which variables may be neglected (ref. 1).

Since turbulent flows vary in both space and time, useful insight into turbulent structure can be gained from space-time correlations in compressible flows. Two approaches will be described. In the first, let us locate two wires at points A and B normal to the flow direction such that

$$e_A = -s_A m_A + s_{\theta A} \Theta_A \quad 6.62$$

$$e_B = -s_B m_B + s_{\theta B} \Theta_B \quad 6.63$$

Cross-correlating, we obtain

$$\begin{aligned} \overline{e_A e_B} &= s_A s_B \overline{m_A m_B} + s_{\theta A} s_{\theta B} \overline{\theta_A \theta_B} \\ &\quad - s_A s_{\theta B} \overline{\theta_B m_A} - s_B s_{\theta A} \overline{m_B \theta_A} \end{aligned} \quad 6.64$$

or

$$z = \overline{\theta_A \theta_B} - r_B \overline{m_B \theta_A} + r_A (r_B \overline{m_A m_B} - \overline{m_A \theta_B}) \quad 6.65$$

where

$$z = \frac{\overline{e_A e_B}}{s_{\theta A} s_{\theta B}}, \quad r_A = \frac{s_A}{s_{\theta A}}, \quad r_B = \frac{s_B}{s_{\theta B}}$$

This plots linearly in the z, r_A plane with intercept

$$(\overline{\theta_A \theta_B} - r_B \overline{m_B \theta_A})$$

and slope

$$(r_B \overline{m_A m_B} - \overline{m_A \theta_B})$$

So that, if we fix $r_B = r_{B1}$ which is a known constant, and test with known values $r_A = r_{A1}$ and r_{A2} to obtain z_1 and z_2 , we obtain

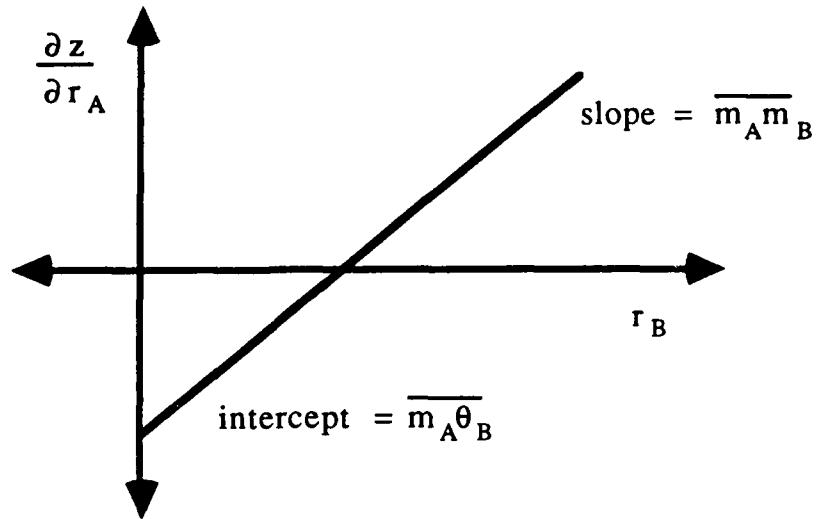
$$\frac{\partial z}{\partial r_A} = (\text{slope})_{r_{B1} = \text{const}} = r_{B1} \overline{m_A m_B} - \overline{m_A \theta_B} \quad 6.66$$

and

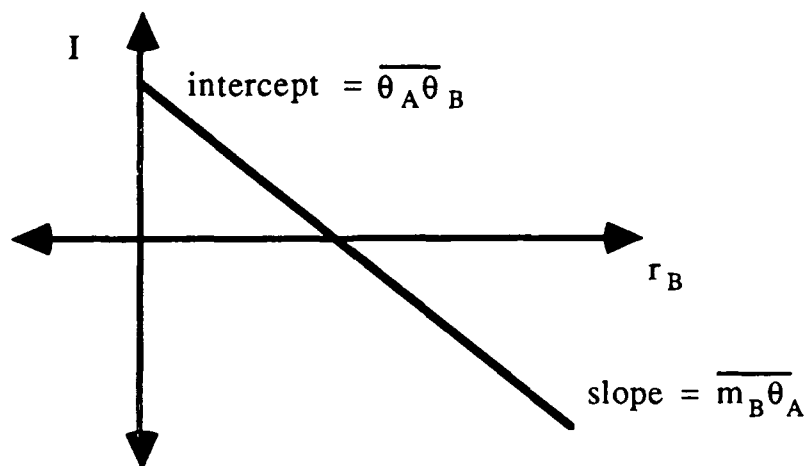
$$(\text{intercept})_{r_{B1} = \text{const}} = \overline{\theta_A \theta_B} - r_{B1} \overline{m_B \theta_A} \quad 6.67$$

If we repeat procedure with a new known constant r_{B2} we obtain four equations and four unknowns. To improve our accuracy we can continue the test sequence and determine the four unknowns graphically as shown on the next page.

First plot $\left(\frac{\partial z}{\partial r}\right)$ vs (r_B)



Then plot (intercept, I) = $\overline{\theta_A \theta_B} r_B - \overline{m_B \theta_A}$ vs (r_B)



Space-time correlations in compressible flows may be obtained with two wires at points A and B in the flow as follows:

$$e_A = \alpha_A m_A + \beta_A \theta_A \quad \text{at time } t \quad 6.68$$

$$e_B = \alpha_B m_B + \beta_B \theta_B \quad \text{at time } t' \quad 6.69$$

If we adjust the anemometer gains such that $r_A = r_B = r$ and measure

$$\frac{(\overline{e_A + e_B})^2 - (\overline{e_A - e_B})^2}{(\overline{e_A + e_B})^2 + (\overline{e_A - e_B})^2}$$

we obtain

$$R_{e_A e_B} = \frac{r^2 \overline{m_A m_B} + r (\overline{m_A \theta_B} + \overline{m_B \theta_A}) + \overline{\theta_A \theta_B} + c}{r^2 \overline{m_A^2} + 2r_A \overline{m_A \theta_A} + \overline{\theta_A^2}} \quad 6.70$$

where

$$r = \sqrt{\frac{\alpha_A}{\beta_A} \frac{\alpha_B}{\beta_B}}, \quad r_A = \frac{\alpha_A}{\beta_A}$$

and

$$c = \left(\sqrt{\frac{\alpha_A}{\beta_A}} - \sqrt{\frac{\alpha_B}{\beta_B}} \right) \left(\sqrt{\frac{\alpha_A}{\beta_A}} \overline{m_A m_B} - \sqrt{\frac{\alpha_B}{\beta_B}} \overline{m_B \theta_A} \right) \quad 6.71$$

When the wires are made of the same material and operated at the same overheat ratio then

$$\sqrt{\frac{\alpha_A}{\beta_A}} \approx \sqrt{\frac{\alpha_B}{\beta_B}} \quad \therefore c = 0 \quad \& \quad r_A^2 = r^2$$

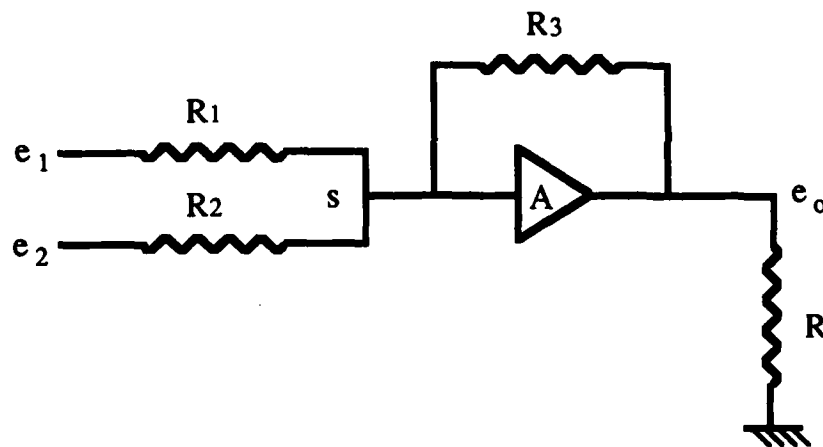
Furthermore, as the overheat $\rightarrow 0$, $\alpha/\beta \rightarrow 0$ and equation 6.70 reduces to the temperature-temperature correlation

$$\frac{\overline{\theta_A \theta_B}}{\overline{\theta_A' \theta_B'}}$$

At high overheat ratios $\alpha/\beta \rightarrow 1.0$, or $\gg 1.0$, so that if $\theta \ll m$, or $\theta = m$, the equation reduces to the mass flux - mass flux correlation

$$\frac{\overline{m_A m_B}}{\overline{m'_A m'_B}}$$

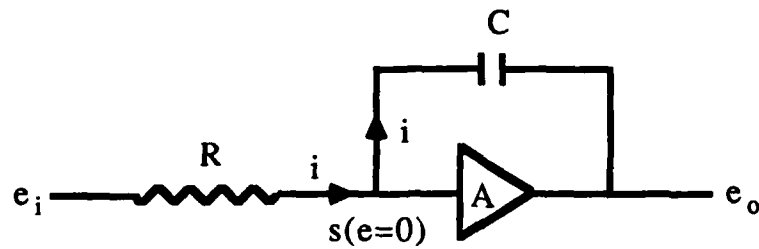
To determine the statistical values outlined earlier, we have to add, subtract and multiply the fluctuating outputs and sometimes delay them in time and filter with frequency. Addition and subtraction are accomplished by converting signal voltages to currents and applying them to resistors as shown in the circuit below.



In the circuit, A has a high input resistance ($\gg R_3$), so that all current goes through R_3 , a large voltage amplification occurs at A and the voltage at s which is equal to e_o/A , tends to 0. Now

$$e_o = -R_3 \left(\frac{e_1}{R_1} + \frac{e_2}{R_2} \right) \quad 6.72$$

so that if $R_1 = R_2$ then $e_o = -(e_1 + e_2)$. Also, if $e_2 = 0$ then $R_1 = R_3$ and $e_o = -e_1$. In these ways we are able to add and subtract hot-wire voltages. We can integrate hot-wire signals as follows



Again if $A \rightarrow \infty$, $e_s \approx 0$ and the input impedance of $A \rightarrow \infty$. For the capacitance $Q = Ce_o$ we may write

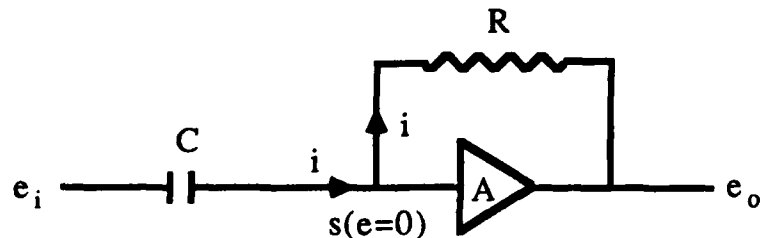
$$\frac{dQ}{dt} = i = C \frac{de_o}{dt} = \frac{e_i}{R} \quad 6.73$$

so that

$$e_o = \int \frac{e_i}{RC} dt \quad 6.74$$

and if $e_i = a \sin \omega t$ then $e_o = -(a/\omega RC) \cos \omega t$.

Differentiation may be accomplished as follows



where we may write

$$C \frac{de_i}{dt} = i = \frac{e_o}{R} \quad 6.75$$

so that

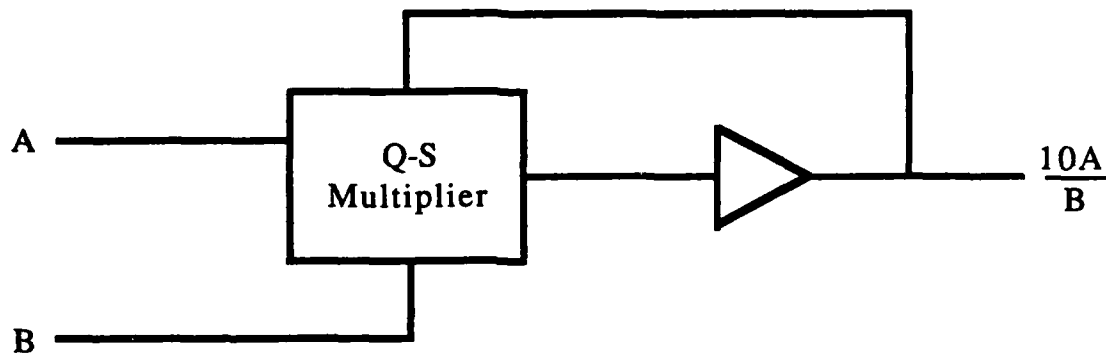
$$e_o = RC \frac{de_i}{dt} \quad 6.76$$

In general, what is termed the quarter-square-technique is used for multiplication. In this case two squaring circuits are used, one to square the quantity $(x + y)$ and the other to square the quantity $(x - y)$. The outputs of the two squaring circuits are then scaled such that

$$(1/4)[(x + y)^2 - (x - y)^2] = xy$$

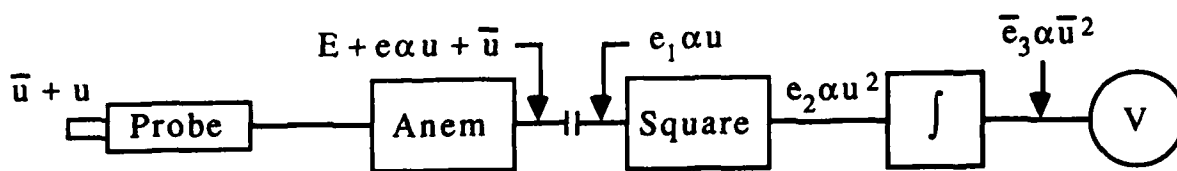
6.77

The input is usually scaled such that the output is $(1/10)xy$. This scaling is necessary to use the full dynamic range of the two input amplifiers without saturation of the output amplifier. Division can be accomplished by placing a squaring network in a feedback loop as shown below

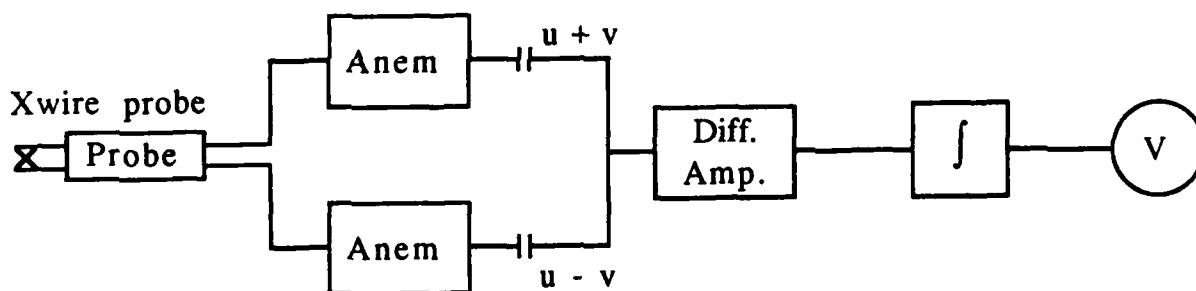


The power spectrum of a hot-wire signal can be obtained by Fourier transformation of the auto-correlation or by spectrum analysis using inductance-capacitance band pass filters. However, filters with band width of $1/3$ octave, ie. $2^{1/3} \times$ center frequency, are not suitable for measuring spectra with sharp peaks. Typical turbulent velocity spectra drop off rapidly with frequency. But, in supersonic flows, there may still be significant energy beyond 50 kHz. The sharp drop off can cause changes in the effective filter band width and, at extremely high frequencies, the spatial resolution of the hot-wire sensing element renders spectral measurements open to question. Although spectra of higher order correlations have been reported at low speeds, care must be exercised to match the phase shifts of the two filter sets, when making these measurements in high-speed flows.

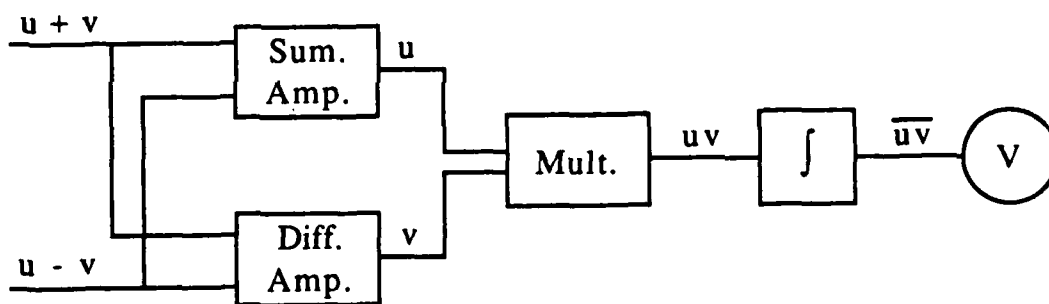
Some practical hot-wire signal analysis set ups are shown below



Measurement of \bar{u}^2



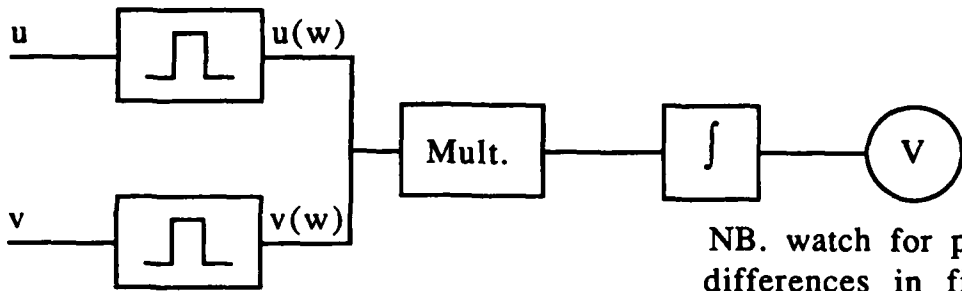
Measurement of \bar{v}^2



Measurement of \bar{uv}

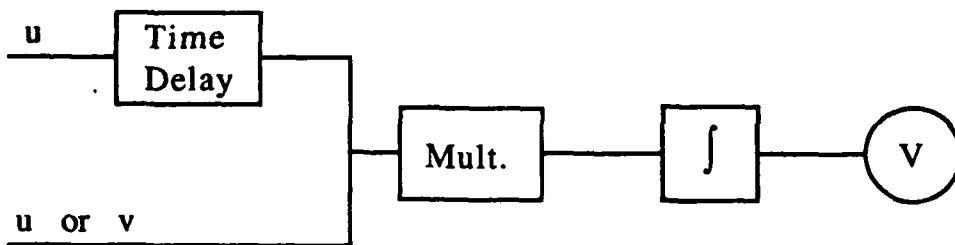


Intensity Spectrum



NB. watch for phase differences in filters

Cross Spectrum

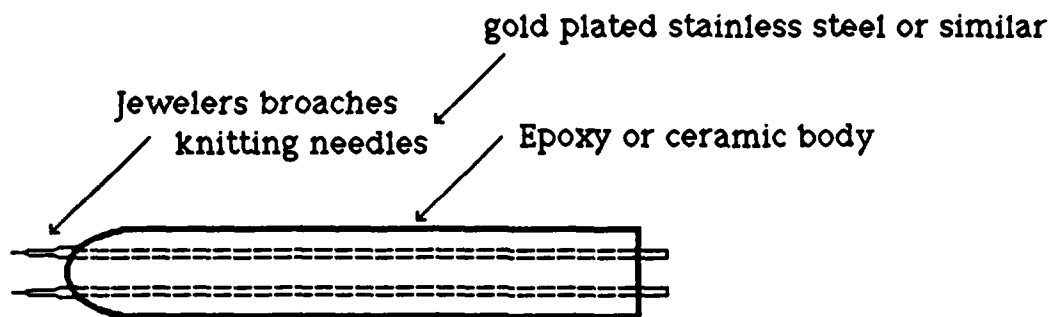


Auto or Cross Correlations

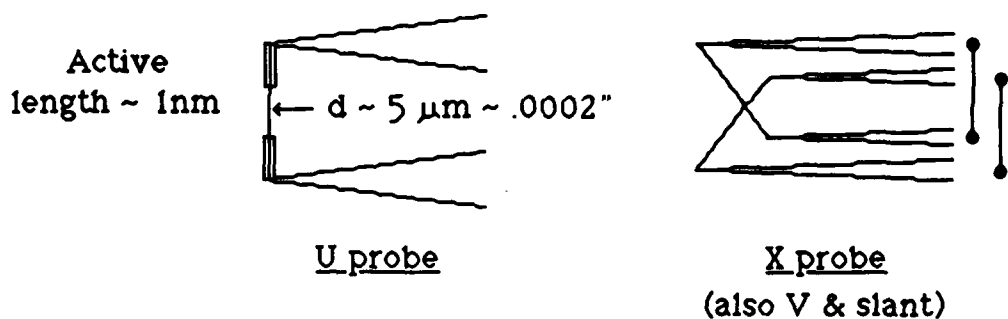
Details of the properties of materials used in the fabrication of hot-wire probes are given in an attached list. Generally hot-wire probes are welded or soft-soldered to the supports. Conventional or etched wollaston wires are used. Film gages have much less directional sensitivity because of conduction to the glass (ie. their effective aspect ratio is lower). They also have a complex time-constant so it is difficult to compensate for quantitative measurements. Some examples of probe

fabrication sequences are given on the following pages.

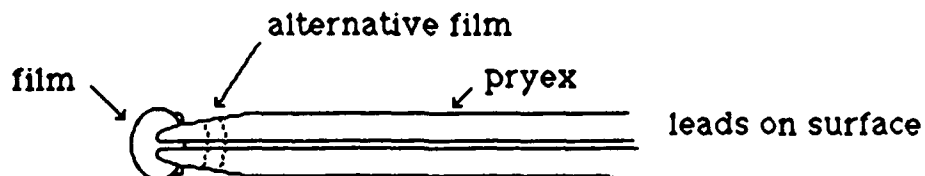
Hot-wire probes

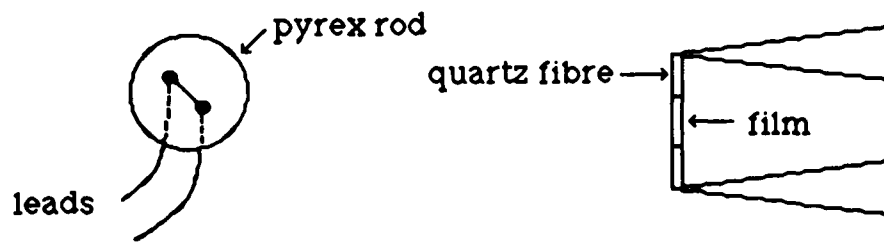


To avoid strain gage oscillations, we must maintain slack in the wires.

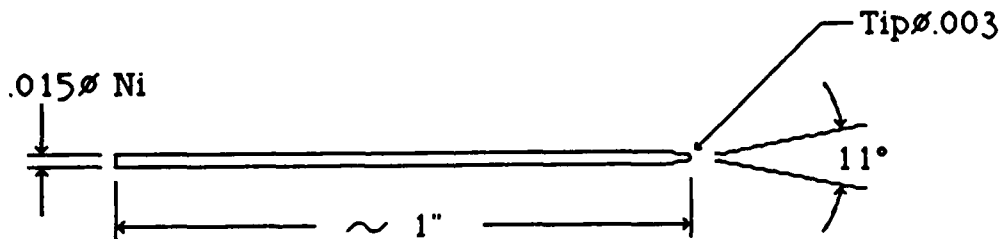
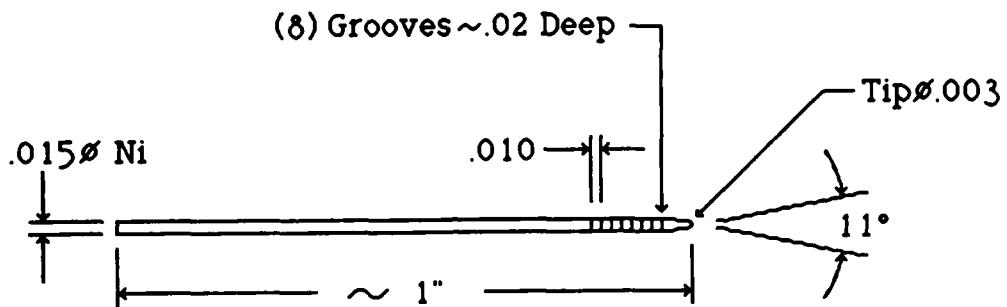


Film Probes

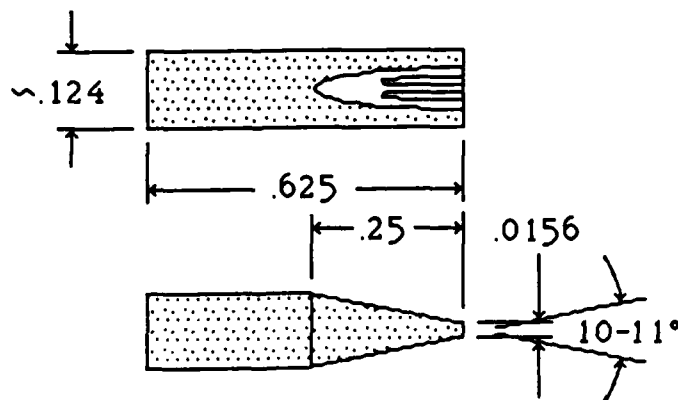




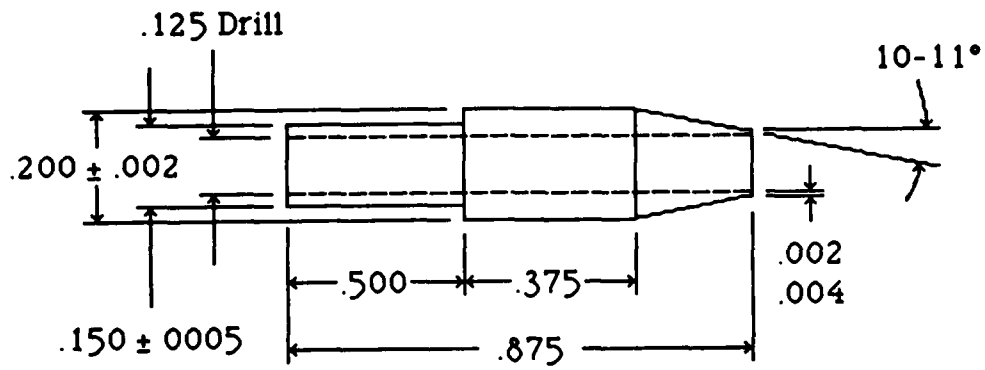
The fabrication sequence for double sensor with straight or coiled wires is shown as follows:



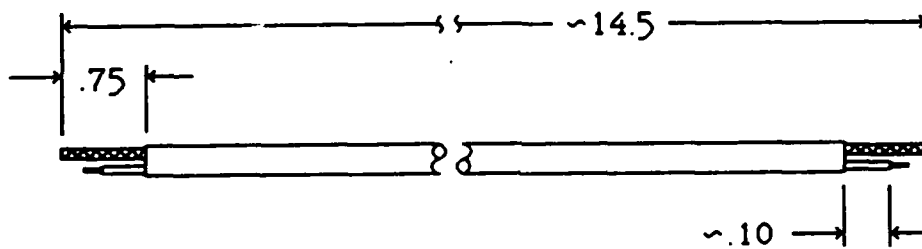
Nickel Support Pins



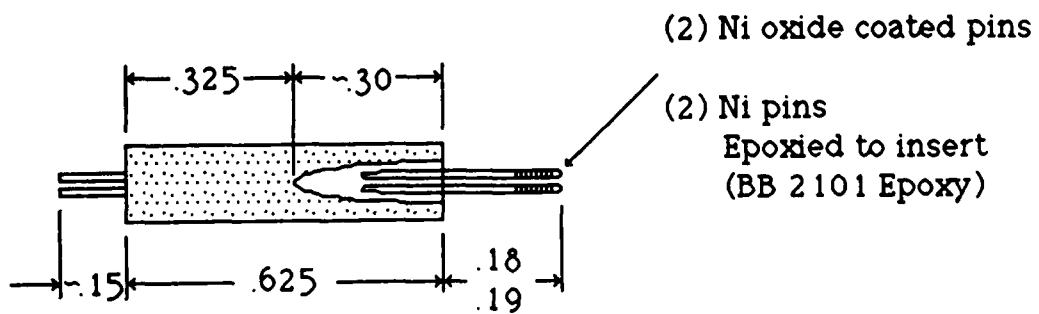
Ceramic Insert



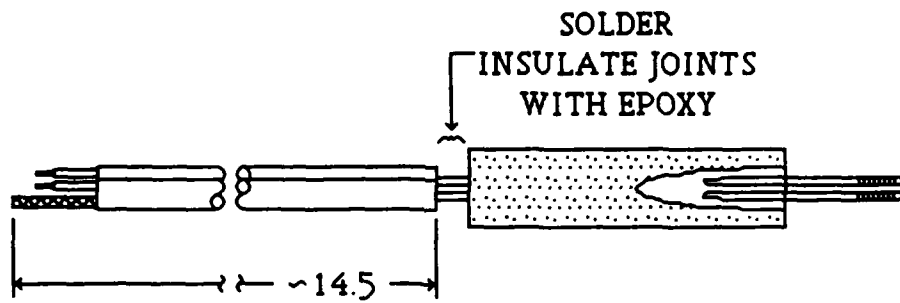
Aluminum or Stainless Steel Body



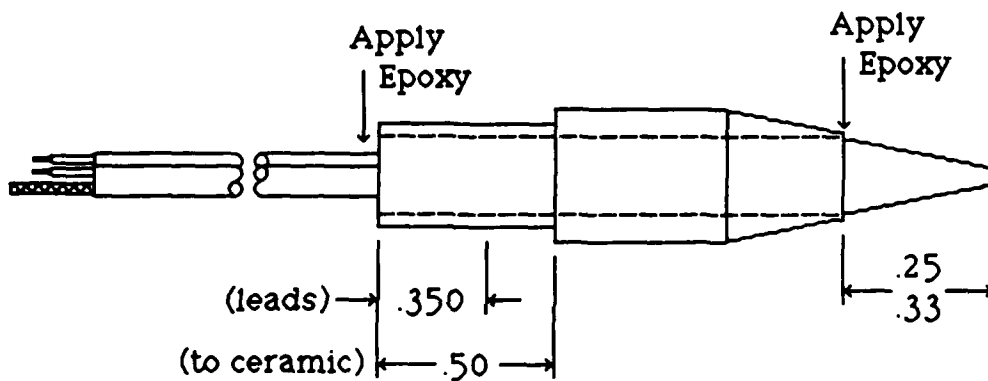
Miniature Co-axial Cable Beldon 8700, 28AWG



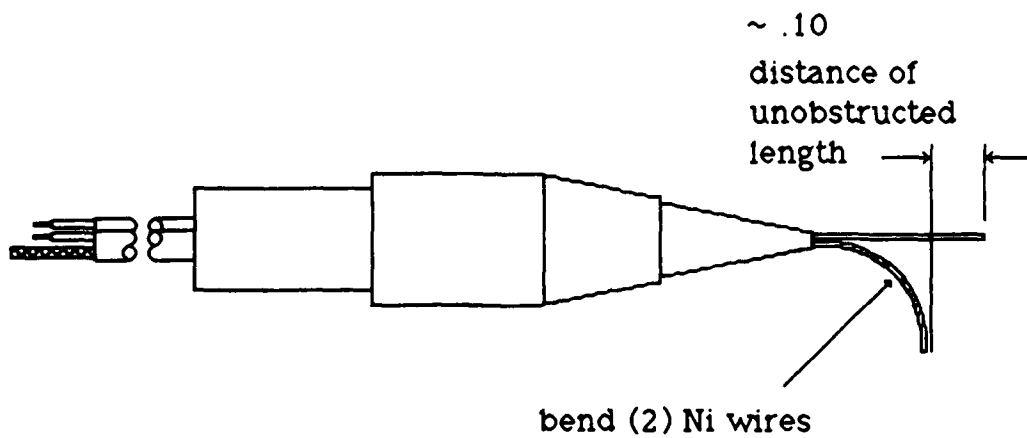
Pin/Ceramic Assembly



Cable/Pin/Ceramic Assembly



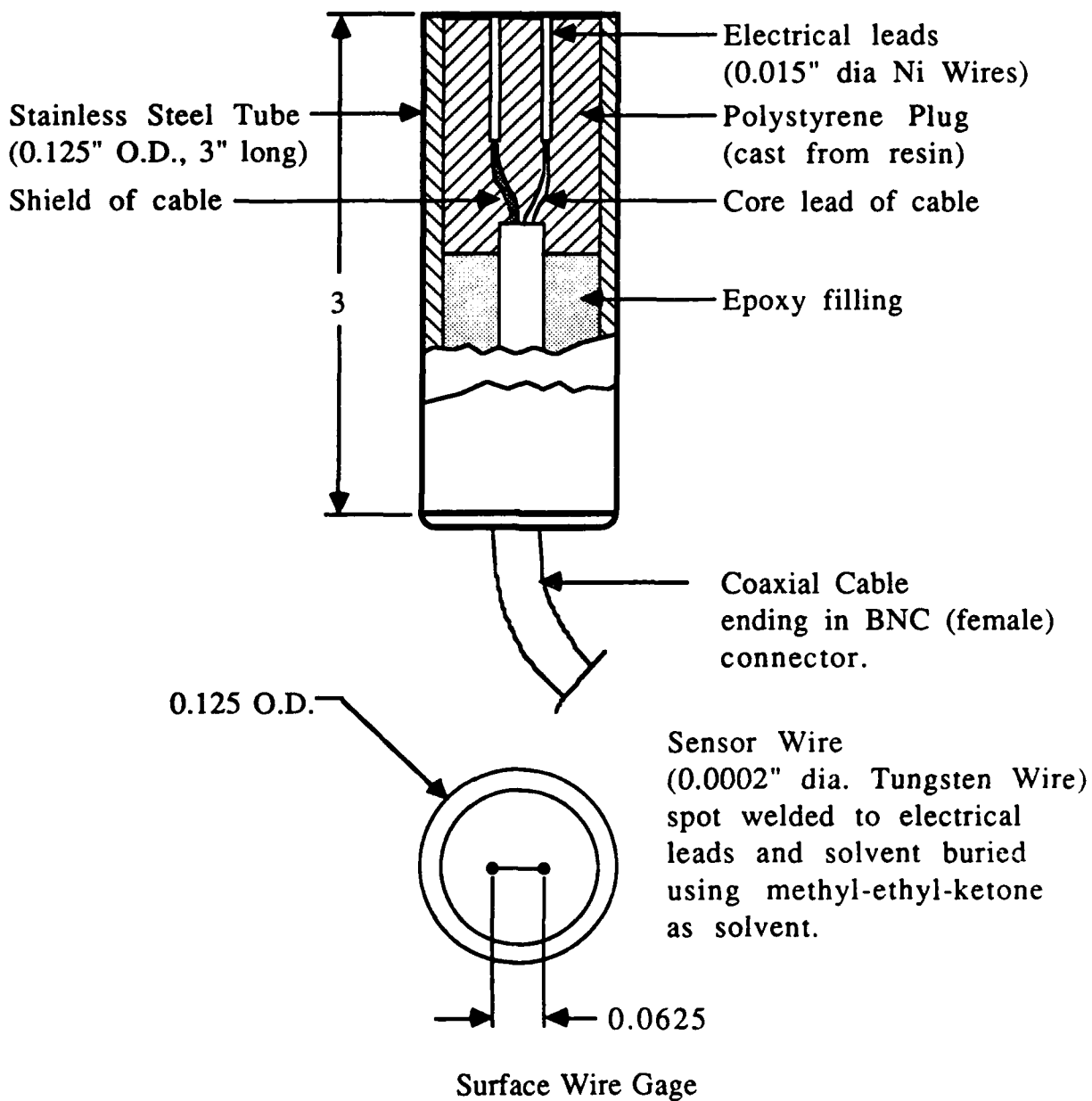
Assembled Probe

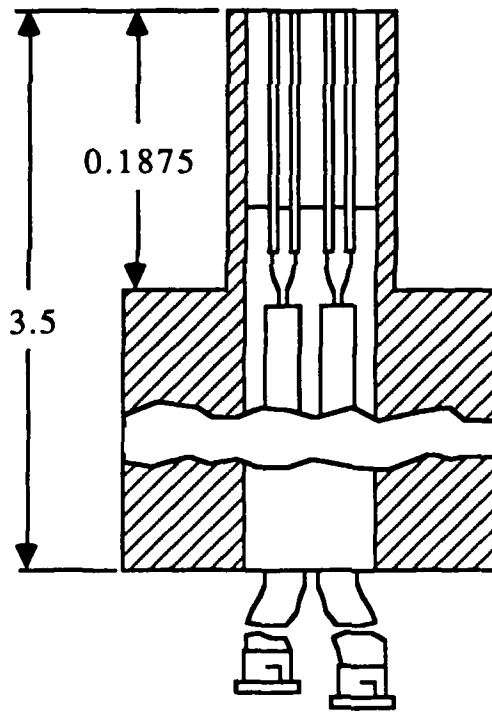
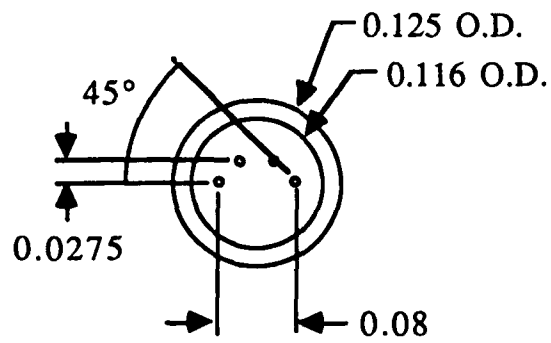


Preparation of Pins for Coil Winding

Finally wind the coil, straighten bent pins, spot weld single wire to Ni pins, record resistances; check for shorts to ground, and coat spot-weld with conductive epoxy (E3021).

The procedure for the construction of surface wire gages is shown on the following pages. These probes can be used for transition and separation detection without disturbing the flow. Surface flow direction can also be sensed with a pair of wires on a single gage (ref. 11).





Surface Flow Direction Sensor (ref. 12).

Summary of Materials						
	Platinum	80% Pt 20% Iridium	Tungsten	Nickel	Pt Film on Glass	
Strength	low	high	high	moderate	very high but brittle	
Temperature Range	to 2000° F	to 2000° F	to 600° F (oxidation)	to 1000° F	to 600° F	
α	0.003/°C moderate, stable and linear	0.00085/°C low, stable	0.004/°C moderate, non linear fairly stable	high, fairly stable and linear	moderate, depends upon plating	
Availability	d to 0.000025" pure or Wollastan	d to 0.0001"	d to 0.00015" pure or copper plated	d to 0.001"	d to 0.001"	
Clean by Burning	yes	yes	no	yes	?	
Miscellaneous	R very precise		Difficult to weld or solder		Sensor replaced only by mfr.	
	catalytic at large T		to 4000° F if no oxygen		Frequency response questions	

Section 7 Hot-Wire and Laser Velocimeter Measurements

In the first part of this section, the results of our hot-wire freestream turbulence measurements in the $M = 6.0$ and $M = 3.0$ high Reynolds number facilities will be described. Comparisons with previous data obtained at much lower unit Reynolds numbers in the Ames 3.5 foot HWT (fig. 7.1) are very encouraging as they show superior flow quality in the AFWAL facility at high unit Reynolds numbers. The mass flow fluctuations increase with tunnel total pressure and range from 0.6 to 1.6 percent. Our previous Ames data were taken in 1972 and after the tunnel was converted to a free jet test section. These latter data were taken in 1974.

If we assume that the disturbances sensed by the hot-wire are predominantly sound waves radiated from the turbulent nozzle wall boundary layers, then the pressure fluctuation levels can be estimated from our hot-wire data. Hot-wire theory shows this assumption to be consistent with linear mode diagrams, (fig. 7.2). The results of these calculations are shown in fig. 7.3 and comparisons made with the Ames HWT and the Langley VDT. This figure clearly shows better flow quality in the $M = 6$ facility. But, sound is not the only disturbance mode, as temperature spottiness, probably due to non-uniform heating of the supply gas, is not negligible (fig. 7.1). Thus, the pressure level estimates from the hot-wire data should be viewed as upper bounds. The actual levels should be somewhat lower. Direct pressure measurements should confirm this.

Two hot-wire signals are shown in fig. 7.4; one for a pressure of 930 psi, the other for a pressure of 1860 psi. These traces clearly show the increased high frequency (smaller length scale) contribution at the higher tunnel total pressure. Low-frequency (large scale) contributions are also apparent in both hot-wire traces. In general, most of the energy is concentrated at low frequencies. Auto-correlation measurements show the turbulent integral length scales to be of the order of the jet exit diameter. Freestream turbulence measurements have also been made in the $M = 3$ facility. These results are shown in fig. 7.5.

The laser velocimeter data were obtained across flat plate boundary layers in the FDL $M = 6.0$ wind tunnel. Zero pressure gradient and adverse, ramp induced, pressure gradient flows were investigated. In the latter case, the capability for both streamwise and vertical velocity measurements was demonstrated. Previously, problems with particle arrival rates, run to run velocity variations and probe volume location within the boundary layer had been encountered. These problems had led to significant uncertainties and scatter in the measured velocity profiles.

Although more costly, laborious and tedious to operate, the laser velocimeter probably represents the instrument of last resort for the measurement of flow in compression corners, shock boundary layer interactions and other large scale unsteady turbulent flows. Once in operation, linear, non-intrusive unambiguous turbulent velocity and shear stresses can be obtained once seeding and sampling bias problems

have been overcome. Flows of most practical interest and importance often involve high turbulence, flow separation and large scale unsteadiness. Here the inherent linearity, non-perturbing, directionally sensitive properties of the laser velocimeter come to bear. However, it is also at these conditions that laser velocimeter sampling bias comes to the forefront.

Most researchers agree that continuous-wave mode signals are free from bias. However, in high-speed wind tunnel applications where particle concentrations are low, individual realization processing is required. In these cases the potential errors attributable to sampling bias can become significant at high turbulence levels. In a recent paper (ref. 12) the existence of "sampling bias" in individual realization laser velocimeter measurements has been experimentally verified and shown to be independent of the sample rate. The results clearly demonstrate that, for the individual realization mode of laser velocimetry, sampling bias exists and that it increases approximately with the square of the turbulence intensity. It was also demonstrated that these bias effects are independent of sampling rate provided the seeding concentration is sufficiently low to insure individual realization measurements. A two-dimensional weighting of the velocity samples was shown to be effective in correcting the individual realization measurements for sampling bias.

With particle bias problems identified and corrected, the seeding problem was the first to be addressed during the present work. A fluidized bed of

carbon particles which proved to be ineffective was replaced by an atomizer ahead of the throat. The accelerations and shear through the nozzle were sufficient to break up and provide an ample supply of scattering centers in the laser velocimeter focal volume. Signal to noise was also improved by the use of pre-amplifiers on the photomultiplier tube outputs. With these improvements, valid velocity data rates were increased to 3,000 samples per second.

The improved data acquisition rate also alleviated the thermal growth problem and its effect on probe volume location within the boundary layer. Increased data rates in the wall region enabled shorter run times, reduced model heating and less thermal distortion. Measurements can now be made through the wall region without excessive model heating, thus minimizing measurement location uncertainties. Reliable measurements of the axial velocity component were made within 0.010 inches of the wall. Vertical velocity measurements were limited to 0.03 inches from the wall.

The problem of run to run edge velocity variations was first noticed during preliminary freestream shakedown runs. These variations were corrected by correlating each set of shear layer measurements with individual run total temperature measurements. A more elusive data reduction problem was also identified. It concerns the relatively crude filter ranges on the laser velocimeter signal processor. Since the mean flow velocity and turbulence measurements were made with a dual beam velocimeter utilizing Bragg cell frequency shift, a stationary particle

produced a doppler frequency of (f_0) 14 mHz for example in fig. 7.6. Thus, in the flow field, particles generated doppler frequencies $f_0 \pm f$ depending on their direction normal to the moving fringes. However, even with this offset errors can arise due to incorrect filter settings. Extra care in their selection must be exercised not only in separated flow regions but also in the wall region of attached flows where local turbulence levels are high. The effect of 16 mHz and 8 mHz filter settings are shown by the solid and dashed lines on fig. 7.6. The problem would be more pronounced closer to the wall.

Fig. 7.7 shows a zero pressure gradient flat plate velocity profile. It can be seen that the comparison with the Van Driest theory is excellent. Fig. 7.8 shows a profile measured across the ramp induced pressure gradient flow field. A direct comparison of ramp induced effects on the mean and turbulent flow fields can be seen in fig. 7.9 where measurements obtained at the same streamwise station are presented. These measurements obtained at a station 0.3δ ahead of the 30-deg. ramp clearly show retardation of the flow and a significant increase in turbulence level over a wide region. The vertical velocity profile measured at the same location ahead of the interaction is shown in fig. 7.10. Local flow angularity profiles across the boundary layer have been calculated from the two component laser measurements. These results (fig. 7.11), show that local flow angles close to the wedge deflection angle are present in the shear layer just upstream of the interaction.

Comparison of the two turbulence level profiles shows that the

streamwise turbulent kinetic energy for the ramp flow is more than three times that for the flat-plate boundary layer. Turbulent mixing length scales, calculated using local rms levels and mean gradients, are an order of magnitude larger. Turbulence levels based on local mean flow values exceed 30 percent in the wall region so that we can see from section 4 that significant hot-wire measurement errors would arise. At this high intensity, large-scale turbulence results in directional intermittency of up to 15 percent ahead of the time-averaged recirculation zone. Hot-wire measurement errors associated with directional intermittency are discussed in detail in ref. 7.

To conclude, diagnostic tools are now available to attempt the measurement of turbulent high-speed flows, an area where comprehensive studies are lacking. However, measurement techniques must be used with understanding and care in appropriate situations. All too often experimental methods have been stretched beyond their reliable limits and misleading results have been reported. Apparent discrepancies between measurements and calculations cannot solely be attributed to deficiencies in turbulence modeling until reliable assessments have been made of measurement errors. Although the potential of laser velocimetry for the non-intrusive measurement of mean velocity, turbulence intensity and shear stress in complex wind tunnel flow fields has long been recognized, the design, construction and successful operation of systems in other than small, closely controlled laboratory situations still presents a formidable engineering challenge. Thus, it is important that redundant hot-wire and laser velocimetry

experiments be carried out to determine the reliable range of hot-wire application.

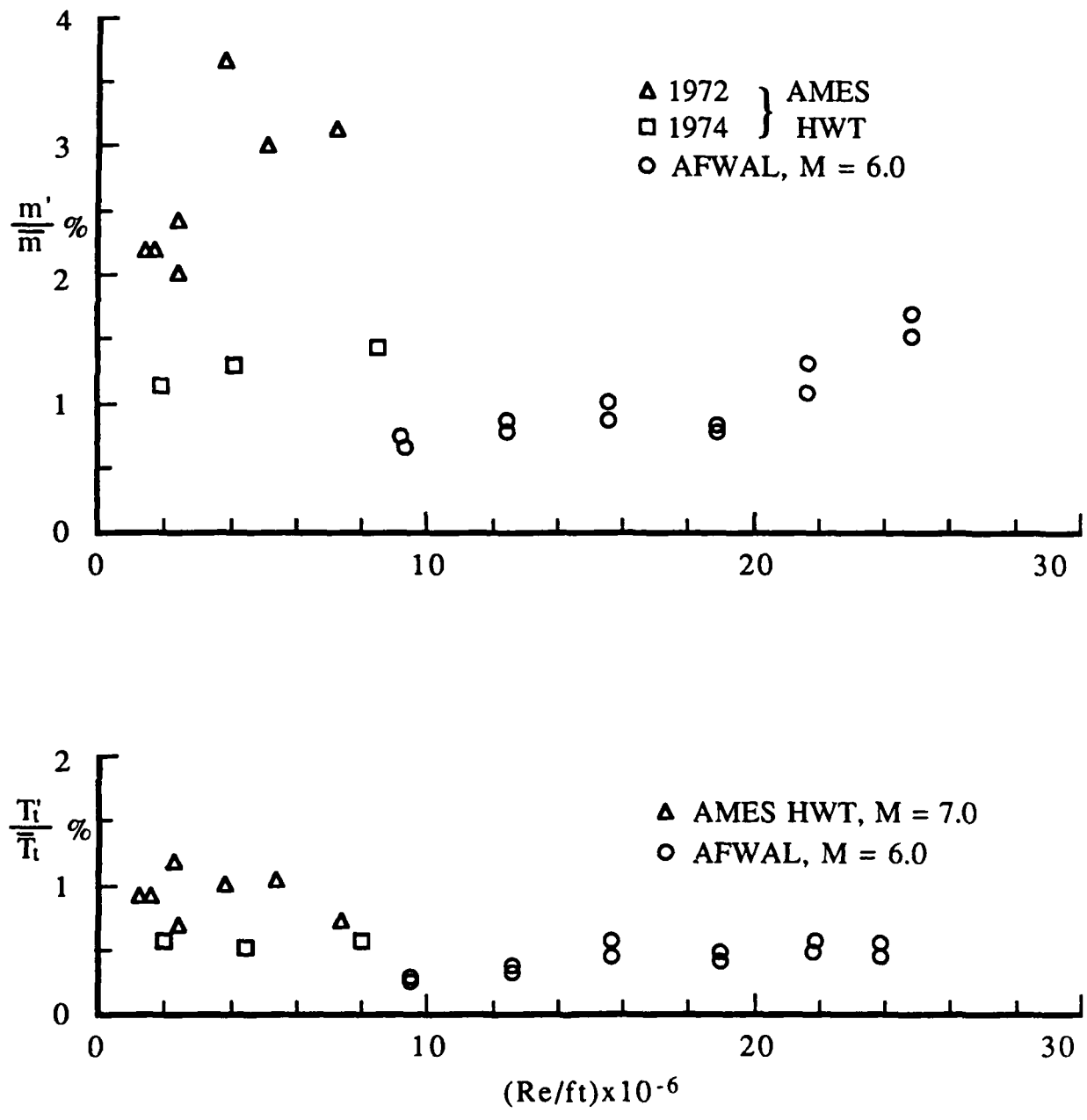


Fig. 7.1 Mass flow and total temperature fluctuations

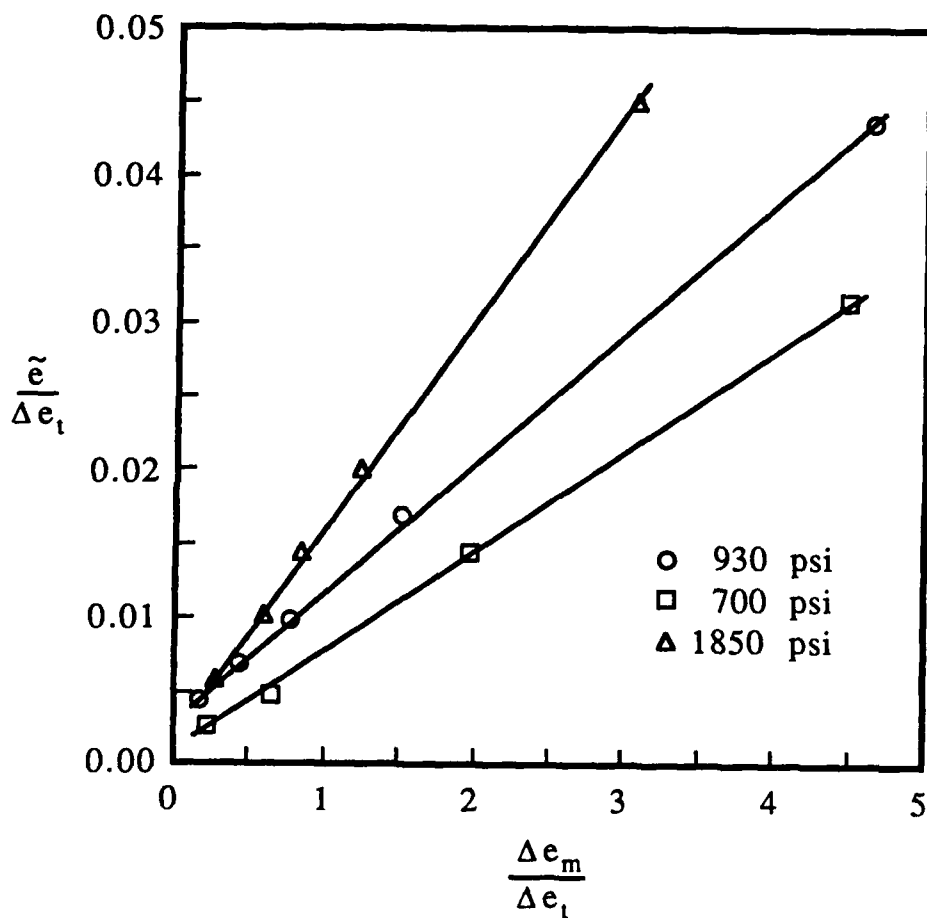


Fig. 7.2 Mode diagrams, AFWAL, M = 6.0

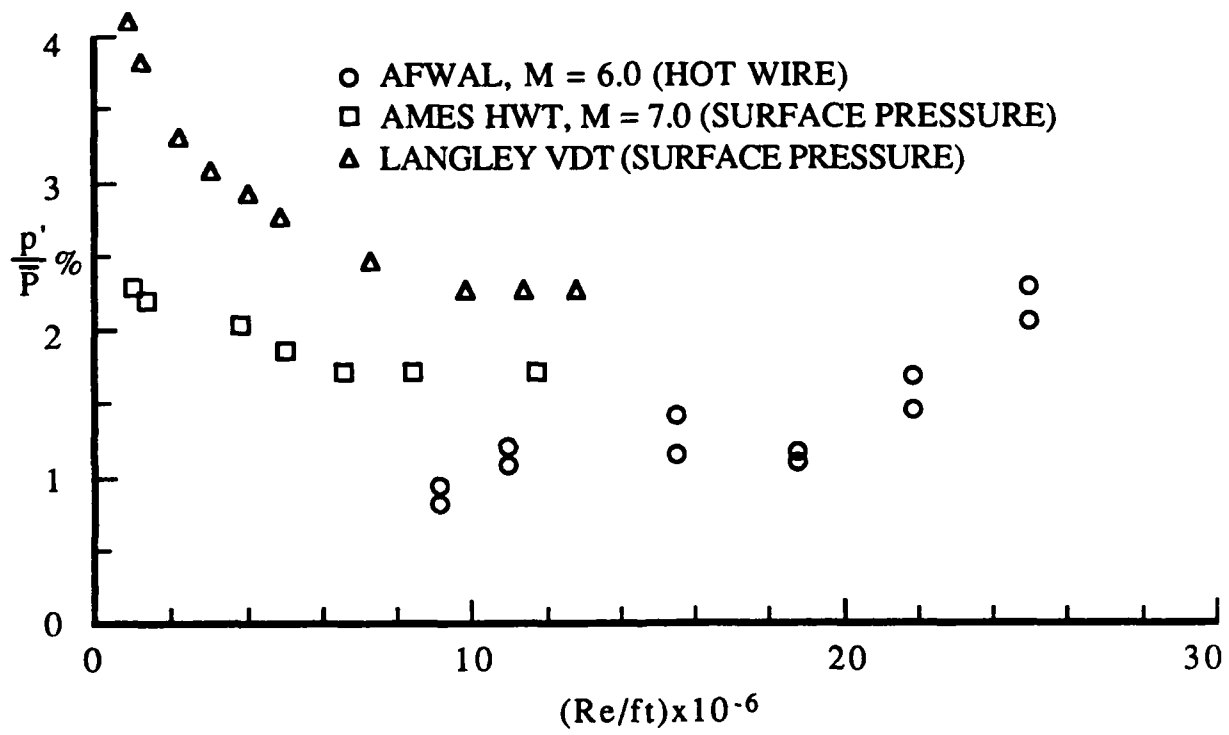
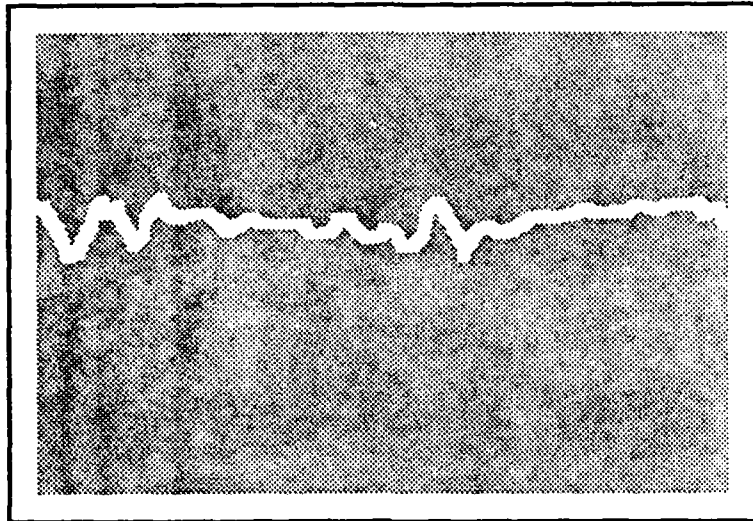
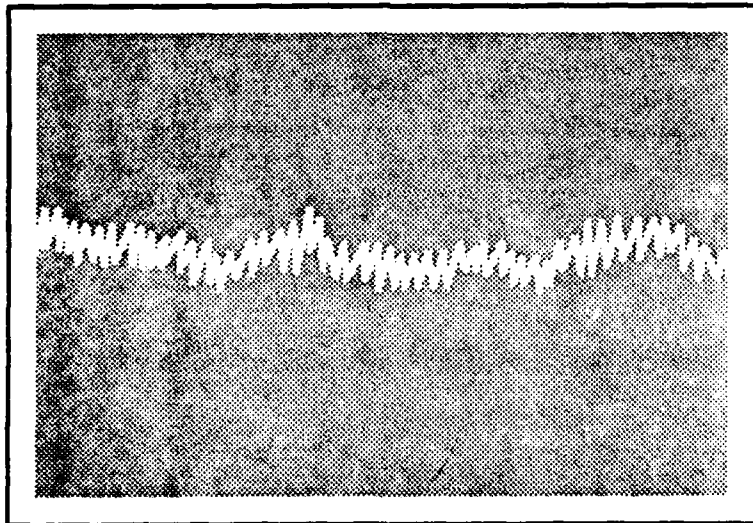


Fig. 7.3 Freestream pressure fluctuations



$p_o = 930$



$p_o = 1860$

Fig. 7.4 Hot-wire traces, AFWAL, $M = 6.0$,
time scale 1 ms/cm.

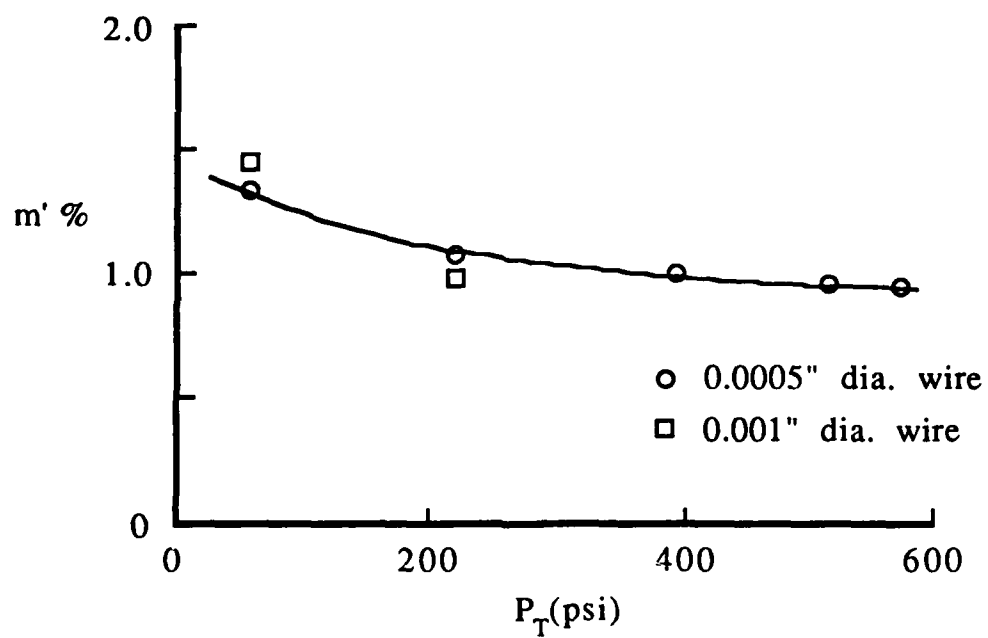


Fig. 7.5 Hot-wire turbulence measurements, AFWAL, $M = 3.0$

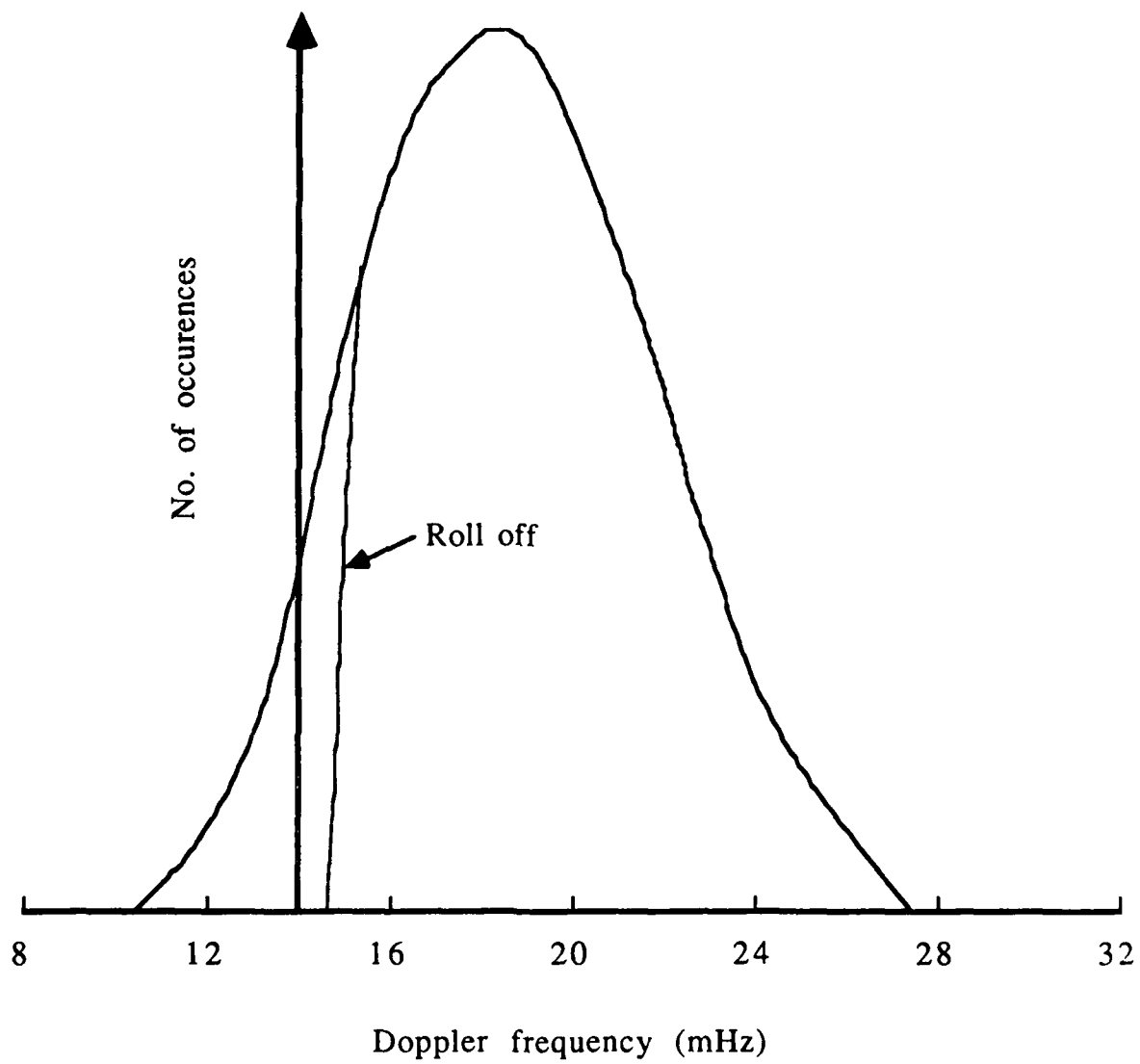


Fig. 7.6 Effect of filter settings on PDF, $y = 0.015$ inches

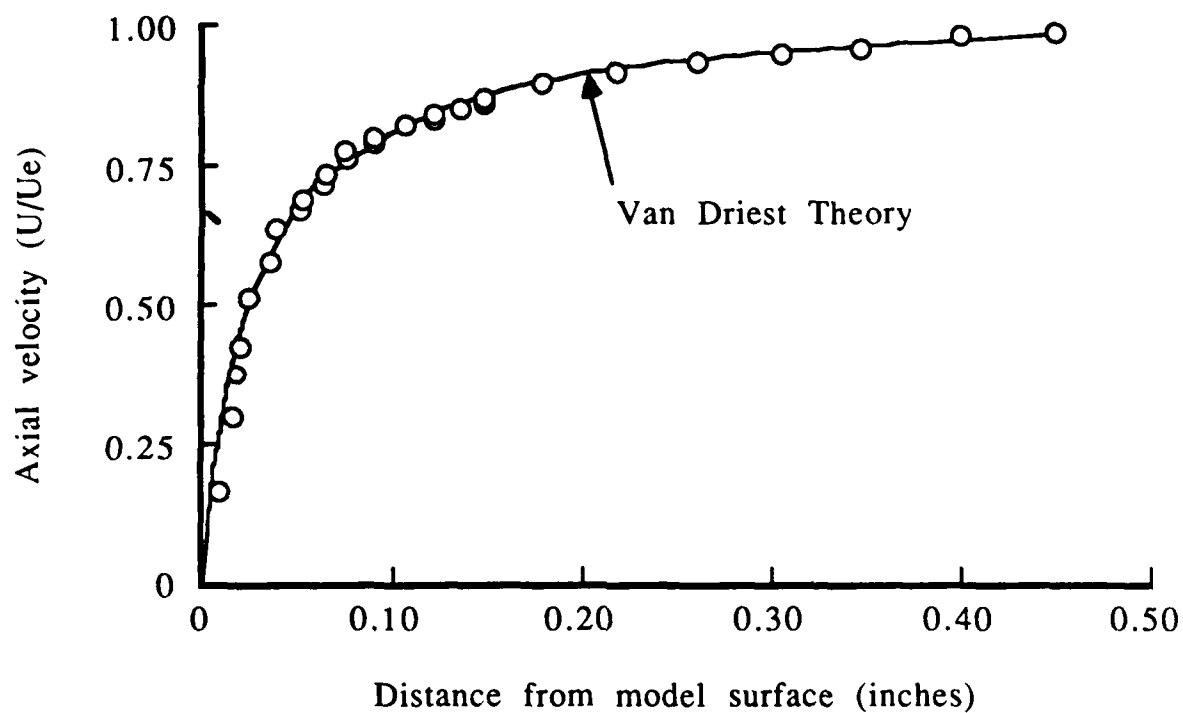


Fig. 7.7 Flat plate axial velocity profile

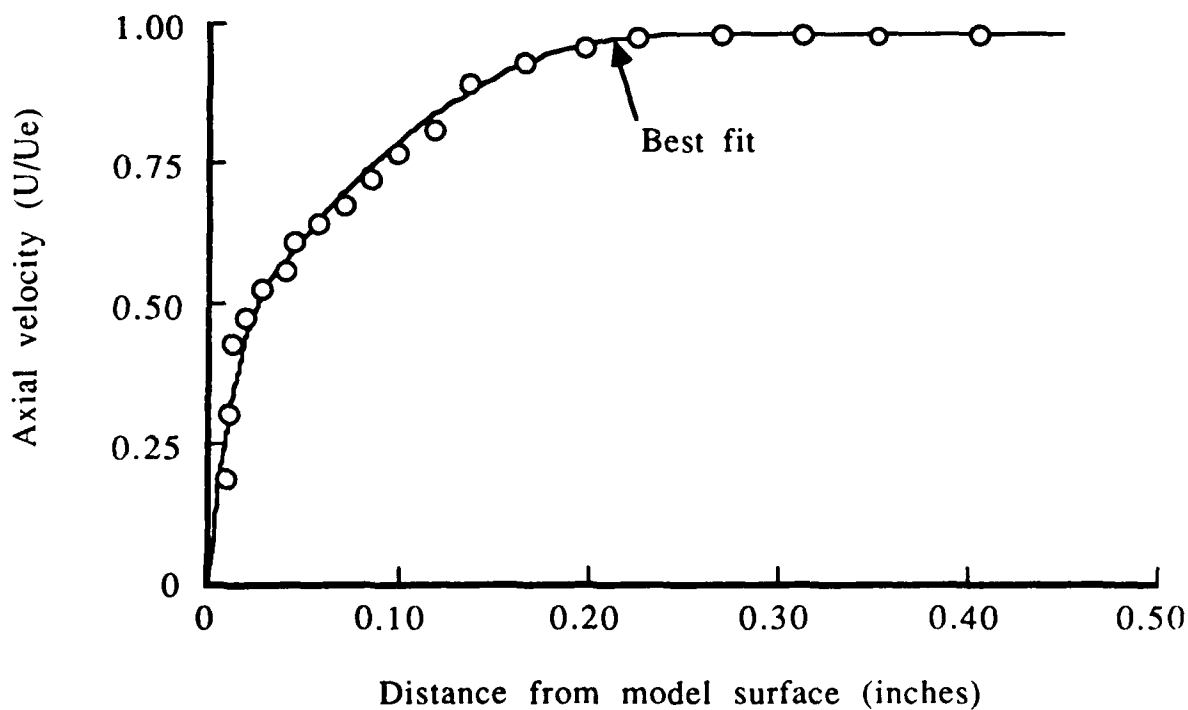


Fig. 7.8 Axial velocity profile ahead of interaction,
 $M_\infty = 6.0$, $p_o = 700$ psia

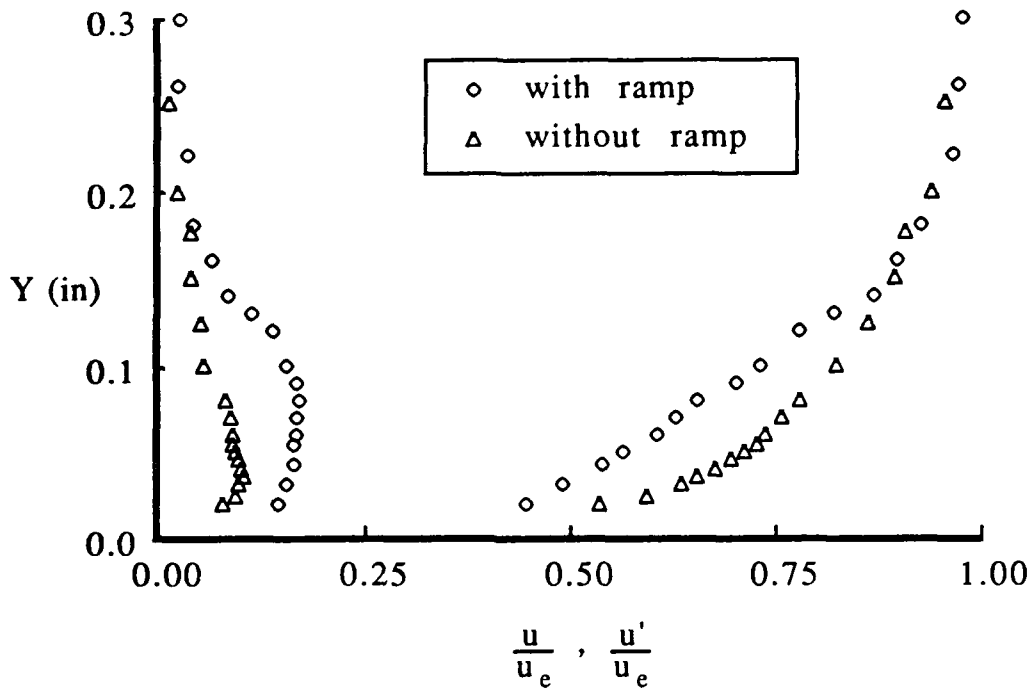


Fig. 7.9 Mean and turbulent velocity profiles

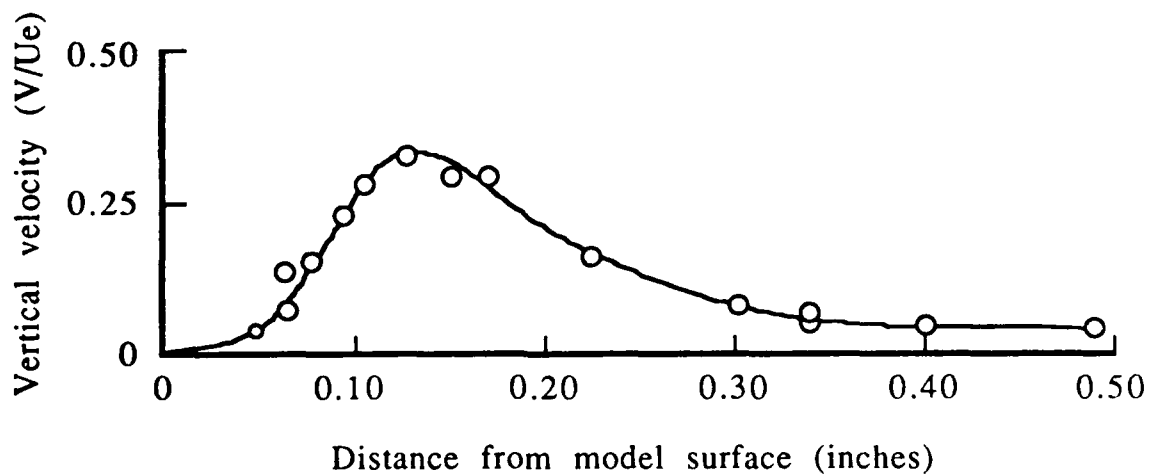


Fig. 7.10 Vertical velocity profile ahead of interaction,
 $M_\infty = 6.0$, $p_0 = 700$ psia

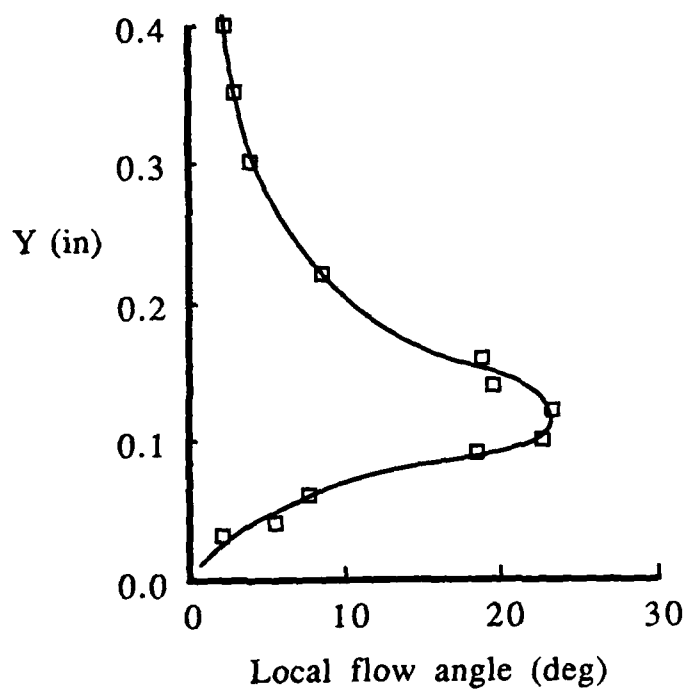


Fig. 7.11 Flow angularity across the boundary layer, wedge angle = 30 deg.

References

1. Morkovin, M. V., *Fluctuations and Hot Wire Anemometry in Compressible Flows*, AGARDograph 24, 1956.
2. Owen, F. K., *An Assessment of Flow Field Simulation and Measurement*, AIAA—83—1721, 1983.
3. Owen, F. K., Harvey, W. D. and Stainback, P. C., *An Evaluation of the Factors Affecting the Flow Quality in Wind Tunnels*, Paper No. 12 AGARD CP 348, 1983.
4. Horstman, C. C. and Owen, F. K., *Turbulent Properties of a Compressible Boundary Layer*, AIAA Journal Vol. 10, No. 11, p. 1418, 1972.
5. Owen, F. K. and Horstman, C. C., *On the Structure of Hypersonic Turbulent Boundary Layers*, J. Fluid Mech., Vol. 53, pt. 4, p. 611, 1972.
6. Owen, F. K., Horstman, C. C. and Kussoy, M. I., *Mean and Fluctuating Flow Measurements of a Fully Developed, Non-adiabatic Hypersonic Boundary Layer*, J. Fluid Mech., Vol. 70, pt. 4, p. 393, 1975.

7. Owen, F. K. and Johnson, D. A., *Separated Skin Friction — Source of Error, an Assessment and Elimination*, AIAA—80—1409, 1980.
8. Stainback, P. C. and Owen, F. K., *Dynamic Flow Quality Measurements in the Langley Low Turbulence Pressure Tunnel*, AIAA—84—0621, 1984.
9. Kovaszny, L. S. G., *Turbulence in Supersonic Flow*, Journal of the Aeronautical Sciences, Vol. 20, No.10, p. 657, 1953.
10. Morkovin, M. V. and Phinney, R. E., *Extended Applications of Hot-Wire Anemometry to High-Speed Turbulent Boundary Layers*, AFOSR TN—58—469, Johns Hopkins University, Department of Aeronautics, 1958.
11. Peake, D. J., Owen, F. K. and Higuchi, H., *Symmetrical and Asymmetrical Separations about a Yawed Cone*, Paper No. 16, AGARD CP 247, 1978.
12. Johnson, D. A., Modares, D. and Owen, F. K., *An Experimental Verification of Laser Velocimeter Sampling Bias and its Correction*, J. of Fluids Engineering, Vol. 106, p. 5, 1984.

List of Symbols

A_w	Overheat parameter, $\frac{1}{2} \frac{I}{R_w} \left(\frac{R_w}{dI} \right)$
a_w	Overheat parameter, $\frac{R_w - R_r}{R_r}$
C	Thermal capacity, electrical capacitance
C_{xy}	Modulus of cross spectral density function
c	Specific heat
E, \bar{e}	DC voltage
$e', \Delta e$	Unsteady voltages
$\Delta e_{\rho u}, \Delta e_{T_t}, \Delta e_{\phi}$	Mass flux, total temperature and angle sensitivities
f	Frequency
$G_x(t)$	Power spectral density
$G_{xy}(t)$	Cross spectral density
Gr	Grashof number
I	DC current
$i, \Delta i$	Unsteady currents
K	$\frac{d \log R_w}{d \log T_w}$
K_2	constant in equation 3.13
k	Thermal conductivity
L	Wire length, turbulent mixing length
M	Mach number, wire time constant
m	Mass flow fluctuation

m_t	$\frac{d \log \mu}{d \log T_w}$
Nu	Nusselt number
n_t	$\frac{d \log k}{d \log T_w}$
\bar{p}	Pressure
$P(x), P(x,y)$	Probability, joint probability functions
Pr	Prandtl number
q^2	Defined inequation 3.3 (turbulent energy)
$Q(x,y)$	Modulus of cross spectral density function
Re	Reynolds number
R	Wire resistance, correlation function
r	Sensitivity ratio, fluctuating wire resistance
s	Sensitivity
T, \bar{T}	Temperature
$\bar{u}, \bar{v}, \bar{w}$	Mean velocity components
u_1, u_2, u_3	Fluctuating velocity components in section 4
u', v', w'	Fluctuating velocity components
V, v	Mean and fluctuating voltage
Z_c	Impedence
x, y, z	Cartesian Coordinates

α, γ	Temperature coefficients of resistance
α	$1 / \left(1 + \frac{\gamma - 1}{2} M^2 \right)$
β	$\alpha(\gamma - 1)M^2$
γ	Ratio of specific heats
δ	Boundary layer thickness
δ^*	Displacement thickness
ϵ	Finite circuit factor - $\frac{\partial \log I_w}{\partial \log R_w}$, viscous dissipation
η	Recovery factor
θ	Temperature fluctuation, overheat parameter $\frac{T_w}{T_t}$
λ	Wavelength, heat transfer coefficient
μ	Viscosity, wire time constant
ρ	Density
ν	Kinematic viscosity, voltage ratio
τ_{wr}	Temperature loading $\frac{T_w - T_r}{T_r}$
τ_w	Skin friction
σ	RMS value
τ	Time delay
ϕ	Wire inclination angle
ψ	Mean square value
ω	Time constant

Subscripts denote values evaluated at

c	Compensated	
f	Film temperature	$\frac{T_w + T_g}{2}$
g	Gas temperature	
m	Measured	
n	Noise	
o, t	Total temperature	
r	Recovery temperature	
w	Wire temperature	
∞	Freestream	
ρ	Due to density	
ρu	Due to mass flux	
u	Due to axial velocity	
v	Due to vertical velocity	

Superscripts denote

'	Fluctuating component, rms value
~	rms value

END

1-87

DTIC